Impact of Pressure and Added Diluents on Rheological Properties of Heavy Oils

by

Sepideh Mortazavi Manesh

A thesis submitted in partial fulfillment of the requirements for the degree of

Doctor of Philosophy

in

Chemical Engineering

Department of Chemical and Materials Engineering
University of Alberta

Abstract

The rheological properties of heavy oil and bitumen depend on factors such as temperature, pressure, diluent type and diluent composition, as well as sample shear and thermal histories and shear conditions during measurements. Each of these factors can affect the value of apparent viscosity significantly. Uncertainties in the available literature data arise when one or more of these factors have not been considered and have not been reported. Heavy oil and bitumen exhibit non-Newtonian rheological behaviors at lower temperatures. Methods for detecting and quantifying non-Newtonian behaviors are developed, presented and explored in this work using a well-characterized heavy crude oil. The methods and results presented for Maya crude oil provide a reliable database for rheological model development and evaluation, and a template for assessing the rheological behavior of other heavy crude oils.

The thixotropic behavior of Maya crude oil was explored systematically using a stress-controlled rheometer. Thixotropy affects the efficiency and length scale of mixing during blending operations, and flow behaviors in pipes and pipelines following flow disruption where it affects the pressure required to reinitiate flow. Maya crude oil is shown to be a shear thinning fluid below 313 K. The thixotropic behaviors are explored using transient stress techniques (hysteresis loops, step-wise change in shear rate, start-up experiments). The magnitude of the thixotropy effect is larger at lower temperatures. Relationships are identified between rest

times and other thixotropic parameters such as hysteresis loop area and stress decay in start-up experiments. Stress growth, which occurs as a result of a step-down in shear rate, is shown to correlate with temperature. The interrelation between rheological behavior of Maya crude oil and its phase behavior is discussed. The effect of pressure on the non-Newtonian rheological properties of Maya crude oil is also investigated over broad ranges of temperature from (258 to 333) K and at pressures up to 150 bar. At fixed temperature, the magnitude of the non-Newtonian behaviors of Maya crude oil appears to increase with increasing the pressure and shear thinning is shown to persist to higher pressures below 313 K. Boundaries of the non-Newtonian region with respect to temperature, pressure and viscosity are identified and discussed. The thixotropic behavior of Maya crude oil is also shown to persist at higher pressure and the recovery of the moduli at rest appears to be faster at elevated pressures than at atmospheric pressure.

Understanding the rheological properties of mixtures of heavy oil or bitumen and diluents, specifically at low temperatures, is key in designing different processes employed in production or transportation of these resources reliably and efficiently. The effect of diluents (n-heptane, toluene and toluene + butanone (50/50 vol. %)) on the non-Newtonian behavior of Maya crude oil including shear thinning and thixotropy at temperatures from (258 to 333) K are discussed. Toluene + butanone (50/50 vol.%) addition to Maya crude oil induces the greatest reduction in shear thinning behavior irrespective of temperature. Thixotropic properties of mixtures of Maya crude oil and diluent were studied through start-up

experiments. It was shown that toluene + butanone (50/50 vol.%) is the best diluent in moderating the thixotropic effect, while n-heptane showed the most pronounced thixotropic effect. It was shown that toluene + butanone (50/50 vol. %) is more promising in decreasing oil viscosity in comparison to two other diluents tested. Less of this diluent is required to decrease the viscosity to a certain value, which confirms its potential application to be used in the industry as a diluent.

Preface

Chapter 2 of this thesis has been published as S. Mortazavi-Manesh, J. M. Shaw, "Thixotropic Rheological Behavior of Maya Crude Oil", *Energy and Fuels*, 2014, 28, 972-979. I was responsible for the data collection and analysis as well as the manuscript composition. Prof. J. M. Shaw was the supervisory author and was involved with analysis, concept formation and manuscript composition.

Dedication

To

my parents, Hossein Mortazavi-Manesh and Manzar Esnaashari

my husband, Abazar and my son, Sepehr

my brother, Soheil

Acknowledgments

I would like to express my sincerest gratitude to my supervisor, Prof. John M. Shaw, who has supported me throughout my PhD program. I acknowledge his encouragement, patience and invaluable comments and advice. I would never forget his support during this period of my life, especially the toughest moments.

I would like to thank my supervisory committee members, Prof. Janet Elliott and Dr. Neda Nazemifard for their brilliant comments and suggestions. I would also like to thank my former supervisory committee member, Prof. Jos Derksen, for his great comments.

I would like to acknowledge Dr. Ala Bazyleva, now at Colorado School of Mines, for the discussions about rheological concepts and also her feedback and help.

I am also grateful to Prof. Jan Mewis from the Katholieke Universiteit Leuven for the excellent discussions and his comments.

I gratefully acknowledge the University of Alberta PhD program scholarship and Provost Doctoral Entrance Award.

I also acknowledge the financial support from Alberta Innovates, Energy and Environment Solutions, British Petroleum, ConocoPhillips Inc., Imperial Oil Resources, Halliburton Energy Services Ltd., Kellogg Brown and Root, NEXEN Energy ULC., Shell Canada, Total E & P Canada, VMG Inc., and the Natural Sciences and Engineering Research Council of Canada (NSERC).

I would like to acknowledge Mildred Becerra, the lab manager in the Petroleum Thermodynamics Research Group, for her amazing help and support during my research. She made my time in the lab enjoyable and memorable. Thank you Mildred.

I am grateful to Linda Kaert, financial administrator of our group, for her great support and help in organizing everything I needed.

I would like to acknowledge the feedback offered by all of my friends and colleagues as well as their support and encouragements.

My deepest appreciation goes to my parents, Hossein Mortazavi-Manesh and Manzar Esnaashari, my brother, Soheil Mortazavi-Manesh, my husband, Abazar Shamekhi and my son, Sepehr Shamekhi. My parents helped me, supported me and encouraged me at every stage of my life. Being a parent myself, I always admire them for being the most special and amazing parents I have ever seen. My brother, Soheil, was more than a brother to me. He was my best friend, who encouraged me, helped me, offered me feedback on my research and never left me alone. Words cannot express how grateful I am to my husband, Abazar. He accompanied me in every moment of my time during my studies and inspired me to go forward. Since he is a brilliant Mechanical Engineer, I have also greatly benefited from his insightful comments towards my research. Without his sacrifices, I could not have accomplished my goals. I am indebt to him. Finally, my dear son, Sepehr, has always been the best reason for me to smile and be happy even at the toughest moments.

Table of Contents

List of Tables

List of Figures

List of Abbreviations and Symbols

A	Thixotropic loop enclosed area
$\overline{A}$	Reduced enclosed area of thixotropic loop
a1	Model parameter
a2	Model parameter
G	Rigidity modulus
G'	Storage modulus
G''	Loss modulus
HP	n-heptane
n	The number of data points at fixed T & P
NN-Index	Non-Newtonian Index
P	Pressure
P_{atm}	Atmospheric pressure
P_R	Reference pressure
R	Universal gas constant
SAOS	Small Amplitude Oscillatory Shear
SAXS	Small Angle X-ray Scattering
t	Time
T	Temperature
T_{ref}	Reference temperature

TL	Toluene
TLBT	Mixture of toluene+butanone 50/50 volume %
w_d	Weight fraction of diluent in a mixture

Greek letters

β	Model parameter
γ	Shear strain
γ_A	Amplitude of the sinusoidal shear stress
$\dot{\gamma}$	Shear rate
$\dot{\gamma}_i$	Shear rate at data point number i
$\delta(\%)$	Percentage of shear stress growth
δ	Phase angle between stress and strain
$\Delta\dot{\gamma}$	Shear rate domain explored during a measurement
$\Delta\tau$	Stress decay
η	Apparent viscosity
η_i	Apparent viscosity at data point number i
η_0	Viscosity contribution when λ equals 1
η_λ	Viscosity contribution for the degree of structuring equal to λ
η_∞	Viscosity when all the structures present in the fluid are broken down at λ equals zero
$\kappa_1, \kappa_2, \kappa_3$	Model parameters
λ	Structural parameter

τ	Shear stress
τ_A	Amplitude of the sinusoidal shear stress
τ_o	Yield stress
τ_{yield}	Yield stress
τ_i	Initial measured shear stress
τ_f	Final measured shear stress
τ_{max}	Overshoot stress
τ_{min}	Last shear stress value detected after imposing start up shear rate
τ^*	Dimensionless stress parameter
ω	Frequency of the sinusoidal shear strain

Chapter 1 : Introduction

As energy demands grow globally and conventional oil and gas reserves become depleted, exploitation and production of heavy hydrocarbon resources become inevitable. However, heavy oil and bitumen have typically very high viscosity and show complex rheological properties, which result in extreme challenges at many stages during their production, transport and processing. In spite of many studies that have been carried out on the viscosity of heavy oil and bitumen on their own and when mixed with diluents, there are still many uncertainties and in many cases lack of data related to their true rheological behavior at various conditions. Most of the complexities arise from the fact that these resources are non-Newtonian materials. This leads to apparent viscosity values that depend on shear conditions during measurement as well as shear and thermal histories prior to it. As dilution is one of the treatment methods widely used in industry to improve the rheological properties of heavy oil and bitumen, the nature and concentration of diluent are other factors that play an important role in affecting the apparent values of viscosity.

Heavy crude oils and bitumen contain high concentrations of asphaltenes, heavy metals, and sulfur and nitrogen enriched compounds. While some researchers have attributed the high viscosity of these resources to the complex properties of asphaltenes, there are still unsolved questions related to the underlying physics behind their complex rheological behavior and whether this complexity is more related to asphaltenes or maltenes, and whether it is a purely hydrodynamic effect

or whether it is related to the phase behavior of asphaltenes and/or maltenes as well.

1.1 Thesis Objectives

Rheological properties of heavy oil and bitumen depend on factors such as reservoir location, depth within a formation, temperature, pressure, diluent type and diluent composition, as well as sample shear and thermal histories and shear conditions during measurements. Each of these factors can affect the value of the measured apparent viscosity significantly. Uncertainties in the available literature data arise when one or more of these factors have not been considered and have not been reported. Sample shear and thermal histories are among the factors that are mostly ignored and not reported in the literature. Consequently, reported viscosity data vary by over two orders of magnitude at fixed values of temperature and pressure for nominally similar samples. This outcome is associated with non-Newtonian behavior of heavy oil and bitumen. While standard measurement techniques are sufficient for measuring the viscosity of a Newtonian material, obtaining a meaningful and reliable value for the apparent viscosity of a non-Newtonian material at various ranges of temperature and pressure requires sophisticated rheological measurements and equipment, including experimental protocols with well-defined shear and thermal histories for the samples. The first objective of this project is to evaluate the rheological properties of a heavy crude oil over wide ranges of temperature and pressure and shear conditions. Well-defined initial shear conditions and clear shear and thermal histories will be

presented that are expected to provide a "finger print" of a fluid. Closer attention will be paid to low temperature conditions that are encountered in cold climates, and to high pressures. A rheometer capable of performing rheological measurements over a broad range of shear conditions at high pressures as well as low temperatures will be applied that will make it possible to investigate non-Newtonian behavior. The data are expected to provide a benchmark for rheological model development and evaluation. The experimental procedures adopted are expected to provide a template for reducing the ambiguity of heavy oil and bitumen rheological properties reported in the literature.

In spite of some efforts that have been made to understand the underlying physics behind the observed rheological behavior of heavy oil and bitumen[1-3], there are still many doubts related to the possible roles of asphaltenes and maltenes and whether non-Newtonian behavior is a purely hydrodynamic effect or is related to the phase behavior of the heavy oil and bitumen constituents as well. Advancing the understanding of the relationship between phase behavior and hydrodynamics comprises a second objective of this work.

Various techniques are applied in industry that lower the apparent viscosity of heavy oil and bitumen including heating, dilution, oil-in-water emulsion, upgrading, and core annular flow[4, 5]. Dilution is one of the techniques that has drawn much attention. Numerous efforts have been carried out to study impacts of adding diluents[1, 6, 7]. The viscosities of mixtures of bitumen or heavy oil with a diluent[8-17] have been reported, and viscosity correlations[18-22] and mixing rules[23, 24] have been developed for the viscosity of mixtures of bitumen or heavy oil and

diluents based on the available data in the literature. Non-Newtonian behavior is neglected in most of these studies, leaving residual questions and doubts related to the true rheological behavior of these heavy hydrocarbon resources when mixed with diluents particularly at low temperatures and high pressures where data are lacking. This leads to setting another objective for this project, namely, investigating the effect of shear rate and shear history on the value of apparent viscosity of a heavy crude oil mixed with different kinds of diluents in order to have reliable and accountable sets of experimental data bases, which may be used to develop adequate rheological models capable of taking all of the rheological features of mixtures of these resources into account. Different types of chemical compounds will be studied in order to examine their effectiveness in improving the rheological behavior of heavy hydrocarbon resources from which eventually the best potential candidate for industrial use may be introduced.

1.2 Literature Review

1.2.1 Rheological concepts

According to the Society of Rheology that was officially formed on December 9, 1929, the word “Rheology” represents the science of the deformation and flow of matter. Rheological research provides information about the flow of a material in a given environment under specified applied stresses. This type of research can lead to a better understanding of microstructures present in different kinds of materials because there is a direct link between the kind of non-Newtonian behavior that a material exhibits on one hand and the type of response of the

structures present within the material to the exerted shear forces on the other[25]. The type of rheological behavior that any material shows lies somewhere between that of a pure viscous liquid and an elastic solid. Any behavior in between these two extremes is referred to as viscoelastic behavior. Newton's law for purely viscous liquids implies that the applied shear stress τ is proportional to the rate of shear strain $\dot{\gamma}$, also called shear rate. The constant of proportionality η, is called viscosity. For a Hookean solid, the applied shear stress is proportional to the shear strain γ where the constant of proportionality G is called the rigidity modulus or modulus of elasticity. Newton's law and Hook's law are linear, meaning that they have constant proportionality constants. While the viscoelastic behavior between these two extreme linear frameworks can be also linear, non-linear viscoelastic behavior is also possible, because material properties such as viscosity and rigidity modulus can change with applied stress[26]. This results in a wide range of non-linear behaviors. Some examples of non-linearity are non-linear viscoelastic behavior, non-linear pure viscous behavior (such as shear thinning) and non-linear pure elastic behavior.

In general, any material whose rheological behavior does not conform with Newton's law of liquids is called non-Newtonian. There are different types of non-Newtonian behavior such as, shear thinning, shear thickening, viscoplasticity, thixotropy, linear and non-linear viscoelasticity. These are briefly defined below.

Shear thinning: In a material that shows shear thinning or pseudoplasticity behavior, the apparent value of viscosity decreases when the shear rate increases

(Figure 1-1). Many constitutive equations have been developed to correlate this type of behavior, with the most well-known ones being the Carreau model[27, 28], the Cross viscosity equation[29], the Ellis fluid model[30] and the Power-Law model explained in detail elsewhere[31].

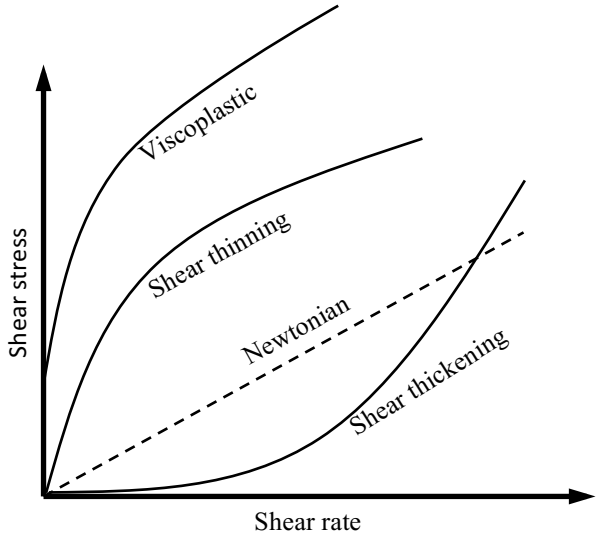

Figure 1-1. Schematic representation of shear thinning and shear thickening behaviors in comparison to Newton's law of liquids.

Shear thickening: The apparent viscosity of a shear thickening material increases with increasing the value of shear rate (Figure 1-1). The Power-Law model can be used to represent the flow behavior of this kind of behavior.

Viscoplasticity: A viscoplastic material will not flow if the external applied shear stress is smaller than a specific fixed value, called the yield stress τ_0. It just deforms elastically (Figure 1-1). If the applied shear stress increases to values higher than the yield stress, the material flows either according to a Newtonian fluid, in which case it will be called a Bingham plastic or it flows based on a non-linear flow curve. The Bingham Plastic model[32], the Herschel-Bulkley fluid model[33] and the Casson fluid model[34] are some of the most widely used constitutive equations for correlating this kind of behavior.

Viscoelasticity: Viscoelastic materials display a combination of viscous and elastic behaviors. The Maxwell model and the Kelvin model are two famous and at the same time simple viscoelastic models, explained in detail elsewhere[31]. More sophisticated constitutive equations have also been developed[35, 36]. In the linear theory of viscoelasticity, differential equations are linear and the material parameters such as viscosity and rigidity modulus have constant values, while the opposite applies for non-linear viscoelastic behavior[26].

Thixotropy: Thixotropic behavior is characterized by a continuous decrease of viscosity with time when a sample that has been previously at rest is subjected to flow and a subsequent increase in viscosity with time when the flow is terminated[37]. This kind of behavior is associated with particulate networks in a material under shear flow that break down into flocs (Figure 1-2). These networks rebuild over time if flow is terminated. A thixotropic material can theoretically be completely viscous or viscoelastic which leads to different kinds of results in a

start-up experiment[37] (Figure 1-3). Several models have been developed for thixotropy correlation and prediction[38-44]. Models that are based on a structural kinetics approach, where shear history is related to a temporal structural parameter $\lambda(t)$, have attracted much attention.

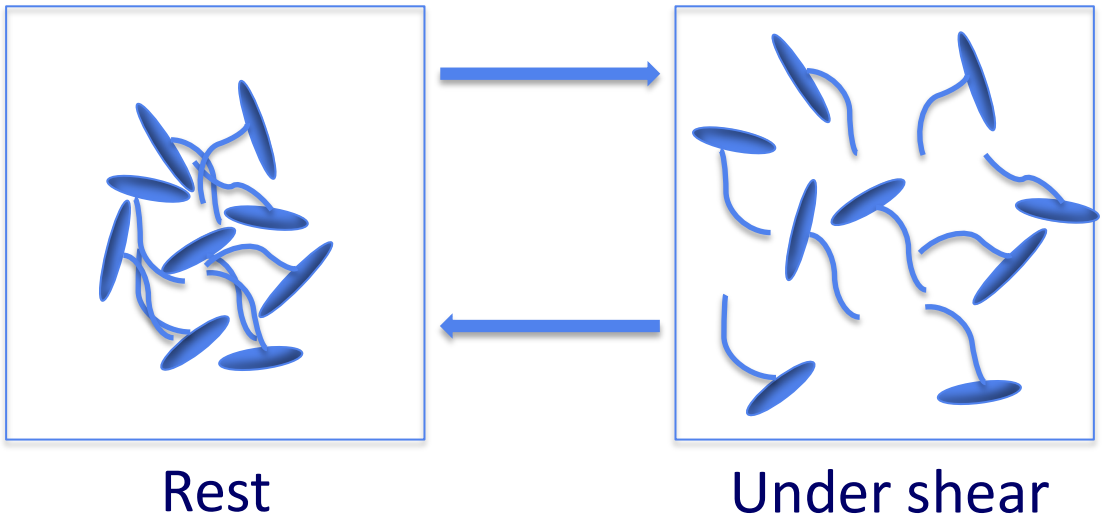

Figure 1-2. Thixotropic behavior under shear and at rest.

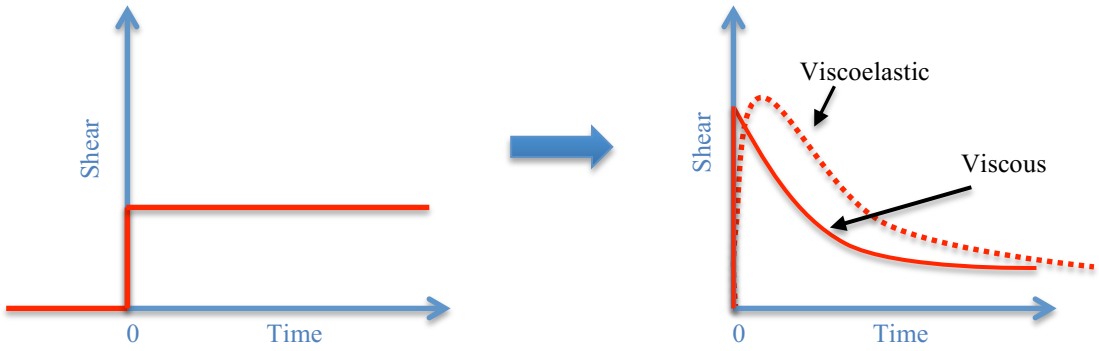

Figure 1-3. The response of a thixotropic material, which is purely viscous, compared to a thixotropic material, which has also viscoelasticity, to a start-up test.

1.2.2 Experimental viscosity data for heavy oil and bitumen available in the literature

A large number of data-bases can be found in the literature, where viscosity of heavy oil and bitumen at different temperatures and/or pressure have been reported[8, 13, 16, 17, 45, 46]. In a study, W. Y. Svrcek and A. K. Mehrotra reported on the viscosity of Athabasca bitumen and its mixtures with CO_2, CH_4 and N_2 over the temperature range of (298 to 373) K. The pressure was varied up to 10 MPa. In another study, L. L. Schramm reported the viscosity of Athabasca bitumen and its mixtures with naphtha at temperatures from (288 to 353) K and at atmospheric pressure, where they described Athabasca bitumen as a Newtonian fluid. M. A. Barrufet and A. Setiadarma performed viscosity measurements for mixtures of a heavy crude oil and n-decane at temperatures ranging from ambient to 450 K and at pressures up to 34 MPa. However, in most cases little or no attention has been

paid to the non-Newtonian features of these resources, which can affect the apparent values of viscosity dramatically[47-50]. This has consequently led to unnecessary uncertainties in the "viscosity" data available in the literature, particularly at higher pressures[51-53]. There are a number of studies where heavy oil and bitumen viscosity is measured or correlated at higher pressures[16, 17, 54-58]. Many studies have been performed, reporting the viscosity of mixtures of bitumen or heavy oil with a light hydrocarbon such as CO_2, methane, propane or butane[8-15]. Others have measured the viscosity of mixtures of bitumen or heavy oil and a liquid solvent[1, 16, 17, 46]. Once again, the non-Newtonian aspects have been widely ignored.

1.3 Thesis Outline

The non-Newtonian behavior of heavy oil and bitumen on their own and when mixed with diluents, which affect the values of their apparent viscosity at different shear conditions and shear histories, is widely ignored in the literature and the available literature data contain significant uncertainties. The main objective of this project is to provide a comprehensive rheological data set of a heavy crude oil on its own and when mixed with diluents with well-defined shear conditions during the measurements and clear shear and thermal histories at various conditions of temperature and pressure, as well as understanding the underlying physics behind the observed rheological behavior. In Chapter 1, an introduction to the literature review is presented, where different types of non-Newtonian behavior are discussed. Past studies on the rheological properties of heavy oil and

bitumen are briefly reviewed from this perspective. Chapters 2, 3 and 4 present detailed studies that address specific objectives. These chapters are in a paper format. Chapter 2 concerning “Thixotropic rheological behavior of Maya crude oil” was published in Energy & Fuels. In Chapter 2, thixotropic rheological behaviors of Maya crude oil (a commercial heavy oil blend from Mexico) are explored systematically using a stress-controlled rheometer at temperatures ranging from (254 to 338) K and atmospheric pressure. Maya crude oil is shown to be a shear thinning fluid below 313 K. The thixotropic behaviors are identified and explored using transient stress techniques (hysteresis loops, step-wise change in shear rate, start-up experiments). The magnitude of the thixotropy effect is larger at lower temperatures. The results also provide a benchmark data set for validation of rheological models for heavy oil that are immerging in the literature. Chapter 3 entitled “Effect of pressure on the rheological properties of Maya crude oil” is dedicated to investigating the effect of pressure on the non-Newtonian rheological properties of Maya crude oil. Measurements were performed from (258 to 333) K, using a stress-controlled rheometer, at pressures up to 150 bar and over a broad range of shear rates. Boundaries of the non-Newtonian region with respect to temperature, pressure and viscosity are identified and discussed. The thixotropic behavior of Maya crude oil is also shown to persist at higher pressure. Chapter 4 entitled “Effect of diluents on the rheological properties of Maya crude oil”, concerns the effect of diluents (n-heptane, toluene and toluene + butanone (50/50 vol. %)) on the non-Newtonian behavior of Maya crude oil including shear thinning and thixotropy at temperatures from (258 to 333) K. The boundary

between shear thinning and Newtonian behavior is found to be between (273 to 283) K, depending on the diluent type and concentration. The thixotropic behavior is explored using the transient stress technique (start-up experiments) at 273 K and different compositions. The effectiveness of these diluents in decreasing the apparent viscosity of Maya crude oil is examined in comparison to the effect of increasing the temperature. The results presented also provide a reliable database for model development and evaluation. Chapters 3 and 4 are being submitted for publication to Energy & Fuels during the Spring of 2015. Finally, Chapter 5 presents the over all conclusions and recommendations for future work for the thesis as a whole.

1.4 References

1. Gateau, P.; Hénaut, I.; Barré, L.; Argillier, J., F., Heavy Oil Dilution. *Oil & Gas Science and Technology - Rev. IFP* 2004, 59, (5), 503-509.
2. Pierre, C.; Barré, L.; Pina, A.; Moan, M., Composition and Heavy Oil Rheology. *Oil & Gas Science and Technology - Rev. IFP* 2004, 59, (5), 489-501.
3. Behzadfar, E.; Hatzikiriakos, S. G., Rheology of bitumen: Effects of temperature, pressure, CO2 concentration and shear rate. *Fuel* 2014, 116, (0), 578-587.
4. Saniere, A.; Hénaut, I.; Argillier, J., F., Pipeline Transportation of Heavy Oils, a Strategic, Economic and Technological Challenge. *Oil & Gas Science and Technology - Rev. IFP* 2004, 59, (5), 455-466.
5. Bensakhria, A.; Peysson, Y.; Antonini, G., Experimental Study of the Pipeline Lubrication for Heavy Oil Transport. *Oil & Gas Science and Technology - Rev. IFP* 2004, 59, (5), 523-533.

6. Li, X.; Sun, W.; Wu, G.; He, L.; Li, H.; Sui, H., Ionic Liquid Enhanced Solvent Extraction for Bitumen Recovery from Oil Sands. *Energy Fuels* 2011, 25, (11), 5224-5231.

7. Hupka, J.; Miller, J. D.; Drelich, J., Water-Based Bitumen Recovery from Diluent-Conditioned Oil Sands. *The Canadian Journal of Chemical Engineering* 2004, 82, (5), 978-985.

8. A.Yazdani; Maini, B. B., Measurements and Modelling of Phase Behaviour and Viscosity of a Heavy Oil/Butane System. *J. Can. Pet. Technol.* 2010, (02), 9-14.

9. Bazyleva, A.; Akeredolu, B.; Liberatore, M. W., Viscosity of Alaska Heavy Oil Saturated with Methane. *Energy Fuels* 2013, 27, (2), 743-751.

10. Badamchi-Zadeh, A.; Yarranton, H. W.; Svrcek, W. Y.; Maini, B. B., Phase Behaviour and Physical Property Measurements for VAPEX Solvents: Part I. Propane and Athabasca Bitumen. 2009, (01), 54-61.

11. Badamchi-Zadeh, A.; Yarranton, H. W.; Maini, B. B.; Satyro, M. A., Phase Behaviour and Physical Property Measurements for VAPEX Solvents: Part II. Propane, Carbon Dioxide and Athabasca Bitumen. 2009, (03), 57-65.

12. Li, H.; Zheng, S.; Yang, D., Enhanced Swelling Effect and Viscosity Reduction of Solvents-CO2-Heavy Oil Systems. In *SPE Heavy Oil Conference and Exhibition 2011*, Society of Petroleum Engineers: Kuwait City, Kuwait, 2011; pp 196-217.

13. Mehrotra, A. K.; Svrcek, W. Y., Viscosity, Density and Gas Solubility Data for Oil Sand Bitumens. Part I: Athabasca Bitumen Saturated with CO and C2H6. *AOSTRA J. Res.* 1985, 1, (4), 263-268.

14. Mehrotra, A. K.; Svrcek, W. Y., Viscosity, Density and Gas Solubility Data for Oil Sand Bitumens. Part II: Peace River Bitumen Saturated with N2, CO, CH4, CO2 and C2H6. *AOSTRA J. Res.* 1985, 1, (4), 269-279.

15. Mehrotra, A. K.; Svrcek, W. Y., Viscosity, Density and Gas Solubility Data for Oil Sand Bitumens. Part III: Wabasca Bitumen Saturated with N2, CO, CH4, CO2 and C2H6. *AOSTRA J. Res.* 1985, 2, (2), 83-93.

16. Guan, J. G.; Kariznovi, M.; Nourozieh, H.; Abedi, J., Density and Viscosity for Mixtures of Athabasca Bitumen and Aromatic Solvents. *J. Chem. Eng. Data* 2013, 58, (3), 611-624.

17. Barrufet, M. A.; Setiadarma, A., Experimental Viscosities of Heavy Oil Mixtures up to 450 K and High Pressures using a Mercury Capillary Viscometer. *J. Pet. Sci. Eng.* 2003, 40, (1-2), 17-26.

18. Mehrotra, A. K.; Svrcek, W. Y., Correlations For Properties of Bitumen Saturated With CO2 , CH4 And N2 , And Experiments With Combustion Gas Mixtures. *J. Can. Pet. Technol.* 1982, 21, (6), 95-104.

19. Motahhari, H.; Schoeggl, F. F.; Satyro, M. A.; Yarranton, H. W., Prediction of the Viscosity of Solvent Diluted Live Bitumen at Temperatures up to 175C. In *Canadian Unconventional Resources Conference 2011*, Society of Petroleum Engineers: Alberta, Canada, 2011; Vol. 3, pp 2065-2083.

20. Miadonye, A.; Doyle, N. L.; Britten, A.; Latour, N.; Puttagunta, V. R., Modelling Viscosity and Mass Fraction of Bitumen-Diluent Mixtures. *J. Can. Pet. Technol.* 2001, 40, 52-57.

21. Novak, L. T., Entity-Based Eyring−NRTL Viscosity Model for Mixtures Containing Oils and Bitumens. *Industrial & Engineering Chemistry Research* 2006, 45, (21), 7329-7335.

22. Wen, Y.; Kantzas, A., Evaluation of Heavy Oil/Bitumen- Solvent Mixture Viscosity Models. *J. Can. Pet. Technol.* 2006, 45, 56-61.

23. Barrufet, M. A.; Setiadarma, A., Reliable Heavy Oil–Solvent Viscosity Mixing Rules for Viscosities up to 450K, Oil–Solvent Viscosity Ratios up to 4 × 105, and any Solvent Proportion. *Fluid Phase Equilib.* 2003, 213, (1-2), 65-79.

24. Mehrotra, A. K., A Mixing Rule Approach for Predicting the Viscosity of CO2-Saturated Cold Lake Bitumen and Bitumen Fractions. *J. Pet. Sci. Eng.* 1992, 6, (4), 289-299.

25. Chhabra, R. P., Rheology of Complex Fluids, Chapter 1: Non-Newtonian Fluids. In Springer: New York, 2010.

26. Barnes, H. A.; Hutton, J. F.; Walters, K., *An Introduction to Rheology*. Elsevier Science Publishers: Amsterdam, Netherlands, 1993.

27. Carreau, P. J. Ph.D. Thesis, University of Wisconsin, Madison, Wisc., 1968.

28. Carreau, P. J., Rheological Equations from Molecular Network Theories. *Transactions of The Society of Rheology (1957-1977)* 1972, 16, (1), 99-127.

29. Cross, M. M., Rheology of Non-Newtonian Fluids: A New Flow Equation for Pseudoplastic Systems. *J. Colloid Interface Sci.* 1965, 20, (5), 417-437.

30. Ellis, S. B. Thesis, Lafayette College, 1927.

31. Mezger, T. G., *The Rheology Handbook*. Vincentz Network: Hanover, 2011.

32. Bingham, E. C., An Investigation of the Laws of Elastic Flow. *Bull. U.S. Bur. of Standards* 1916.

33. Herschel, W. H. B., R., Measurement of Consistency as Applied to Rubber Benzene Solutions. *Proc. ASTM* 1925, 82.

34. Casson, N., *A Flow Equation for Pigment-Oil Suspensions of the Printing Ink Type, in: Rheology of Disperse Systems*. ed. C.C. Mill, Pergamon Press: New York, 1959.

35. McLeish, T. C. B.; Larson, R. G., Molecular Constitutive Equations for a Class of Branched Polymers: The Pom-Pom Polymer. *Journal of Rheology (1978-present)* 1998, 42, (1), 81-110.

36. Drozdov, A. D.; Jensen, E. A.; Christiansen, J. d. C., Thermo-Viscoelasticity of Polymer Melts: Experiments and Modeling. *Acta Mech* 2008, 197, (3-4), 211-245.

37. Mewis, J.; Wagner, N. J., Thixotropy. *Adv. Colloid Interface Sci.* 2009, 147-148, 214-27.

38. de Souza Mendes, P. R., Modeling the Thixotropic Behavior of Structured Fluids. *J. Non-Newtonian Fluid Mech.* 2009, 164, (1–3), 66-75.

39. de Souza Mendes, P. R., Thixotropic Elasto-Viscoplastic Model for Structured Fluids. *Soft Matter* 2011, 7, (6), 2471-2483.

40. Dullaert, K.; Mewis, J., A Structural Kinetics Model for Thixotropy. *J. Non-Newtonian Fluid Mech.* 2006, 139, (1-2), 21-30.

41. Quemada, D., Rheological Modelling of Complex Fluids: IV: Thixotropic and "Thixoelastic" Behaviour. Start-up and Stress Relaxation, Creep Tests and Hysteresis Cycles. *Eur. Phys. J.: Appl. Phys.* 1999, 5, (02), 191-207.

42. Roussel, N.; Le Roy, R.; Coussot, P., Thixotropy Modelling at Local and Macroscopic Scales. *J. Non-Newtonian Fluid Mech.* 2004, 117, (2-3), 85-95.

43. Yziquel, F.; Carreau, P. J.; Moan, M.; Tanguy, P. A., Rheological Modeling of Concentrated Colloidal Suspensions. *J. Non-Newtonian Fluid Mech.* 1999, 86, (1–2), 133-155.

44. Dion, M. Modelling the Rheology of Complex Fluids: Cases of Bitumen and Heavy Oils at Low Temperatures. M.Sc. Thesis, University of Alberta, Edmonton, 2011.

45. Svrcek, W. Y.; Mehrotra, A. K., Gas Solubility, Viscosity and Density Measurements for Athabasca Bitumen. *J. Can. Pet. Technol.* 1982, 31-38.

46. Schramm, L. L. L.; Kwak, J. C. T., The Rheological Properties Of An Athabasca Bitumen And Some Bituminous Mixtures And Dispersions. *J. Can. Pet. Technol.* 1988, 27, (1).

47. Bazyleva, A. B.; Hasan, M. A.; Fulem, M.; Becerra, M.; Shaw, J. M., Bitumen and Heavy Oil Rheological Properties: Reconciliation with Viscosity Measurements. *J. Chem. Eng. Data* 2010, 55, 1389-1397.

48. Hasan, M. D. A.; Fulem, M.; Bazyleva, A.; Shaw, J. M., Rheological Properties of Nanofiltered Athabasca Bitumen and Maya Crude Oil. *Energy Fuels* 2009, 23, (10), 5012-5021.

49. Evdokimov, I. N.; Losev, A. P., Thixotropy in Native Petroleum Emulsions. *J. Dispersion Sci. Technol.* 2011, 32, (8), 1206-1212.

50. Mortazavi-Manesh, S.; Shaw, J. M., Thixotropic Rheological Behavior of Maya Crude Oil. *Energy Fuels* 2014, 28, 972-979.

51. Novak, J. D.; Winer, W. O., The Effect of Pressure on the Non-Newtonian Behavior of Polymer Blended Petroleum Oils. *J. Lubr. Technol.* 1969, 91, (3), 459-462.

52. Hirst, W.; Moore, A. J., Elastohydrodynamic Lubrication at High Pressures. II. Non-Newtonian Behaviour. *Proceedings of the Royal Society of London. Series A, Mathematical and Physical Sciences* 1979, 365, (1723), 537-565.

53. Kioupis, L. I.; Maginn, E. J., Impact of Molecular Architecture on the High-Pressure Rheology of Hydrocarbon Fluids. *The Journal of Physical Chemistry B* 2000, 104, (32), 7774-7783.

54. Puttagunata, V. R.; Singh, B.; Miadonye, A., Correlation of Bitumen Viscosity with Temperature and Pressure. *The Canadian Journal of Chemical Engineering* 1993, 71, (3), 447-450.

55. Mehrotra, A. K.; Svrcek, W. Y., Viscosity of Compressed Athabasca Bitumen. *Can. J. Chem. Eng.* 1986, 64, (5), 844-847.

56. Mehrotra, A. K.; Svrcek, W. Y., Viscosity of Compressed Cold Lake Bitumen. *The Canadian Journal of Chemical Engineering* 1987, 65, (4), 672-675.

57. Khan, M. A. B.; Mehrotra, A. X.; Svrcek, W. Y., Viscosity Models For Gas-Free Athabasca Bitumen. *J. Can. Pet. Technol.* 1984, 23, (3).

58. Johnson, S. E.; Svrcek, W. Y.; Mehrotra, A. K., Viscosity Prediction of Athabasca Bitumen Using the Extended Principle of Corresponding States. *Industrial & Engineering Chemistry Research* 1987, 26, (11), 2290-2298.

Chapter 2 : Thixotropic Rheological Behavior of Maya Crude Oil

2.1 Introduction

Heavy hydrocarbon resources such as heavy oil and bitumen have become essential energy sources globally. Their transport properties in situ, and under production, transport and refining conditions have become key building blocks for decision makers in industry. These resources, which normally contain high asphaltene mass fractions, have been considered to be colloidal in nature for nearly a century[1]. However, in spite of many studies that have been performed on the viscosity of these resources[2-7], uncertainties related to their rheological properties persist. For example, uncertainties arise because reported viscosity data for the same nominal resource are obtained using samples from different locations and depths within formations or reservoirs that are then prepared in different ways[2]. Sample shear histories and shear conditions during measurements also vary and numerous measurement techniques and procedures do not detect Non-Newtonian rheological behavior. Consequently reported viscosity data vary over two orders of magnitude at fixed temperature for nominally similar samples. Non-Newtonian effects such as thixotropy and viscoelasticity may account for a significant fraction of this apparent variation in heavy oil and bitumen rheological behavior[2, 8]. Sample shear history may be responsible for deviations of an order of

magnitude for viscosities of heavy oil or bitumen from the same nominal location[7, 9-14]. While thixotropy and viscoelasticity both reflect memory dependent properties, they can be distinguished through step-down shear rate experiments, where viscoelastic fluids undergo a monotonic decrease of stress to a new plateau value, while thixotropic fluids undergo an instantaneous drop to a lower value followed by a gradual increase in stress to a new plateau value[15].

Thixotropy affects flow in mixers[16-18], flow in pipes and pipelines, and it is particularly evident during restart operations following flow disruption arising from gel formation, asphaltene precipitation, or maintenance among other causes. Impacts are more likely and more severe at low temperatures. During restart, a low-viscosity lubricating layer near the wall and non-linear pressure profiles are just some of the features that make the pipeline flow characterization of thixotropic materials complex[19]. Problems with respect to pump performance may also arise. While a few studies have accounted for thixotropic behavior of oils in characterizing flow start-up in pipelines[20-23], a thixotropic rheological database for heavy oils, which covers lower temperatures found sub-sea or in northern climates, is still lacking in the literature. Such comprehensive sets of information on thixotropic properties of these materials are essential for accurate and reliable characterization of heavy oil and bitumen flow in pipelines.

Thixotropic behavior is characterized by a continuous decrease of viscosity with time when a sample that has been previously at rest is subjected to flow and the subsequent increase of viscosity with time when the flow is terminated[15]. This behavior results from the breaking down of particulate networks in a material

under shear flow into flocs. These networks rebuild over time if flow is terminated. The building process is typically slower than the network breakage process. In thixotropic materials, the microstructural change occurring over time under intermittent flow and rest conditions is competitive[19]. The attractive forces among flocs that drive floc association and network regrowth are weak and consequently the hydrodynamic forces driving break up are strong enough to disrupt association[24].

Several models have been proposed for thixotropy behavior correlation and prediction[25-31]. Among them, models that are based on a structural kinetics approach have attracted much attention. In these models, shear history is related to a temporal structural parameter $\lambda(t)$. These models are specific to individual fluids and do not predict the thixotropic behavior of others well. Therefore, suitable experimental data sets that represent different aspects of thixotropic properties of specific heavy oils and bitumen are necessary in order to validate and subsequently generalize models for these classes of fluids. These data sets include results from start-up experiments, hysteresis flow curves, and step-wise changes in shear rate or shear stress. The results of these experiments serve as a fingerprint for a specific material as well as a fitting or validation tool for thixotropic models for fluids comprising comparable constituents. Care must be taken to avoid artifacts in data sets because the outcomes of thixotropy experiments may vary with the details of the shear history of a sample prior to measurements, and sample handling procedures during experiments. It is crucial

to establish a well-defined initial condition for experiments to get both reproducible and meaningful results.

Typical structural kinetics thixotropic rheological behavioral models possess the general form:

$$\tau(t) = \tau_{yield}(\lambda) + \eta_{\lambda}(\lambda, \dot{\gamma}).\dot{\gamma} + \eta_{\infty}(\dot{\gamma}).\dot{\gamma} \tag{2-1}$$

$$\frac{\mathrm{d}\lambda(t)}{\mathrm{d}t} = f(\lambda, \dot{\gamma}) \tag{2-2}$$

where $\dot{\gamma}$ is the shear rate, τ_{yield} is the yield stress, η_{λ} is the viscosity contribution to the degree of structuring equal to λ and η_{∞} is the viscosity when all the structures present in the fluid are broken down at λ equals zero. Viscosity measurements at conditions where samples are destructured provide information necessary to obtain the shear rate functionality of η_{∞} based on a shear thinning constitutive equation of state. Yield stress experiments provide a basis for modeling the τ_{yield} contribution of the shear stress. Results obtained from step-down and start-up experiments define parameters appearing in specific η_{λ} and dλ/dt models, such as ones proposed by Dullaert and Mewis[27]:

$$\eta_{\lambda} = \lambda\eta_0 \tag{2-3}$$

$$\frac{\mathrm{d}\lambda}{\mathrm{d}t} = \kappa_1\dot{\gamma}\lambda t^{-\beta} + \kappa_2(1-\lambda)t^{-\beta} + \kappa_3(1-\lambda)\dot{\gamma}^{0.5}t^{-\beta} \tag{2-4}$$

where η_0 is the viscosity contribution when λ equals 1 and κ_1, κ_2, κ_3 and β are model parameters.

In this study, the thixotropic behavior of Maya crude oil is explored systematically with the goal of providing high quality data for model development

and testing. Experimental data with well-defined initial shear conditions and clear shear histories are presented that provide a "finger print" for this fluid. These data are expected to provide a benchmark for rheological model development and evaluation. The experimental procedures adopted provide a template for reducing the ambiguity of heavy oil and bitumen rheological properties reported in the literature as we move forward. Relationships identified between rest time and other thixotropic parameters may facilitate reconciliation of rheological data in the literature, and the development of simplified or minimal data sets required to determine the rheological properties of heavy oils and bitumen.

2.2 Experimental Section

2.2.1 Materials

Maya crude oil, a commercial heavy oil blend from Mexico with a reported pour point of 243.15 K[32], was supplied by Dr. Carlos Lira at the Mexican Petroleum Institute. The elemental composition and the SARA analysis (saturates, aromatics, resins, and asphaltenes) of the Maya oil sample were obtained from a previous study[2] according to ASTM D3279 and are given in Table 2-1. Detailed information about methods used for these analyses are available elsewhere[33].

Table 2-1. SARA analysis and elemental composition of Maya crude oil[2].

Saturates	Aromatics	Resins	C5 Asphaltenes
Mass fraction			
0.316	0.425	0.102	0.157

Element	Maya crude oil
	Mass fraction
C	0.845
H	0.113
N	0.003
S	0.033
O	0.012
	Metal analysis/mg.kg^{-1}
Al	1.0
Ba	< 0.1
K	1
Ca	29
Cr	0.8
Fe	4.0
Mg	0.7
Mn	< 0.1
Mo	3.0
Na	112
Ni	56
Si	80
Ti	0.4
V	263
Zn	1.6

2.2.2 Rheological measurements

Rheological measurements were performed using a stress-controlled rheometer (Physica MCR 301 Anton Paar). In this device, a magnetic coupling connected to the rheometer head transmits the motor movement to the geometry inside the pressure cell. All of the measurements in this study were carried out at atmospheric pressure using a double-gap cylinder geometry. The measuring bob

internal and external diameters are 21.03 and 23.04 mm respectively. The internal and external diameters of the measuring cup are 20.33 and 23.85 mm respectively. The amount of sample loaded for each test was 2.37 ml. The small size of this geometry minimizes the thickness of the fluid inside the cup, and hence effects associated with temperature gradients. Sample temperature is measured with a Pt100 DIN/IEC 751 sensor with a resolution of 0.01 K and controlled with an accuracy of ±0.03 K. A peltier system (C-PTD200, Anton Paar), used for temperature control of the sample in the rheometer, has a temperature operating range from (243 to 472) K.

Table 2-2 shows the results of viscosity measurements using the Anton Paar rheometer on some Cannon certified viscosity standards. These standards comprise Newtonian fluids and highlight the accuracy of the reported measurements over the range of temperatures and nominal viscosities explored in this work. The highest relative deviation from these standards, 10 %, is seen at 255.3 K, and the lowest relative deviation, 1 %, is seen at 313 K.

Table 2-2. Deviations of measured viscosities from reported values for certified Newtonian viscosity standards.

Standard	Reported viscosity of standard[34] (Pa.s)	Temperature (K)	$100\times(\eta_{reported}-\eta_{measured})/\eta_{reported}$
Cannon S600	0.4335	313	1.7
	1.056	298	2.1
Cannon S60	0.04684	313	1.2
Cannon N18000	16.04	313	2.2
Cannon N115B	9.575	266.5	5.3
	17.00	260.9	7.8
	31.93	255.3	10.1

Prior to sample loading, the moment of inertia of the applied geometry is measured by the instrument followed by a motor adjustment. During the motor adjustment, the instrument automatically performs a ball bearing adjustment. Since the pressure cell is sealed, the cell head contains a ball bearing in addition to the air bearing of the instrument. The measuring system is attached to the cell head containing the ball bearing, which itself is coupled to the instrument over a stiff magnetic coupling[35].

In order to avoid ambiguity in the shear history of samples being tested, it is essential to follow the same procedure for loading and pre-cooling samples, providing a specific rest time and in some cases pre-shearing samples prior to the main steady shear or transient shear stress measurements. This ensures that the rheological results obtained are comparable, which is extremely important as far as thixotropic materials are concerned. In each experiment, samples were loaded

into the rheometer and cooled to 268 K. The samples then rested for 24 hours, at which point the main test began. All of the experiments were conducted in triplicate to confirm repeatability of the experiments. All of the data obtained are presented as tabulated supplemental data in Tables S1 to S6. These tables include standard uncertainties of the measurements. Summary Figures are presented and discussed below. In these Figures, the error bars are smaller than the data-points in most cases and are not added to the figurers for clarity.

2.3 Results and Discussion

2.3.1 Shear thinning behavior

Linear shear rate ramps from (10 to 500) s^{-1} were imposed on a Maya oil sample and the steady shear stress was measured. The experiments were performed isothermally at temperatures ranging from (254 to 338) K. The results are shown in Figures 2-1 a and b. At each shear rate, a 2 minute conditioning period preceded measurements. During the conditioning period, components of the structural networks that are weak enough to break under the imposed shear rate are eliminated and the shear stress approaches a steady state value. Below 313 K, Maya crude oil exhibits shear thinning behavior. At 313 K and above, response variations with shear rate are not detected. The phase behavior of Maya crude oil was studied previously[36] using a combination of nanofiltration (to partition the crude), differential scanning calorimetry combined with an accurate solid state heat capacity model (to detect phase transitions), and phase angle measurements (to assess the nature of the phase transitions observed). According to that study, at

temperatures between 160 K and 320 K, Maya crude oil comprises three phases, namely: a liquid maltene phase, a solid maltene phase and solid asphaltenes. At 320 K, the solid maltene phase which melts into liquid phase as temperature is increased is absent. Above 320 K, the liquid maltene phase and solid asphaltene phase remain. Thus, the observable shear-thinning behavior of Maya crude oil at temperatures lower than 313 K may in part be attributable to structural and hydrodynamic properties of solid maltenes. As the structure and nature of the solid phase is unknown, the decrease in viscosity with shear rate may result from breakage or alignment of solid domains as both are characteristic of shear-thinning materials[37].

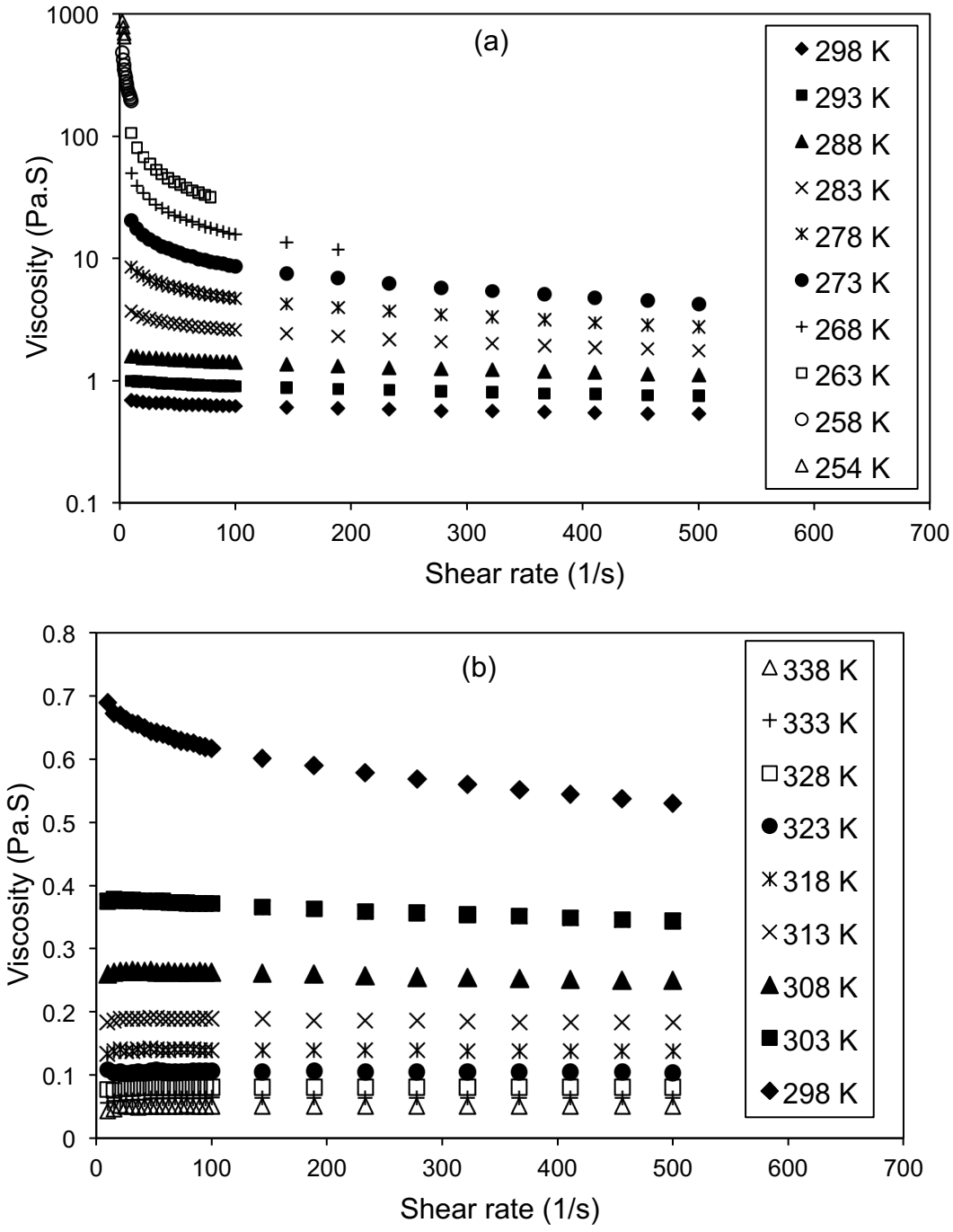

Figure 2-1. Flow curves for Maya oil: a) 254-298 K, b) 298-338 K.

2.3.2 Hysteresis behavior

Hysteresis is identified using *the hysteresis loop technique*, where shear rate is increased linearly from zero to a maximum value followed by decreasing it to zero at the same rate during a single isothermal rheology experiment[38]. This technique quickly demonstrates if thixotropic behavior is present and provides a qualitative measure of the magnitude of the effect of thixotropy. Shear rate profiles were imposed on Maya crude oil, at fixed temperatures, as illustrated in Figure 2-2a. Numerical results are shown in Figures 2-3a and b. The upper flow curves were measured during the increasing shear rate runs ("upper curve") and the lower flow curves were measured during the decreasing shear rate runs ("lower curve"). As the flow curves possess hysteresis loops, Maya crude oil exhibits thixotropic behavior. At temperatures greater than 288 K the observed hysteresis loops become small and hysteresis is not observed experimentally above 293 K at the ramp rate investigated. The hysteresis loops are observed as a result of shear stress lagging shear rate during experiments, because network breakage and build up kinetics differ. Typically, breakage is faster kinetically than build up and at higher ramp rates the hysteresis is expected to persist to higher temperatures. The observation of hysteresis in the rheological response reflects how fluid shear history affects rheological measurements, which in turn has implications for industrial cases[39] such as oil production, transport and refining, where neglecting the shear history of a fluid may impact the measurement and prediction of rheological properties, and consequently lead to inadequate or inappropriate facility designs.

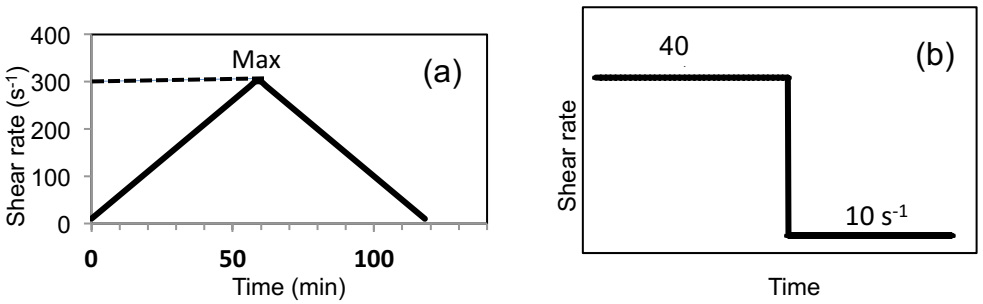

Figure 2-2. Qualitative illustration of (a) a shear rate ramp, imposed to observe the lag between shear stress and shear rate – "hysteresis technique". The maximum value of shear rate imposed is 100 s^{-1} and 20 s^{-1} for temperatures of 263 K and 258 K, respectively; (b) a step down in shear rate, imposed to observe structure build-up behavior.

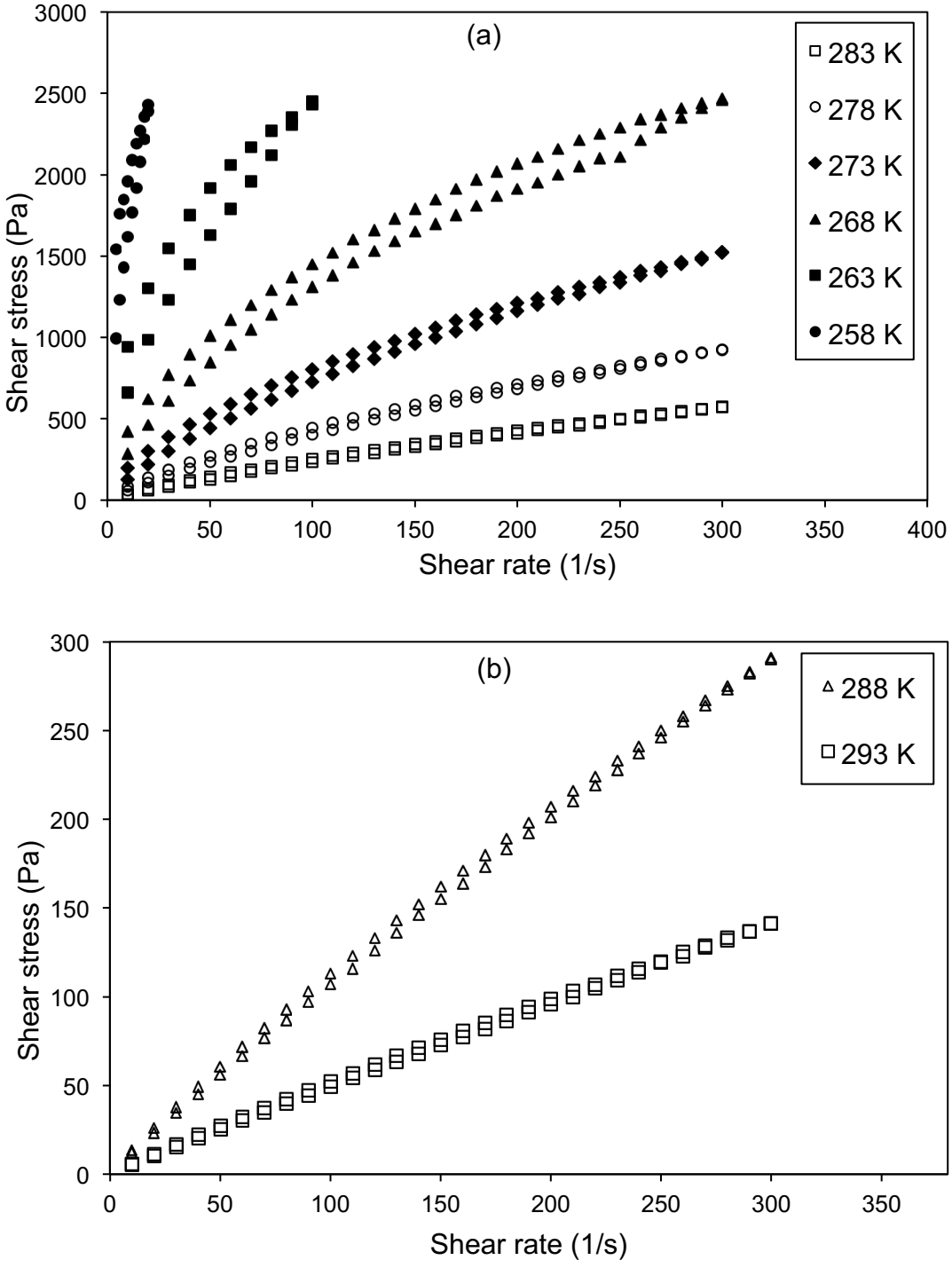

Figure 2-3. Flow curves of Maya oil obtained using the hysteresis technique: (a) 258-283 K, (b) 288-293. At each temperature, the upper curve: increasing shear rate run; the lower curve: decreasing shear rate run.

In order to qualify the magnitude of the thixotropic effect, the area enclosed within the hysteresis loops was calculated. As there is an upper limit to the torque that the equipment can withstand, these experiments were performed over different shear rate domains and the areas, A, were normalized by dividing by $\Delta\dot{\gamma}$, the shear rate domain explored during a measurement and, $\bar{A}$, a reduced enclosed area is defined as:

$$\bar{A} = \frac{A}{\Delta\dot{\gamma}} \tag{2-5}$$

Figure 2-4a shows the reduced enclosed area as a function of temperature. As the mass fraction of solid maltenes is also available from prior work over the same temperature range[36], it is possible to graph the reduced enclosed area as a function of solid maltene mass fraction - Figure 2-4b. The thixotropic behavior of Maya crude oil correlates closely with the solid maltene mass fraction. Thus, the thixotropy arising in Maya crude oil is in agreement with the phase behavior of Maya crude oil[36] and the network formation and breakage phenomena appear attributable to the maltene fraction because the asphaltene fraction is invariant.

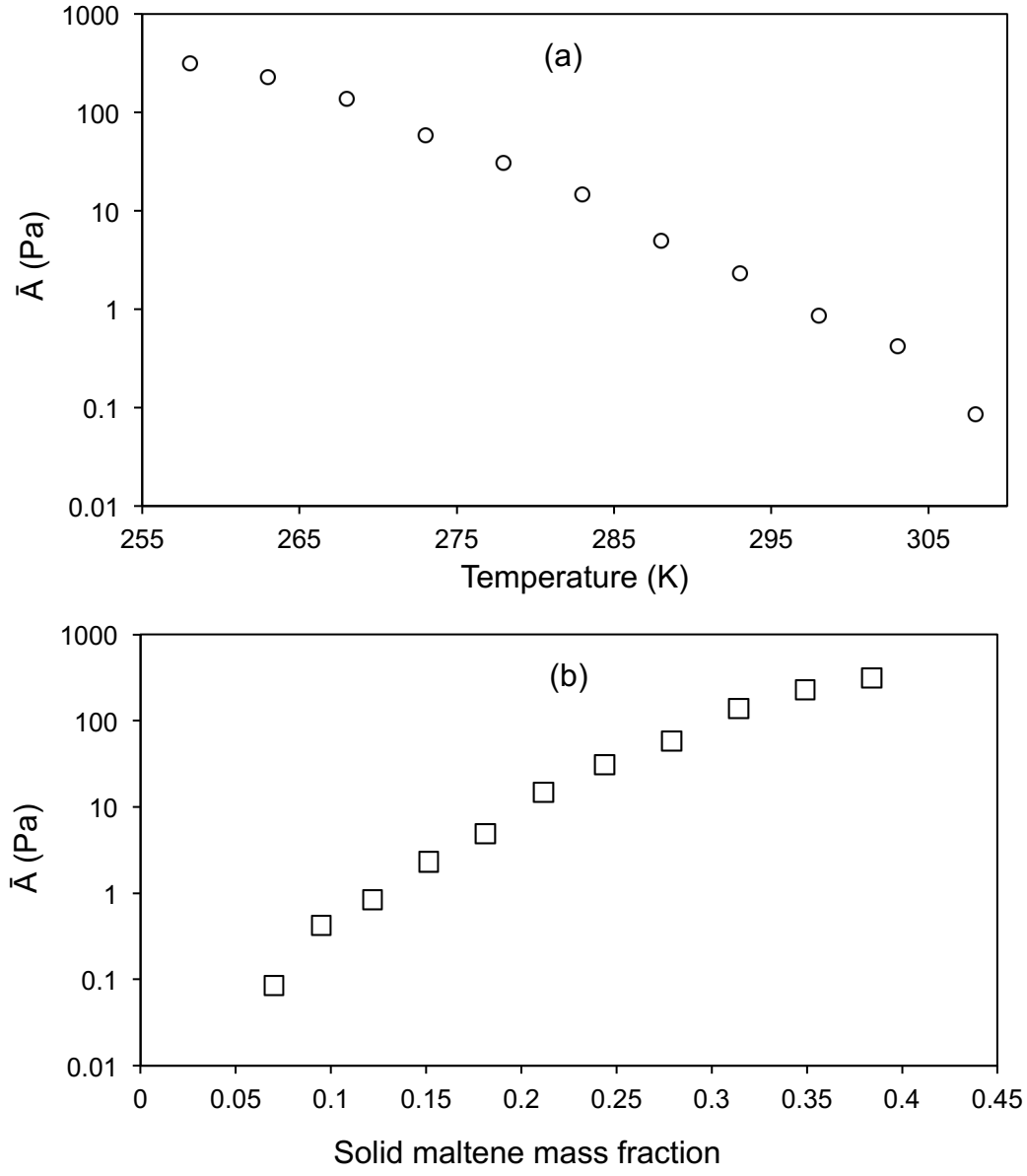

Figure 2-4. Temperature and solid maltene mass fraction dependence of reduced enclosed area, defined in equation 3-5, for Maya oil: (a) Temperature dependence, (b) solid maltene mass fraction dependence. Temperature dependence of solid maltene mass fraction is obtained from our previous work[36].

The impact of rest time on the magnitude of thixotropic behavior was also addressed and the value of *A* was determined as a function of rest time at 278 K. It should be noted that at this temperature, the vapour pressure of Maya crude oil is low relative to atmospheric pressure and the cup holding the sample is sealed. Thus the possible impact of light ends evaporation on results can be ignored. The rest time was defined as the time that the Maya oil sample was at rest after it had been first loaded into the rheometer. The results obtained are shown in Figure 2-5. The magnitude of the hysteresis loop triples in size in 800 hours and continues to increase even after one month, as suggested by the log-linear relationship between rest time and reduced hysteresis area. From a microscopic point of view, hysteresis regrowth can be associated with rebuilding structures broken as a consequence of the shear history of the sample. With increasing rest time, a larger number and potentially stronger structures have a chance to form. Such effects are included in structural kinetic models for thixotropic behavior[25-27, 31]. For Maya crude oil, a termination step for network growth was not observed and hysteresis area is readily defined as a simple logarithmic function of rest time. The lag between shear stress and shear rate, and the impact of rest time both underscore the impact of fluid history on rheological measurements for Maya crude oil and the interplay between shear history and phase behavior.

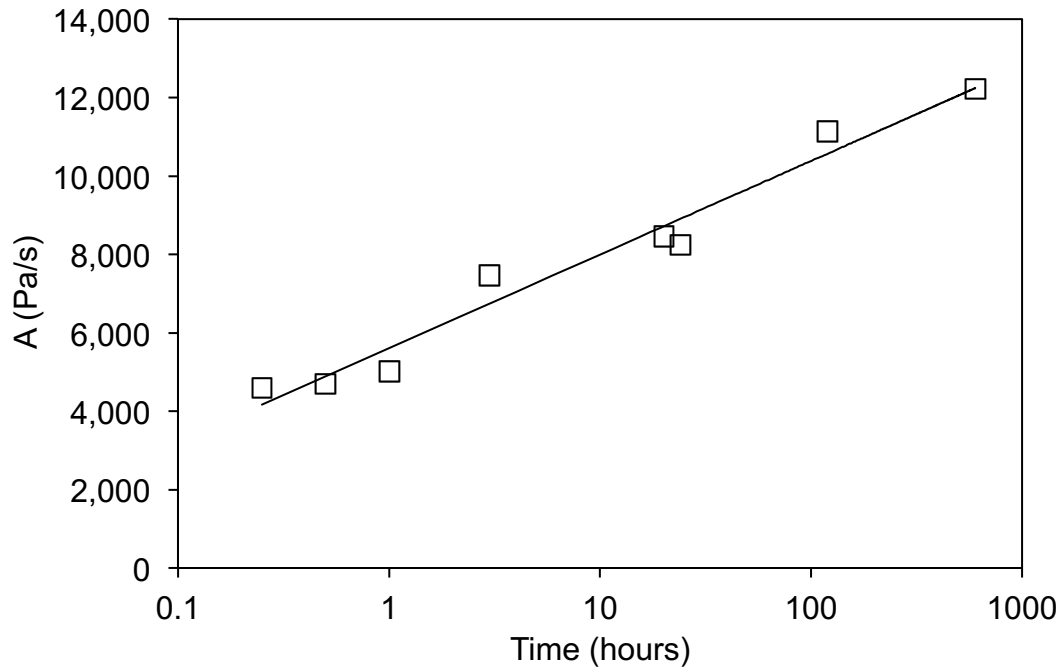

Figure 2-5. Impact of rest period on hysteresis area for Maya oil at 278 K.

2.3.3 Build-up behavior

Thixotropic behavior can be further quantified through measurements where there is a step-down in the imposed shear rate. Step-down experiments provide information on structure regrowth and whether or not samples possess purely thixotropic behavior or a mix of thixotropic and viscoelastic behaviors[15]. However, viscoelastic behavior is only observed, even if is present, if the measurement time scale is short enough to capture it, and does not otherwise appear experimentally. As discussed in detail by J. Mewis and N. J. Wagner[15], the shear stress transient response obtained after imposing a step-down in shear rate

on a purely thixotropic material would appear as an instantaneous decrease followed by an increase to a steady value. However, if a thixotropic material has viscoelastic properties too, then the shear stress response would appear as an instantaneous decrease followed by a slow decrease (stress relaxation due to viscoelasticity) and eventually an increase to a steady value. In this latter case, stress relaxation would be observed only if the measurement time scale is short enough to capture it, and does not otherwise appear experimentally. For Maya crude oil, a thixotropic response was observed. Viscoelasticity was not detected over the range of conditions evaluated. Isothermal shear rate step-down experiments, shown schematically in Figure 2-2b, were performed from (40 to 10) s^{-1} over the temperature interval (258 to 278) K. To insure that all samples had the same shear history, they were pre-sheared at 10 s^{-1} and then the samples were sheared at 40 s^{-1} until a steady shear stress value was obtained. The shear rate was then dropped to 10 s^{-1} and the shear stress responses are reported in Figures 3-6 a-e. The results show that the impact of temperature on the rate and extent of shear stress increases with time after the shear rate is stepped down. This type of shear stress regrowth highlights the thixotropic properties of Maya crude oil. From a micro-scale point of view, the increase arises from particles/small structures within Maya oil that associate to build up larger flocs/networks at low shear rate that do not survive at higher shear rates. At longer times, a new steady shear stress value is approached that reflects a balance between network breakage and regrowth at the lower shear rate.

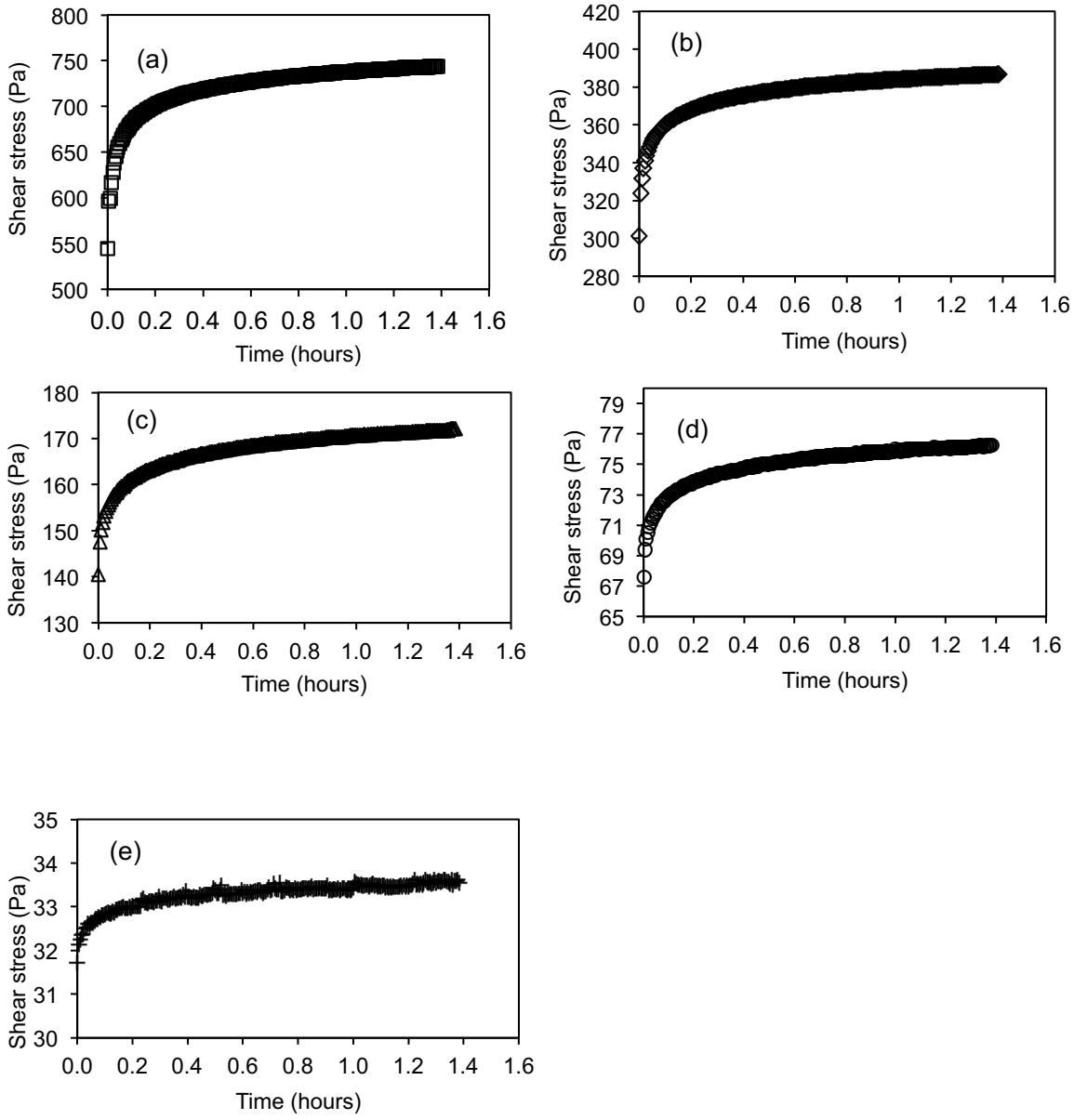

Figure 2-6. Build-up behavior of Maya oil after a step-down in shear rate from 40 to 10 s^{-1}: (a) 258 K, (b) 263 K, (c) 268 K, (d) 273 K, (e) 278 K.

Shear stress growth, δ, defined as:

$$\delta(\%) = \frac{\tau_f - \tau_i}{\tau_i} \times 100 \quad (2\text{-}6)$$

where τ_i is the initial measured shear stress, and τ_f is the final measured shear stress, is a linear function of temperature:

$$\delta(\%) = -1.5539T/\mathrm{K} + 437.62 \quad (2\text{-}7)$$

As temperature increases, both the absolute (Figure 2-6) and relative (Figure 2-7) magnitudes of the build-up process diminish. This behavior is attributed to the transition from more solid to more liquid for the maltene fraction over this temperature interval, which reduces the mass fraction of structured material present in Maya crude oil, and hence the potential for structural change and thixotropic behavior. It should be noted that Equation 2-7 is only valid up to the temperature where shear stress growth reaches zero - (282 K).

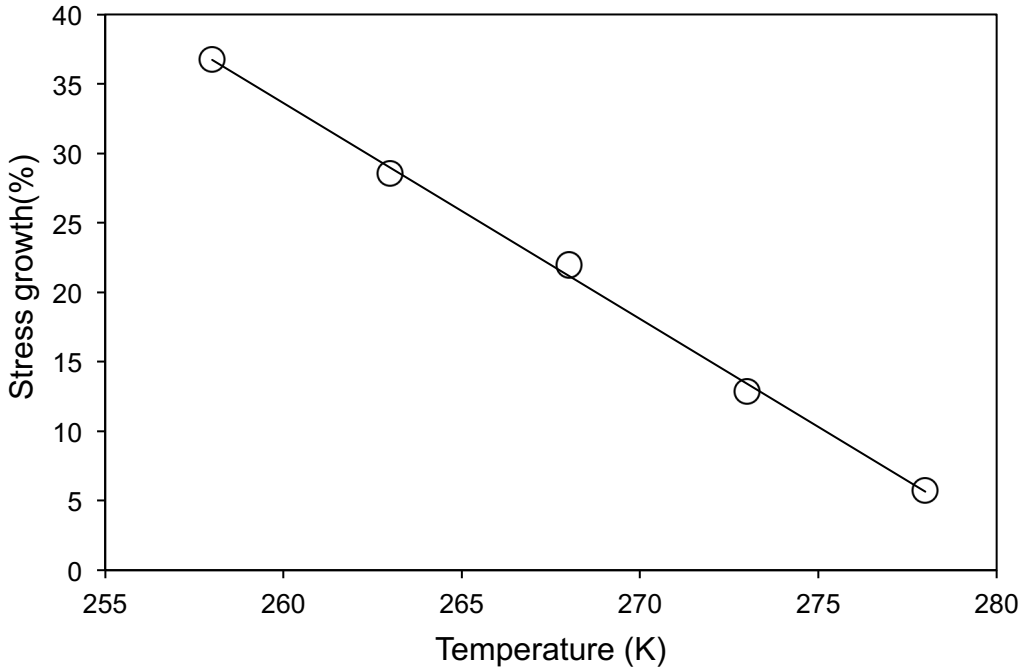

Figure 2-7. Dependence of the stress growth, defined in equation 2-6, on temperature obtained from step-down in shear rate experiments.

Shear stress changes can also be normalized to obtain a dimensionless stress parameter:

$$\tau^* = \frac{\tau - \tau_i}{\tau_f - \tau_i} \tag{2-8}$$

where τ^* is a function of τ_f, τ_i and the measured shear stress at each data-point, τ, and is a temperature independent property. The τ^* master curve is shown in Figure 2-8. Data for the whole temperature range (258 to 278) K map onto a single master curve to a first approximation and this master curve provides a simple and general benchmark for the thixotropy model development.

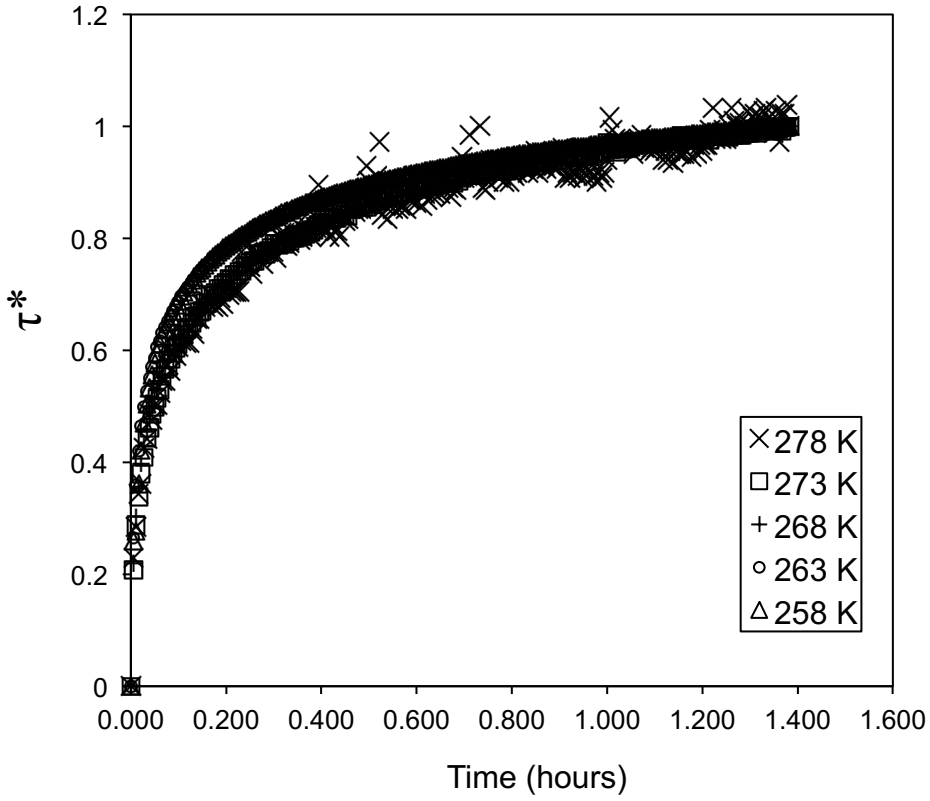

Figure 2-8. Normalized stress response, defined in equation 2-8, to a step-down in shear rate from 40 to 10 s^{-1} for Maya crude oil.

2.3.4 Start-up experiment results

The degree to which Maya oil structuring occurs during rest and the effect of structure on the subsequent flow behavior under stress is studied through start-up experiments. During these tests, a constant shear rate is imposed on the sample following a specific rest time. The change of shear stress over time is then monitored. Measurements were repeated for different values of rest time ranging from 5 minutes to 2 hours at fixed temperatures ranging from (258 to 278) K. The

results obtained from these experiments address the difficulties involved, for example, in heavy oil pipeline restart following a prolonged shutdown.

For the start-up experiments, Maya oil samples were loaded into the rheometer. The samples were first pre-sheared at 50 s^{-1} for 5 minutes, then let rest for a specified rest time, and finally a start-up shear rate equal to 30 s^{-1} was imposed. For 258 K, since the viscosity of Maya oil is high, a start-up shear rate of 10 s^{-1}, instead of 50 s^{-1}, was imposed on the sample in order to avoid exceeding the upper torque limit of the equipment. The pre-shear step was intended to mitigate the impact of differences in shear history of the samples on the results obtained. The shear stress values were measured during the start-up step. Illustrative results, obtained at 273 K, are shown in Figure 2-9. These results show how shear stress during start-up decays with time. Again from a microscopic perspective, the results illustrate how the structures that have had enough time to form during rest are broken down under shear, leading to stress decay over time.

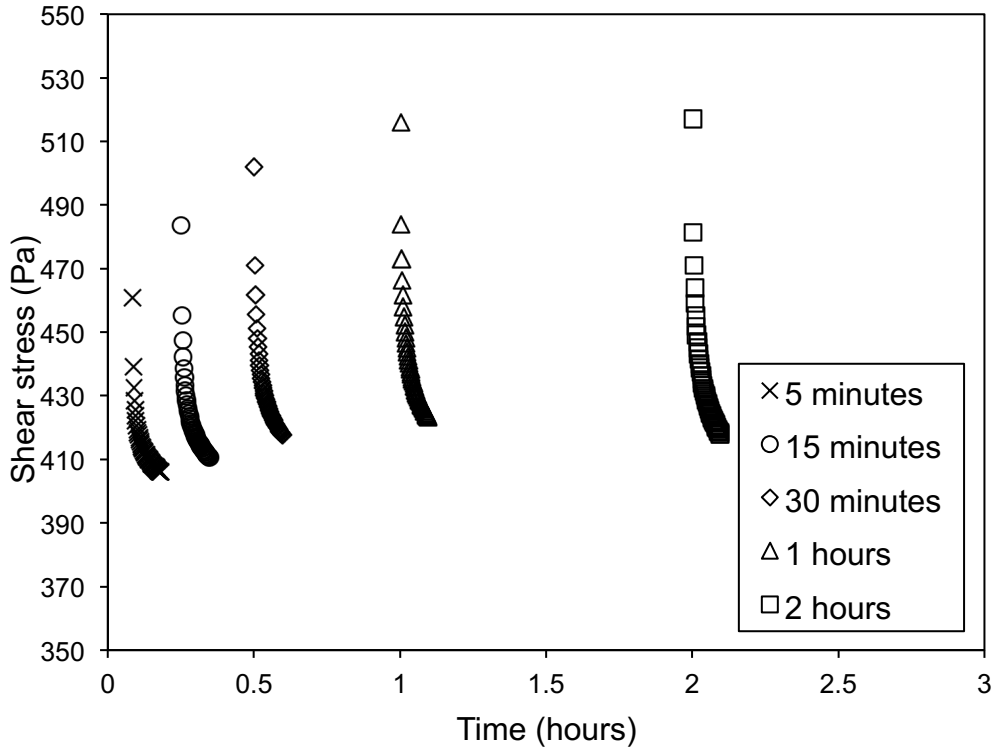

Figure 2-9. Transient shear stress arising during start-up experiment at 273 K, where a 30 s^{-1} shear rate is imposed on samples formerly at rest. Rest time prior to the start-up is a parameter. All samples were pre-sheared at 50 s^{-1} for 5 minutes.

In order to examine the relationship between rest time and stress value decay more closely for the entire data set, a parameter, $\Delta\tau$, called "stress decay" is introduced:

$$\Delta\tau = \tau_{max} - \tau_{min} \tag{2-9}$$

where τ_{max} is the overshoot stress and τ_{min} is the last stress value detected after imposing the start-up shear rate. Stress decay values are presented in Figure 2-10.

The results show the impact of rest time on stress decay values. Longer rest times lead to larger stress overshoots. Again, there is a linear relationship between stress decay and the logarithm of rest time. Hysteresis area, which showed the same behavior, and shear stress decay are functionally related. Neglecting the overshoot effect, during pipeline design, can lead to difficulties when dealing with pipeline restart, particularly at lower temperatures where a greater fraction of the maltenes become solid and can become structured.

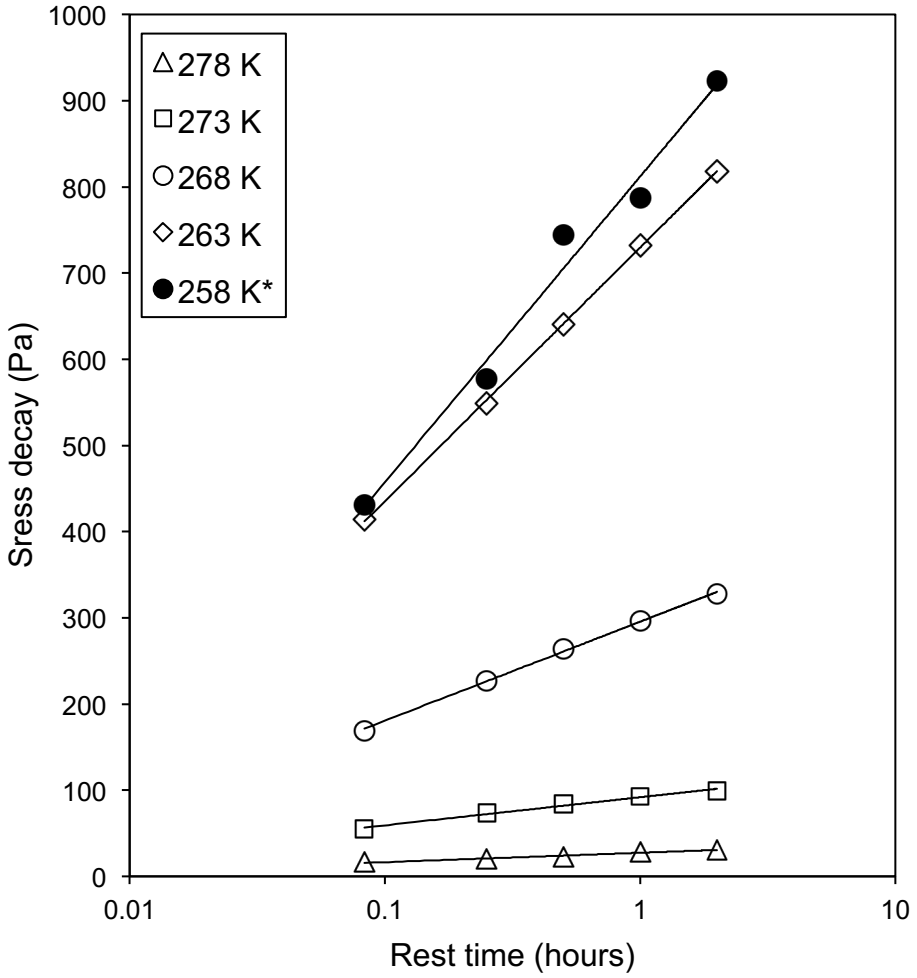

Figure 2-10. Effect of rest time on stress decay during start-up experiments, where a shear rate of 30 s^{-1} is imposed on samples formerly at rest. All samples were pre-sheared at 50 s^{-1} for 5 minutes. Temperature is a parameter. * For 258 K, since the viscosity of Maya oil is high, a start-up shear rate of 10 s^{-1} instead of 50 s^{-1} was imposed on the sample in order to avoid exceeding the upper torque limit of the equipment.

2.4 Conclusions

Thixotropic behaviors of Maya crude oil that lead to time and shear history dependent viscosities have been explored systematically. Maya crude oil exhibits

shear thinning behavior at temperatures lower than 313 K that is consistent with its phase behavior, reported previously, and is attributed to structural and hydrodynamic properties of the maltenes fraction. Viscoelastic effects were not observed. The lag between shear stress and shear rate, and the impact of rest time both underscore the impact of shear history on the rheological response of Maya crude oil and the interplay between shear history and phase behavior. These observations have industrial implications from crude oil production, to transport and refining. By neglecting the impact of shear history on laboratory measurements and the prediction of rheological properties in the field, poor operating practices or inadequate or inappropriate facility designs may arise. The data, correlations and master curve linked to the rheological responses of Maya crude oil provide a simple and general benchmark for rheological response measurement and model development for heavy oils as well as a better understanding of the physical phenomena underlying the rheology. The roles of temperature, rest time, and shear rate are clearly delineated, using well-defined and well-established experimental protocols. The impacts of these variables for example on pipeline restart are explored. The relationships identified between rest time and other thixotropic parameters may facilitate reconciliation of rheological data in the literature, and facilitate the development of minimal data sets required to determine the rheological properties of other heavy oils and bitumen.

2.5 References

1. Nellensteyn, F. J. The Colloidal Structure of Bitumen. PhD Thesis, Delft Technical University, Delft, The Netherlands, 1923.

2. Bazyleva, A. B.; Hasan, M. A.; Fulem, M.; Becerra, M.; Shaw, J. M., Bitumen and Heavy Oil Rheological Properties: Reconciliation with Viscosity Measurements. *J. Chem. Eng. Data* 2010, 55, 1389-1397.

3. Hasan, M. D. A.; Fulem, M.; Bazyleva, A.; Shaw, J. M., Rheological Properties of Nanofiltered Athabasca Bitumen and Maya Crude Oil. *Energy Fuels* 2009, 23, (10), 5012-5021.

4. Hasan, M. D. A.; Shaw, J. M., Rheology of Reconstituted Crude Oils: Artifacts and Asphaltenes. *Energy Fuels* 2010, 24, (12), 6417-6427.

5. Svrcek, W. Y.; Mehrotra, A. K., Gas Solubility, Viscosity and Density Measurements for Athabasca Bitumen. *J. Can. Pet. Technol.* 1982, 31-38.

6. Barrufet, M. A.; Setiadarma, A., Experimental Viscosities of Heavy Oil Mixtures up to 450 K and High Pressures using a Mercury Capillary Viscometer. *J. Pet. Sci. Eng.* 2003, 40, (1-2), 17-26.

7. Schramm, L. L. L.; Kwak, J. C. T., The Rheological Properties Of An Athabasca Bitumen And Some Bituminous Mixtures And Dispersions. *J. Can. Pet. Technol.* 1988, 27, (1).

8. Evdokimov, I. N.; Losev, A. P., Thixotropy in Native Petroleum Emulsions. *J. Dispersion Sci. Technol.* 2011, 32, (8), 1206-1212.

9. Jacobs, F. A.; Donnelly, J. K.; Stanislav, J., Viscosity of Gas-Saturated Bitumen. *J. Can. Pet. Technol.* 1980, 19, (4).

10. Khan, M. A. B.; Mehrotra, A. X.; Svrcek, W. Y., Viscosity Models For Gas-Free Athabasca Bitumen. *J. Can. Pet. Technol.* 1984, 23, (3).

11. Dealy, J. M., Rheological Properties of Oil Sand Bitumens. *Can. J. Chem. Eng.* 1979, 57, (6), 677-683.

12. Mehrotra, A. K.; Svrcek, W. Y., Viscosity, Density and Gas Solubility Data for Oil Sand Bitumens. Part I: Athabasca Bitumen Saturated with CO and C2H6. *AOSTRA J. Res.* 1985, 1, (4), 263-268.

13. Mehrotra, A. K.; Svrcek, W. Y., Viscosity of Compressed Athabasca Bitumen. *Can. J. Chem. Eng.* 1986, 64, (5), 844-847.

14. Bunger, J. W.; Thomas, K. P.; Dorrence, S. M., Compound Types and Properties of Utah and Athabasca Tar Sand Bitumens. *Fuel* 1979, 58, (3), 183-195.

15. Mewis, J.; Wagner, N. J., Thixotropy. *Adv. Colloid Interface Sci.* 2009, 147-148, 214-27.

16. Derksen, J. J., Agitation and Mobilization of Thixotropic Liquids. *AIChE J.* 2010, 2236-2247.

17. Derksen, J. J., Direct Flow Simulations of Thixotropic Liquids in Agitated Tanks. *Can. J. Chem. Eng.* 2011, 89, (4), 628-635.

18. Edwards, M. F.; Godfrey, J. C.; Kashani, M. M., Power Requirement for the Mixing of Thixotropic Liquids. *J. Non-Newtonian Fluid Mech.* 1976, 1, (4), 309-322.

19. Barnes, H. A., Thixotropy-a review. *J. Non-Newtonian Fluid Mech.* 1997, 70, 1-33.

20. Escudier, M. P.; Presti, F., Pipe Flow of a Thixotropic Liquid. *J. Non-Newtonian Fluid Mech.* 1996, 62, (2–3), 291-306.

21. Chang, C.; Nguyen, Q. D.; Rønningsen, H. P., Isothermal Start-up of Pipeline Transporting Waxy Crude Oil. *J. Non-Newtonian Fluid Mech.* 1999, 87, (2–3), 127-154.

22. Vinay, G.; Wachs, A.; Frigaard, I., Start-up Transients and Efficient Computation of Isothermal Waxy Crude Oil Flows. *J. Non-Newtonian Fluid Mech.* 2007, 143, (2–3), 141-156.

23. Negrão, C. O. R.; Franco, A. T.; Rocha, L. L. V., A Weakly Compressible Flow Model for the Restart of Thixotropic Drilling Fluids. *J. Non-Newtonian Fluid Mech.* 2011, 166, (23–24), 1369-1381.

24. Mewis, J., Thixotropy - a general review. *J. Non-Newtonian Fluid Mech.* 1979, 6, (1), 1-20.

25. de Souza Mendes, P. R., Modeling the Thixotropic Behavior of Structured Fluids. *J. Non-Newtonian Fluid Mech.* 2009, 164, (1–3), 66-75.

26. de Souza Mendes, P. R., Thixotropic Elasto-Viscoplastic Model for Structured Fluids. *Soft Matter* 2011, 7, (6), 2471-2483.

27. Dullaert, K.; Mewis, J., A Structural Kinetics Model for Thixotropy. *J. Non-Newtonian Fluid Mech.* 2006, 139, (1-2), 21-30.

28. Quemada, D., Rheological Modelling of Complex Fluids: IV: Thixotropic and "Thixoelastic" Behaviour. Start-up and Stress Relaxation, Creep Tests and Hysteresis Cycles. *Eur. Phys. J.: Appl. Phys.* 1999, 5, (02), 191-207.

29. Roussel, N.; Le Roy, R.; Coussot, P., Thixotropy Modelling at Local and Macroscopic Scales. *J. Non-Newtonian Fluid Mech.* 2004, 117, (2-3), 85-95.

30. Yziquel, F.; Carreau, P. J.; Moan, M.; Tanguy, P. A., Rheological Modeling of Concentrated Colloidal Suspensions. *J. Non-Newtonian Fluid Mech.* 1999, 86, (1–2), 133-155.

31. Dion, M. Modelling the Rheology of Complex Fluids: Cases of Bitumen and Heavy Oils at Low Temperatures. M.Sc. Thesis, University of Alberta, Edmonton, 2011.

32. Manriquez, L.; Moreno, A.; Tenorio, E. R.; Herrera, D., Guide to World Crudes: Four Mexican Crude Assays Updated. *Oil & Gas J.* 2000, 98, (20), 54-57.

33. Zhao, B.; Shaw, J. M., Composition and Size Distribution of Coherent Nanostructures in Athabasca Bitumen and Maya Crude Oil. *Energy Fuels* 2007, 21, 2795-2804.

34. http://www.cannoninstrument.com (Nov 14, 2013),

35. Heyer, P., Guidelines for the Pressure Cell. In Paar, A., Ed. 2007.

36. Fulem, M.; Becerra, M.; Hasan, M. D. A.; Zhao, B.; Shaw, J. M., Phase Behaviour of Maya Crude Oil Based on Calorimetry and Rheometry. *Fluid Phase Equilib.* 2008, 272, (1–2), 32-41.

37. Barnes, H. A.; Hutton, J. F.; Walters, K., *An Introduction to Rheology*. Elsevier Science Publishers: Amsterdam, Netherlands, 1993.

38. Green, H.; Weltmann, R., Analysis of Thixotropy of Pigment-Vehicle Suspensions - Basic Principles of the Hysteresis Loop. *Ind. Eng. Chem., Anal. Ed.* 1943, 15, (3), 201-206.

39. Magda, J. J.; El-Gendy, H.; Oh, K.; Deo, M. D.; Montesi, A.; Venkatesan, R., Time-Dependent Rheology of a Model Waxy Crude Oil with Relevance to Gelled Pipeline Restart. *Energy Fuels* 2009, 23, (3), 1311-1315.

Chapter 3 : Effect of Pressure on the Rheological Properties of Maya Crude Oil

3.1 Introduction

Heavy oil and bitumen reserves, which are found in many countries such as Canada and Venezuela, are comparable to global conventional oil resources assuming that 15% for heavy oil and bitumen, and 33% for conventional oil[1] can be produced. New exploitation and production techniques are making these heavier hydrocarbon reserves easier to exploit but their high viscosities and complex rheological properties, among other characteristics, present challenges for their production, transport, and processing. There is ongoing research on their transport properties, and more specifically on their rheological properties in order to facilitate the design, operation and optimization of production, transport, storage, blending, and refining processes. Rheological properties of heavy oil and bitumen are affected by composition, temperature and pressure as well as sample shear and thermal histories and shear conditions during measurements. While many researchers provide information about the viscosity of heavy oil and bitumen at different temperatures and/or pressures[2-7], most have not considered and have not reported sample shear histories and shear conditions prior to and during measurements. These temporal factors[8-11] affect the reported viscosity values for heavy hydrocarbon resources and consequently these resources must be categorized as non-Newtonian fluids. Ignoring their non-Newtonian behavior has

introduced unnecessary uncertainties in the "viscosity" data available in the literature. This is particularly evident at higher pressures[12-14]. There are a number of studies where heavy oil and bitumen viscosity is measured or correlated at higher pressures[3, 7, 15-19]. However, there are few reports that consider impacts of shear conditions during measurement and that also consider or provide sample shear history.

As described in Chapter 2, Maya crude oil is a thixotropic non-Newtonian fluid. Thixotropy, explained elsewhere in detail[20, 21], leads to time dependent apparent viscosities at fixed shear rate that arise from the breakage or growth of coherent structures within a fluid. Thixotropy can be responsible for order of magnitude changes in reported viscosity values. The impacts of thixotropic behavior are particularly evident during restart operations following flow disruption in a pipeline and during blending and mixing operations[22-24], and tend to become more significant at low temperatures[11]. While one can anticipate that the impact of increasing pressure is equivalent to the impact of decreasing temperature, there do not appear to be extant studies that report the effect of pressure on thixotropic properties of fluids, in general, or within the context of heavy oil and bitumen, in particular.

In this study, the effect of pressure on the rheological properties of Maya crude oil over a range of temperatures is investigated. Care is taken to avoid artifacts by adopting the same experimental procedure for all of the measurements, providing well-defined initial shear conditions and clear shear histories. The effect of pressure on the viscosity at constant temperature and shear rate as well as shear

rate dependence of the viscosity values at different pressures and at the same temperature are presented. The effect of the phase behavior of the maltene fraction of Maya crude oil on the onset of non-Newtonian behavior is discussed. Boundaries between the Newtonian and the non-Newtonian region with respect to temperature, pressure and viscosity are identified and the effect of pressure on the magnitude of non-Newtonian behavior is illustrated using a non-Newtonian Index. The way pressure affects thixotropic behavior of heavy oil is studied for the first time. These data are expected to provide a benchmark for heavy oil rheological model development and evaluation at higher pressures as well as a better understanding of the interrelation between rheological properties and the phase behavior of their constituting compounds such as asphaltenes and maltenes. This study is also expected to reduce the uncertainty of heavy oil and bitumen rheological properties reported in the literature through the provision of measurement protocols and identification of conditions where non-Newtonian effects are significant.

3.2 Experimental Section

3.2.1 Materials

Maya crude oil, a commercial heavy oil blend from Mexico supplied by Carlos Lira-Galena at the Mexican Petroleum Institute, was used in this study. Maya crude oil has a reported pour point of 243.15 K[25]. The elemental composition and the SARA analysis (saturates, aromatics, resins, and asphaltenes) of the Maya oil

sample and detailed information about methods used for these analyses have been reported previously[8, 26].

3.2.2 Rheological measurements

The rheometer used in this work is a stress-controlled high-pressure rheometer (Physica MCR 301 Anton Paar). Isothermal measurements were carried out from (258 to 333) K at pressures up to 150 bar. In this device, a magnetic coupling connected to the rheometer head transmits the motor movement to a measurement unit with a double-gap cylinder geometry inside the pressure cell. The measuring bob internal and external diameters are 21.03 and 23.04 mm respectively. The internal and external diameters of the measuring cup are 20.33 and 23.85 mm respectively. The amount of sample loaded for each test was 2.37 ml. The small size of this measurement unit minimizes the thickness of the fluid inside the cup, and hence minimizes effects associated with temperature gradients. The applied pressure within the pressure cell is imposed by nitrogen gas. A compressed liquid nitrogen bottle is connected to a line through a regulator. The line itself is connected to the rheometer through a valve and after passing through a pressure sensor (Anton Paar) it is connected to the pressure cell. The standard uncertainty of pressure is 0.01 bar. Sample temperature is measured with a Pt100 DIN/IEC 751 sensor with a resolution of 0.01 K and controlled with an accuracy of ±0.03 K. A peltier system (C-PTD200, Anton Paar), used for temperature control of the sample in the rheometer, has a temperature operating range from (243 to 472) K.

Viscosity measurement accuracy was examined at atmospheric pressure using Cannon certified viscosity standards, as shown in Table 3-1. The absolute relative deviations for these standards are less than 7.7 %. At higher pressures, previously reported viscosity values for di-isodecyl phthalate[27] were used as a reference. The absolute relative uncertainty between the current and previously published values, Table 3-2, is less than 3.5% at 100 bar.

Table 3-1. Deviations of measured viscosities from reported values for certified Newtonian viscosity standards at atmospheric pressure.

Standard	Reported viscosity of standard[28] (Pa.s)	Temperature (K)	$100\times(\eta_{reported}- \eta_{measured})/ \eta_{reported}$
Cannon S600	1.479	293	0.2
	1.056	298	0.1
	0.4335	313	-1.3
	0.2596	323	-1.4
Cannon RT500	0.5543	293	-0.5
	0.4992	298	-0.1
	0.3717	313	0.2
Cannon N18000	16.04	313	2.2
Cannon 1400B	168.6	260	-7.7
	151.3	261	-7.5
	136	262	-7.6

Table 3-2. Deviations of measured viscosities from reported values[27] for di-isodecyl phthalate at elevated pressures.

Temperature (K)	Pressure (bar)	Reported viscosity[27] (Pa.s)	$100\times(\eta_{reported}- \eta_{measured})/ \eta_{reported}$
298	2	0.0875	-2.6
298	101	0.11208	-3.5
305	2	0.05704	-2.8
313	2	0.03738	-2.8
313	101	0.04623	-2.4

The moment of inertia of the double-gap geometry was measured by the instrument at the beginning of each measurement and before loading the sample. The rheometer then performed a motor adjustment. The details of this step were reported previously[11]. The sample was then loaded into the double-gap geometry inside the pressure cell. Before applying pressure, the pressure cell was filled and then tightly sealed. A pressure was then imposed on the sample.

As described in Chapter 2, Maya oil is a thixotropic material. It is very important to provide a specific rest time and to pre-shear sub-samples prior to the main rheological measurement in order to make sure that all of the sub-samples have the same shear history and thus avoid ambiguity in the data. For each measurement, sub-samples were loaded into the rheometer and cooled to 268 K. The sub-samples then rested for 24 hours before a pressure was imposed. The

main test began after waiting for about 30 minutes at each pressure in order to avoid artifacts associated with bubbles formed within the Maya crude oil sample[29]. Since the solubility of nitrogen in heavy oil and bitumen is small[30, 31] and it takes hours at a shear rate of 100 s^{-1} to reach saturation[29], the solvation of nitrogen in Maya oil during the measurements performed in this study may be neglected.

All of the experiments were conducted in triplicate to confirm repeatability of the experiments. All of the data obtained are presented as tabulated supplemental data in Tables S7 to S9. These tables include standard uncertainties of the measurements. Summary Figures are presented and discussed below. In these Figures, the error bars are smaller than the data-points in most cases and are not added to the figurers for clarity.

3.3 Results and Discussion

3.3.1 Effect of pressure on viscosity

The pressure dependence of the viscosity of Maya crude oil sub-samples possessing the same shear history was explored over a range of temperatures and shear conditions. The results are presented in Figures 3-1 to 3-7 and are available in tabular form as supplemental material. From (258 to 333) K, linear shear rate ramps from (10 to 200) s^{-1} were imposed on Maya crude oil sub-samples and the steady shear stress values were measured. At lower temperatures, the shear rate domains were reduced to avoid the upper torque limit that the rheometer head can bear. All of the experiments were isothermal and isobaric at temperatures ranging

from (258 to 333) K and pressures ranging from atmospheric pressure to 150 bar. Prior to measurements, samples were pre-sheared for 5 minutes at a shear rate of 5 s^{-1} at 258 K, and at 40 s^{-1} at higher temperatures. Pre-shearing ensures that sub-samples share a common shear history. At each shear rate, sub-samples were sheared for 2 minutes prior to shear stress measurement. In this way, those parts of the structural network that are weak enough to break under the imposed shear rate have done so and the measured shear stress is a steady state value.

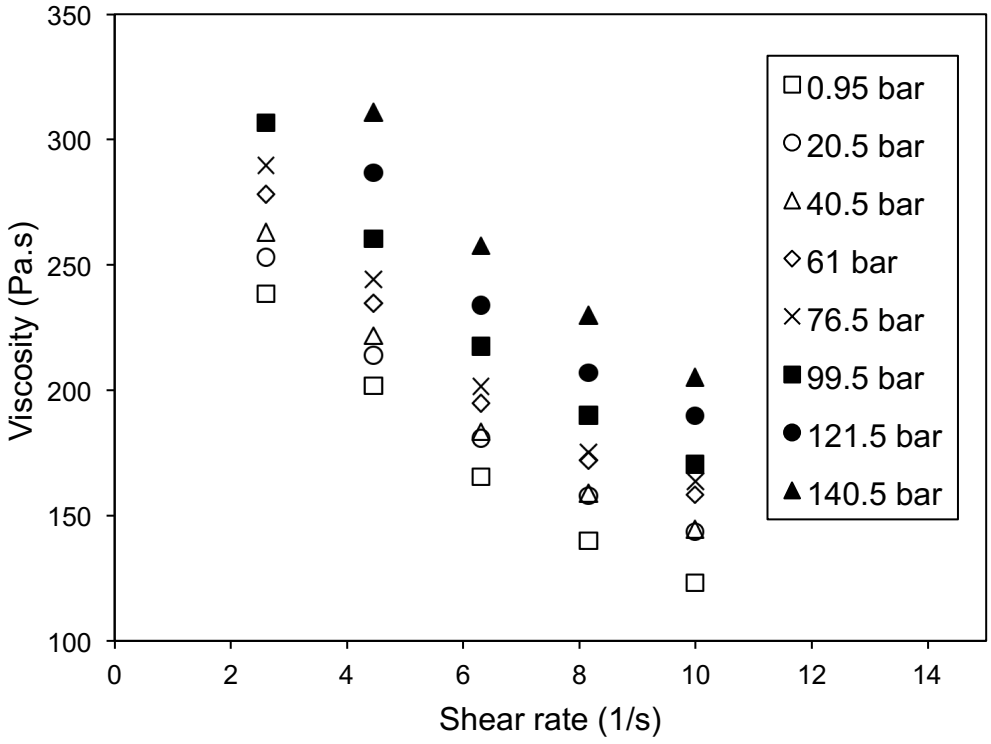

Figure 3-1. Flow curves for Maya crude oil at 258 K. Pressure is a parameter.

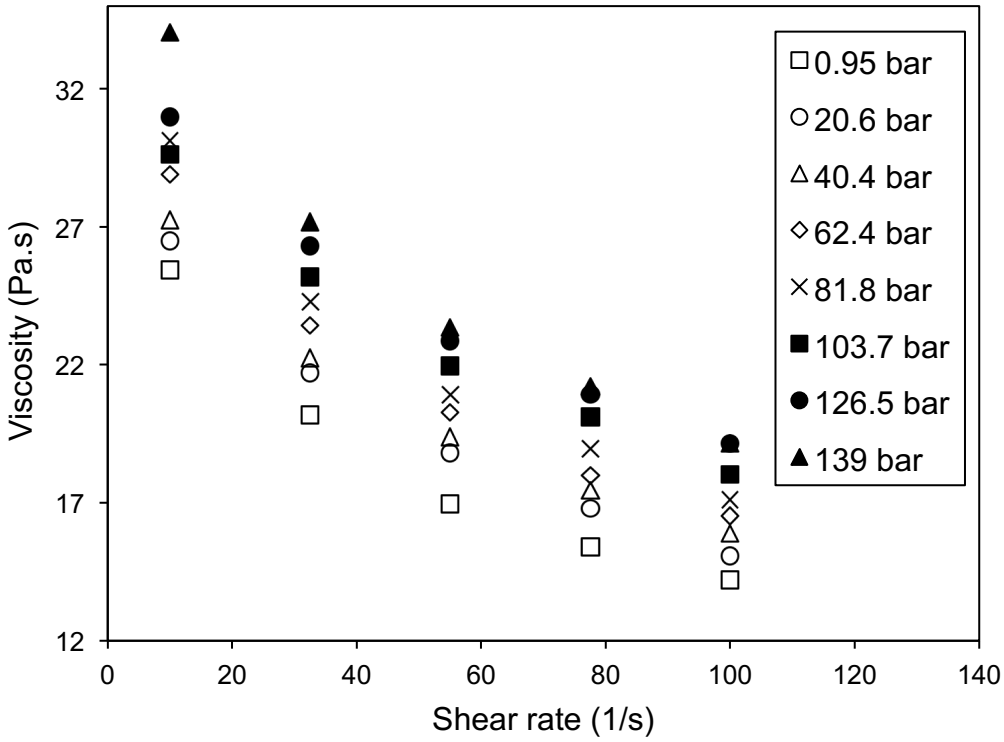

Figure 3-2. Flow curves for Maya crude oil at 268 K. Pressure is a parameter.

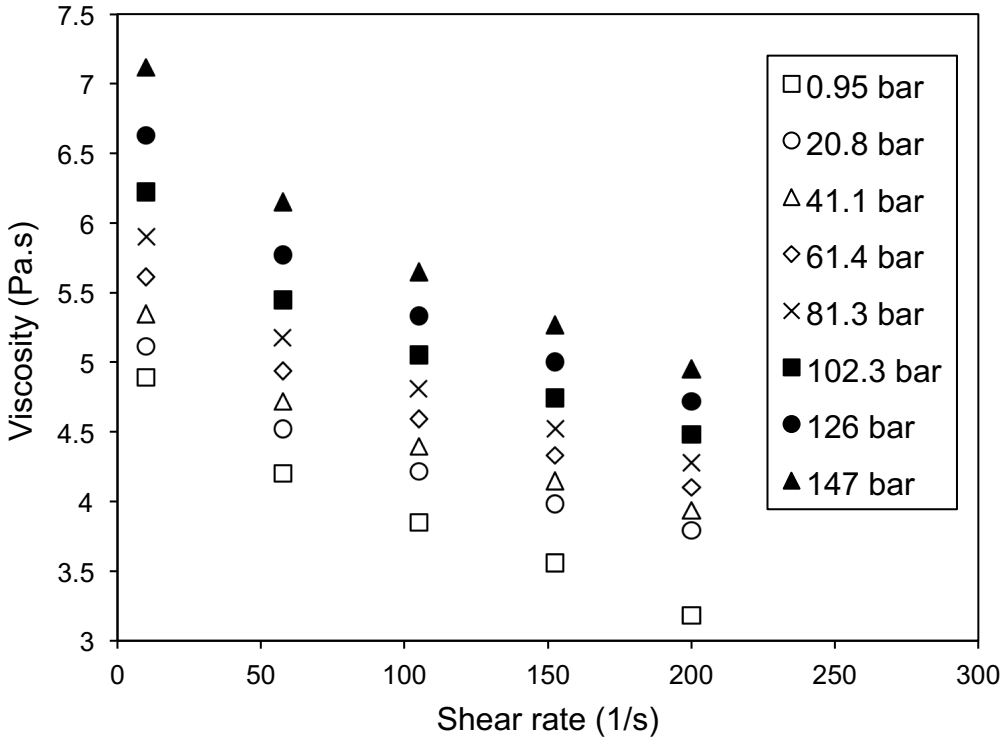

Figure 3-3. Flow curves for Maya crude oil at 278 K. Pressure is a parameter.

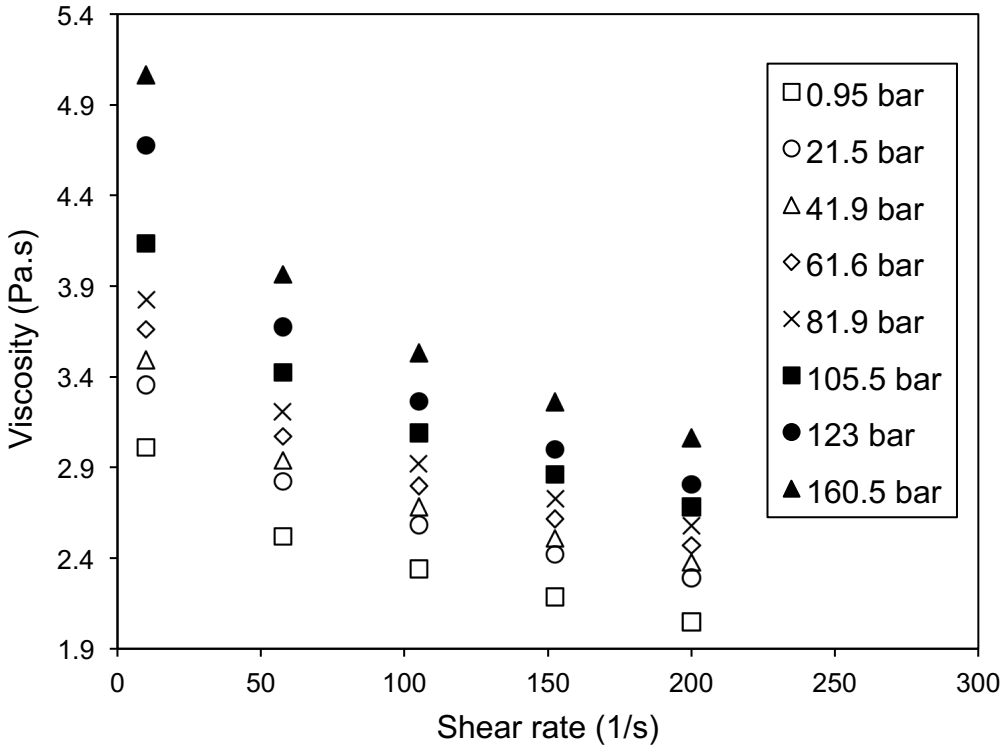

Figure 3-4. Flow curves for Maya crude oil at 283 K. Pressure is a parameter.

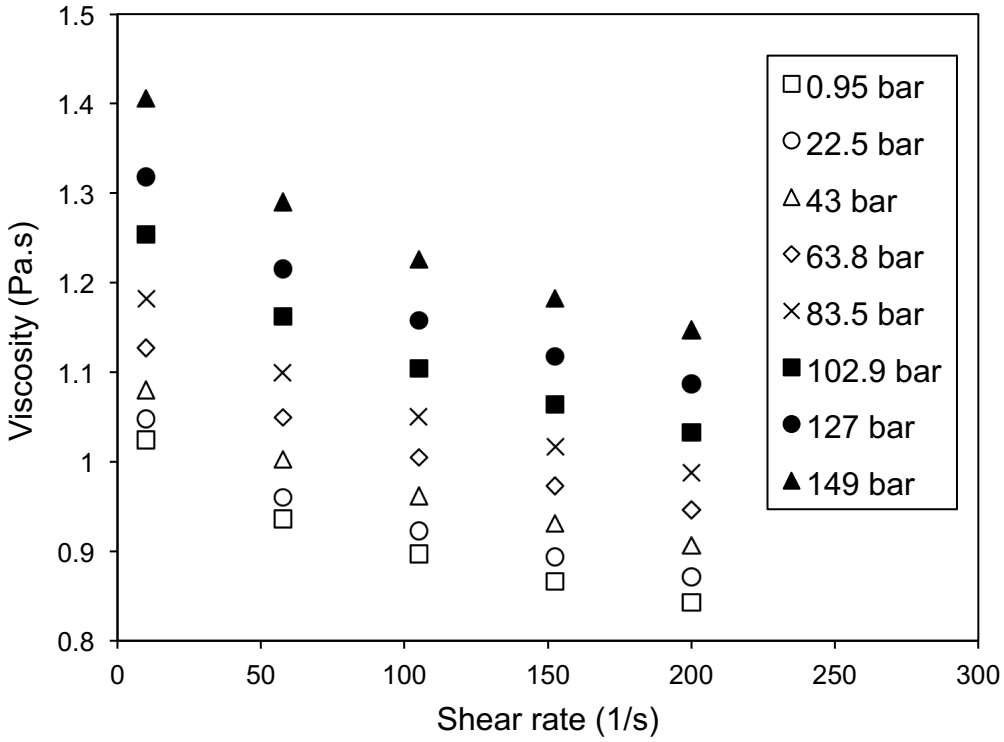

Figure 3-5. Flow curves for Maya crude oil at 293 K. Pressure is a parameter.

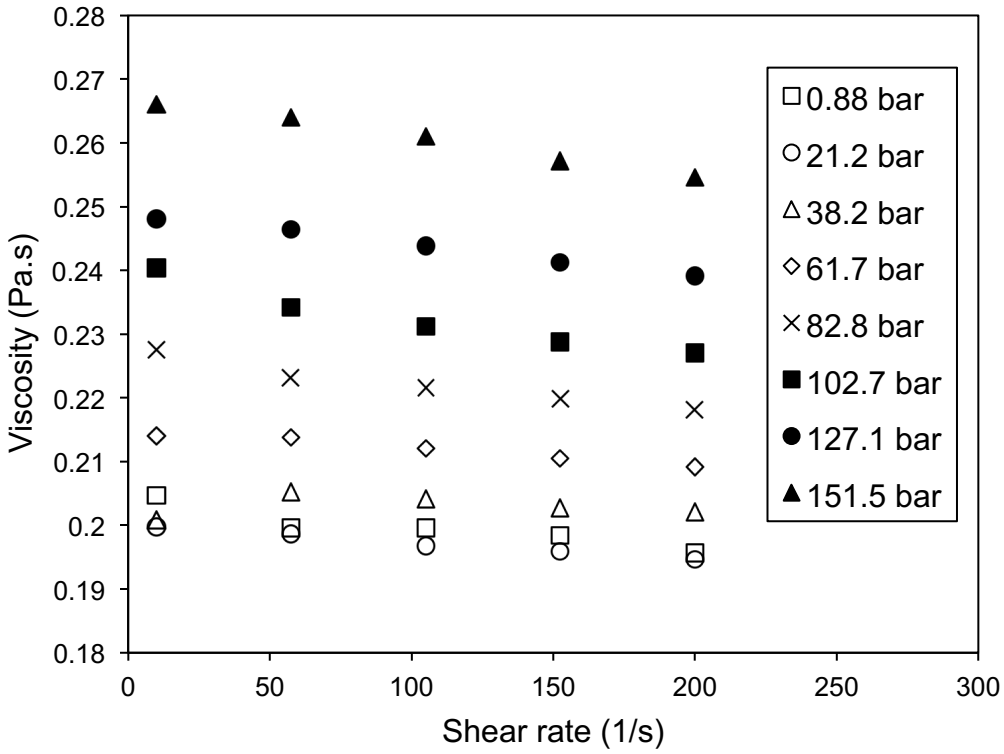

Figure 3-6. Flow curves for Maya crude oil at 313 K. Pressure is a parameter.

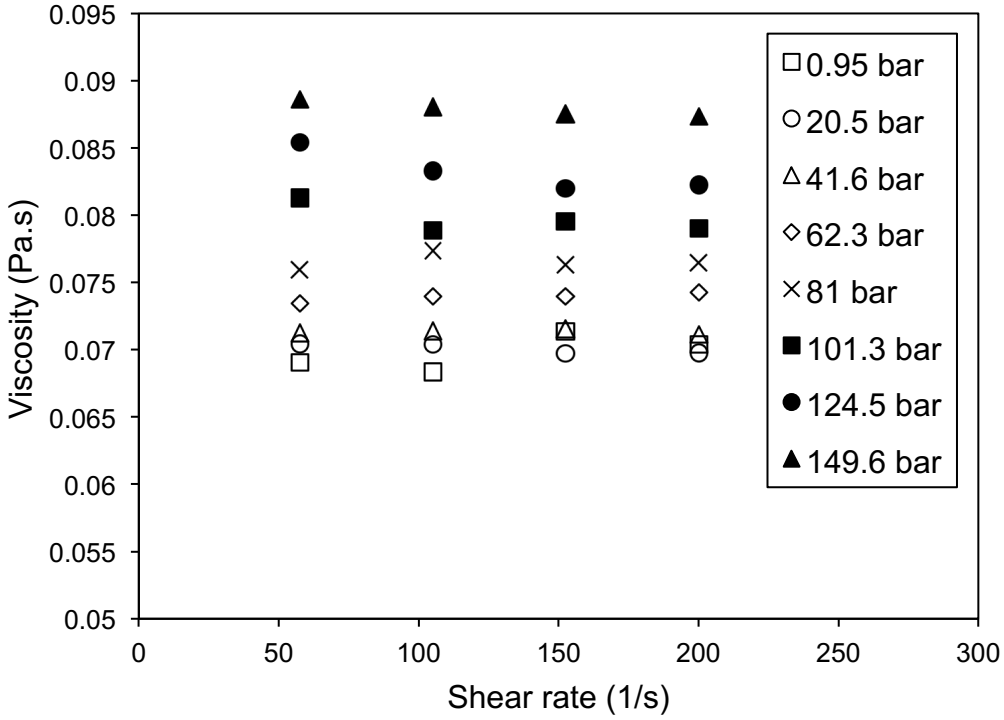

Figure 3-7. Flow curves for Maya crude oil at 333 K. Pressure is a parameter.

From Figures 3-1 to 3-7, it is clear that at fixed temperature and shear rate, viscosity increases with increasing pressure. Such a trend is expected because raising pressure is equivalent to and has an effect similar to decreasing temperature from a thermodynamic perspective and therefore one would expect that as viscosity increases with decreasing temperature, it would also increase with increasing pressure. Figures 3-8 a-g show the pressure dependence of viscosity at a constant temperature and shear rate. At each temperature, shear rate does not appear to affect the pressure dependence of viscosity significantly. The

data can easily be fit by using a shear rate dependent base value and a pressure dependent parameter that is independent of shear rate.

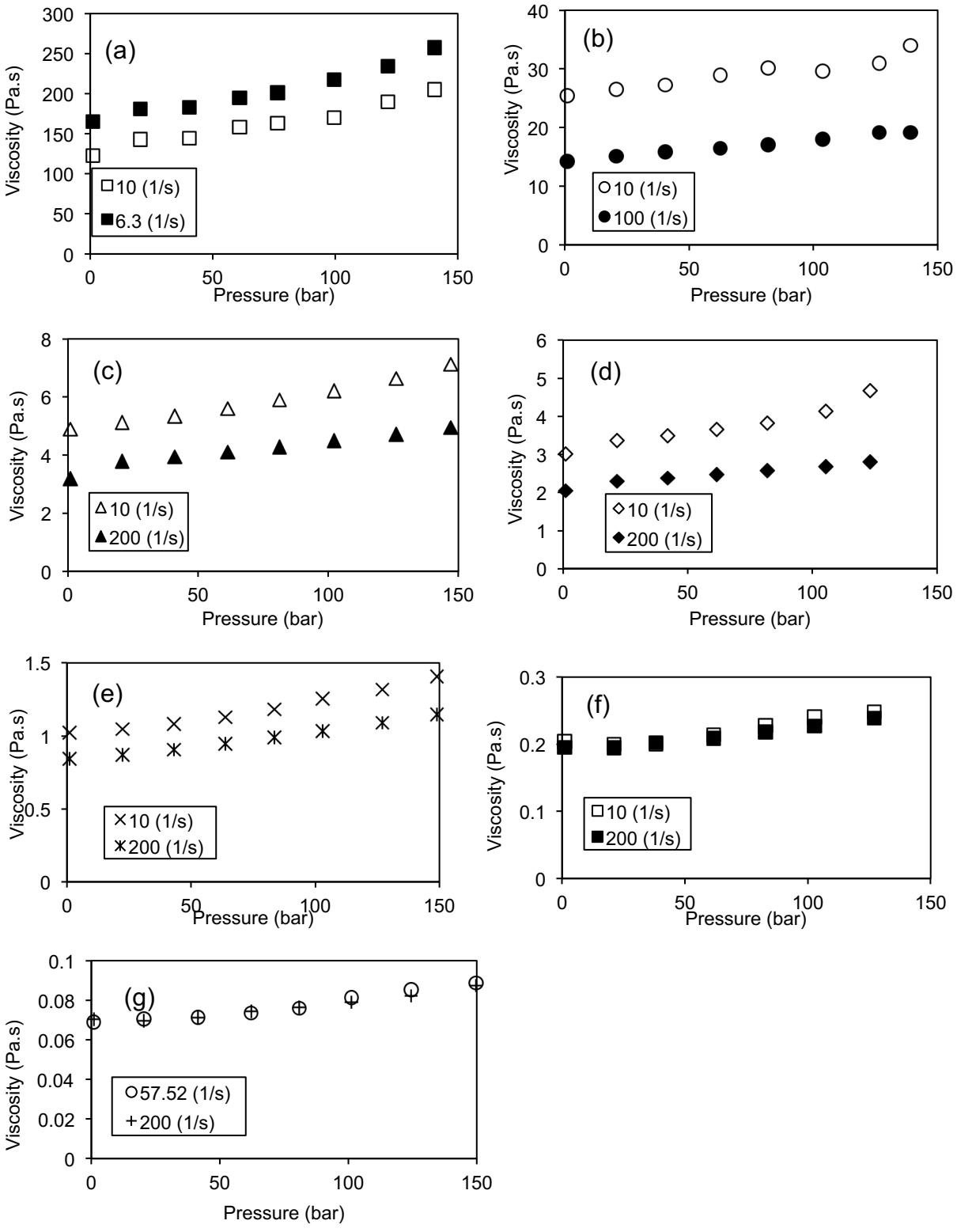

Figure 3-8. Pressure dependence of the viscosity of Maya crude oil: (a) 258 K, (b) 268 K, (c) 278 K, (d) 283 K, (e) 293 K, (f) 313 K, (g) 333 K. Shear rate is a parameter.

Pressure dependency of the apparent viscosity at constant shear rate can be correlated based on Barus equation[32]:

$$\eta_P = \eta_{P_R} \exp(\beta \Delta P) \tag{3-1}$$

where η_P and η_{P_R} is the viscosity at pressure P and reference pressure P_R, respectively. β is the pressure effectiveness constant in bar. It was shown that β has an Arrhenius relationship with temperature[33]. This kind of temperature relationship is also observed in this study, which can be shown as:

$$\beta = a1.e^{\left(\frac{a2}{RT}\right)} \tag{3-2}$$

where T is the temperature in K, *a1* and *a2* are the model parameters and R is the universal gas constant in J/(mol.K). By correlating the experimental data obtained for Maya crude oil in this study at shear rate of 10 s^{-1}, the values of *a1* and *a2* were obtained as 4.239e-5 and 9491.47, respectively. The results are shown in Figure 3-9.

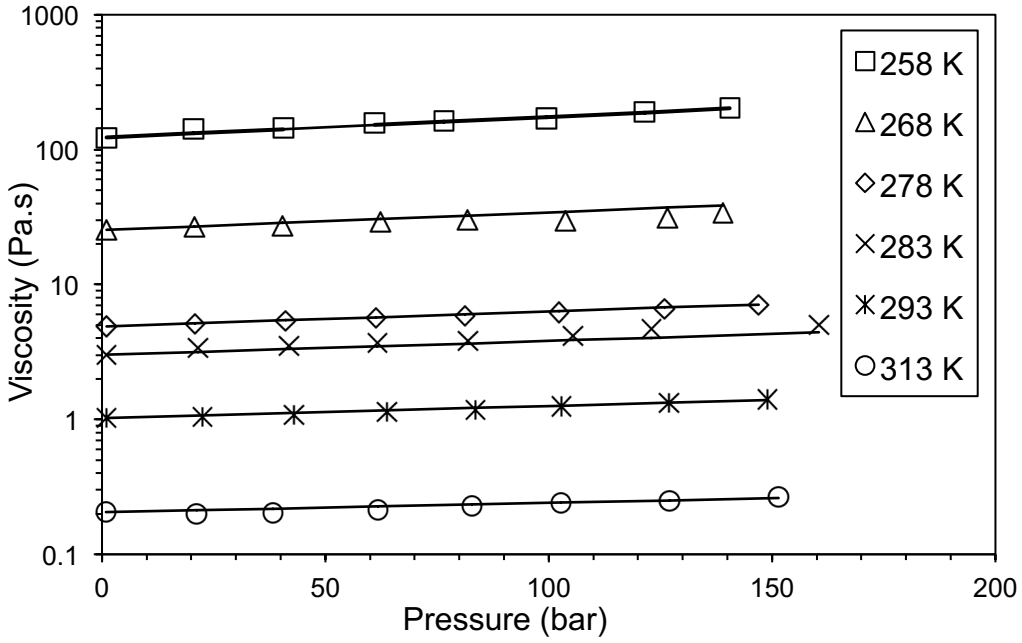

Figure 3-9. Pressure dependence of the viscosity of Maya crude oil at shear rate of 10 s^{-1}. The line represents correlation based on the Barus equation.

3.3.2 Equivalence of pressure and temperature at fixed shear rate

For viscosity values (η) at a reference temperature (T_{ref}) and pressure (P) a temperature (T) at atmospheric pressure (P_{atm}), which has the same viscosity (η) at the same shear rate can be identified. This equivalence of the impact of pressure and temperature, for values of T_{ref} ranging from 258 to 313 K, is presented in Figure 3-10. The overall impact of pressure is weak. Increasing pressure from 1 to 100 bar is equivalent to decreasing temperature by 2 +/- 1 K.

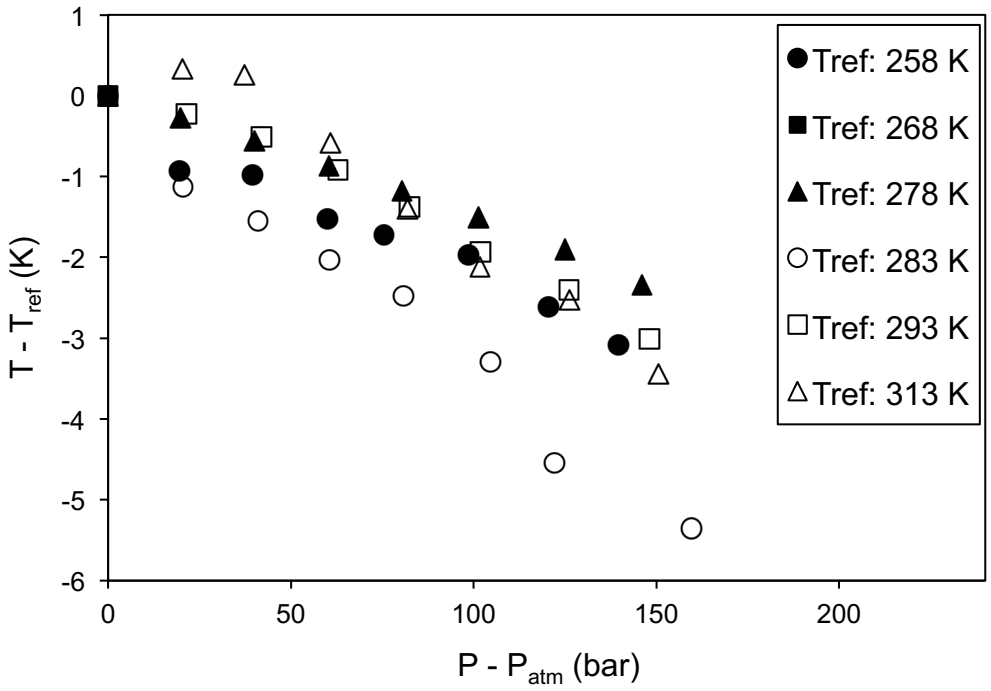

Figure 3-10. Comparison between the equivalent effects of pressure and temperature. Shear rate is 10 s^{-1}.

3.3.3 Quantification of non-Newtonian behavior at steady shear state

It is extremely important to evaluate the shear rate dependence of the viscosity of Maya oil as a function of pressure. This phenomenon is neglected in the literature. From Figures 3-1 through 3-8, Maya oil clearly exhibits shear thinning behavior at temperatures lower than 313 K. A remarkable result that can be achieved from these measurements is that shear thinning behavior persists to higher pressures at temperatures below 313 K. Further, shear thinning is shown to persist and appears to become more important at elevated pressures at temperatures below 313 K. As discussed in detail in Chapter 2, shear thinning

behavior of Maya oil may in part be attributable to structural and hydrodynamic properties of solid maltenes. Solid maltenes are not present in Maya oil at temperature higher than 320 K[34]. Observation of shear thinning behavior at elevated pressures may be an indication of the consistent structural and hydrodynamic roles of solid maltenes towards establishment of shear thinning properties in Maya crude oil up to high pressures, considering that transition to Newtonian behavior occurs at the same temperature at elevated pressures as at atmospheric pressure, namely 313 K.

In order to quantify the impact of pressure on the magnitude of the non-Newtonian behavior at a constant temperature, a new non-Newtonian index (NN-Index), is defined as:

$$\text{NN-Index} = \frac{\sqrt{\sum_{i=1}^{n}\left(\frac{\eta_i-\eta_{ref}}{\dot{\gamma}_i-\dot{\gamma}_{ref}}\right)^2}}{n} \tag{3-3}$$

where n is the number of data points at a fixed temperature and a fixed pressure, Σ is a summation over all of the data points at that particular temperature and pressure, η_i is the viscosity at data point number *i*, $\dot{\gamma}_i$ is the shear rate at data point number *i*, subscript *ref* refers to a reference data point which is chosen to be the data point with the minimum value of shear rate at that particular temperature and pressure. NN-Index values were calculated at each temperature and pressure and the results are presented in Figures 3-11 a-g. The magnitude of the non-Newtonian behavior index increases with increasing the pressure, at fixed temperature, and at fixed pressure with decreasing temperature. This result is

important in terms of the effect of pressure on the flow properties of Maya oil since it implies that high pressures not only lead to higher viscosities, a known phenomenon, but that high pressures also lead to more significant non-Newtonian behaviors which need to be addressed in engineering calculations. At 313 K and higher temperatures, Maya oil is Newtonian and NN-Index values approach zero.

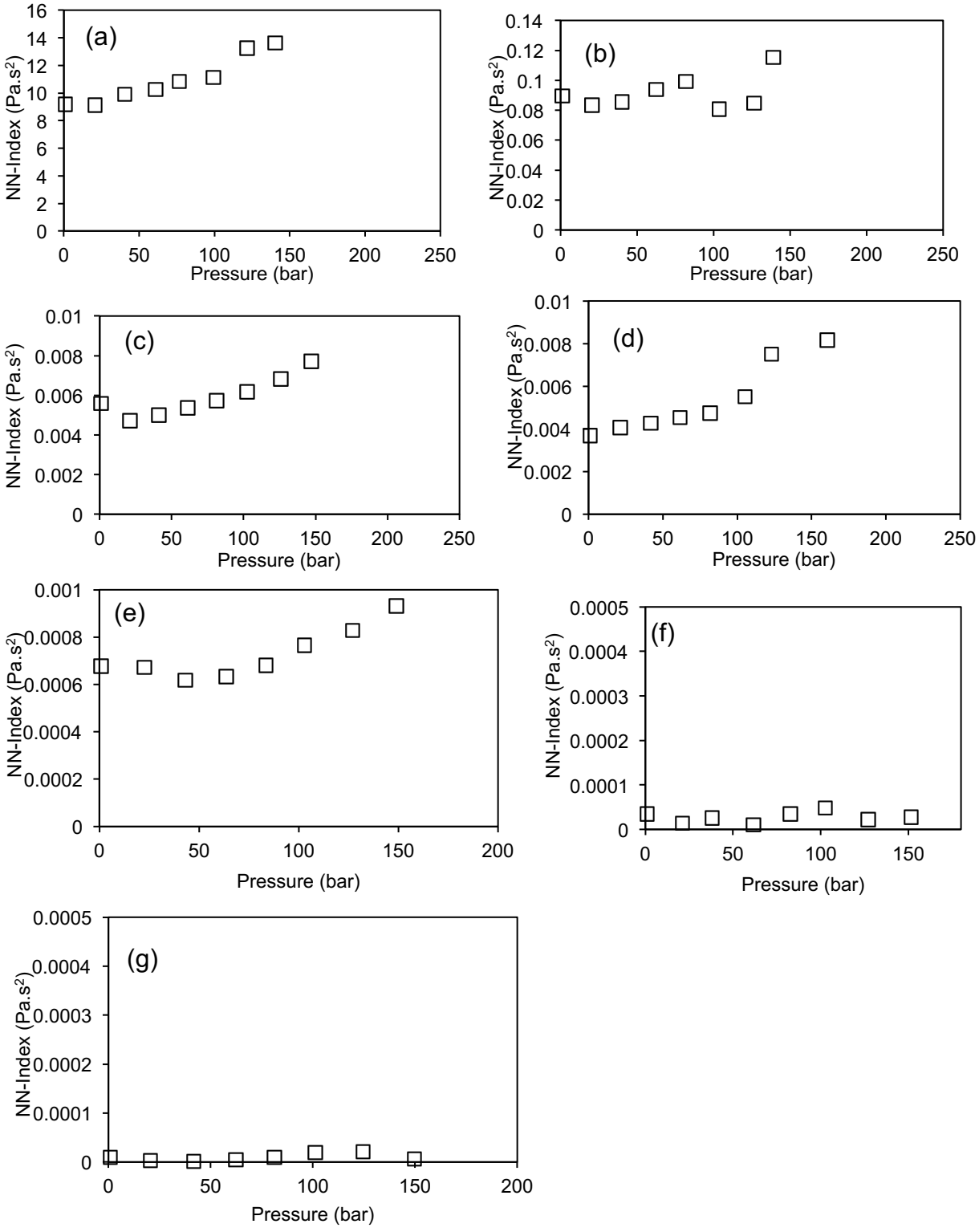

Figure 3-11. Pressure dependence of the non-Newtonian index (NN-Index): (a) 258 K, (b) 268 K, (c) 278 K, (d) 283 K, (e) 293 K, (f) 313 K, (g) 333 K.

3.3.4 Thixotropic behavior

Thixotropic behavior, which is usually explored through transient stress techniques such as hysteresis loop techniques, step-down changes in shear rate or start-up experiments, provides information about the effect of time on the microstructures within a material that impact flow properties and conversely on the impact of flow (hydrodynamic forces) on time dependence of microstructures. In thixotropic materials, any shear rate experience leaves a footprint that then appears as a structure rebuilding process occurring during periods where the fluid is at rest. In order to capture this rebuilding process experimentally and as closely as possible to a rest condition, a few studies have applied Small Amplitude Oscillatory Shear (SAOS) methods[35-38]. The advantage of Small Amplitude Oscillatory experiments over steady shear tests is that during SAOS experiments very small deformations are applied to samples and therefore interference with the rebuilding structures within the material is minimized, providing an environment which is more likely to be considered meaningfully as a "*rest condition*". The storage modulus, which is measured during SAOS experiments at a fixed low frequency, can be representative of the level of microstructure[39].

During an SAOS experiment, the shear strain, γ imposed on the sample changes sinusoidally with time, *t*:

$$\gamma = \gamma_A \sin \omega t \tag{3-4}$$

where γ_A and ω are the amplitude and frequency of the applied sinusoidal shear strain, respectively. For a viscoelastic fluid, the resulting shear stress, τ, changes sinusoidally with time:

$$\tau = \tau_A \sin(\omega t + \delta) \tag{3-5}$$

where τ_A is the amplitude of the stress and δ is the phase angle between stress and strain. The storage (G') and loss (G'') moduli are defined as[40]:

$$G' = \frac{\tau_A}{\gamma_A} \cos\delta \tag{3-6}$$

$$G'' = \frac{\tau_A}{\gamma_A} \sin\delta \tag{3-7}$$

The way pressure affects thixotropic behavior has essentially been ignored in the literature. The results presented here provide basic understanding about the effect of pressure on thixotropic properties that extends beyond the present example, Maya oil.

The effect of pressure on the recovery of structures within Maya oil at rest after being subject to a constant steady shear rate at 0.95 bar and 54.4 bar at 268 K exemplifies the role of pressure. The same procedure was followed for both experiments. In the first step, a high steady shear rate, 50 s^{-1}, was imposed on the Maya oil sample for 10 minutes to breakdown the structures within the sample. In the second step, which immediately followed the first step, the steady shear rate was eliminated and the recovery of the storage (G') and loss (G'') moduli were measured using SAOS experiment (shear strain of 1%, angular frequency of 10 rad/s). Figure 3-12 shows how the storage and loss moduli rebuild over time at atmospheric pressure and at 54.4 bar, meaning that thixotropy persists to higher

pressures. Both moduli rebuild more quickly and to higher values at the higher pressure. Increasing pressure speeds up the rebuilding process of microstructure in Maya oil. It is worth noting that in both experiments, at the beginning of the second step the storage modulus has decreased to values below the values of the loss modulus as a result of the imposition of a steady shear rate. This implies that the structures within the material have been broken down. During the course of the oscillatory experiment, which simulates the rest condition, these structures rebuild. Both moduli increase but especially the storage modulus. Consequently, at each pressure, the storage modulus reaches and then exceeds the loss modulus as both moduli approach their respective asymptotic values. Again, the kinetics of this aspect of moduli growth increases with pressure.

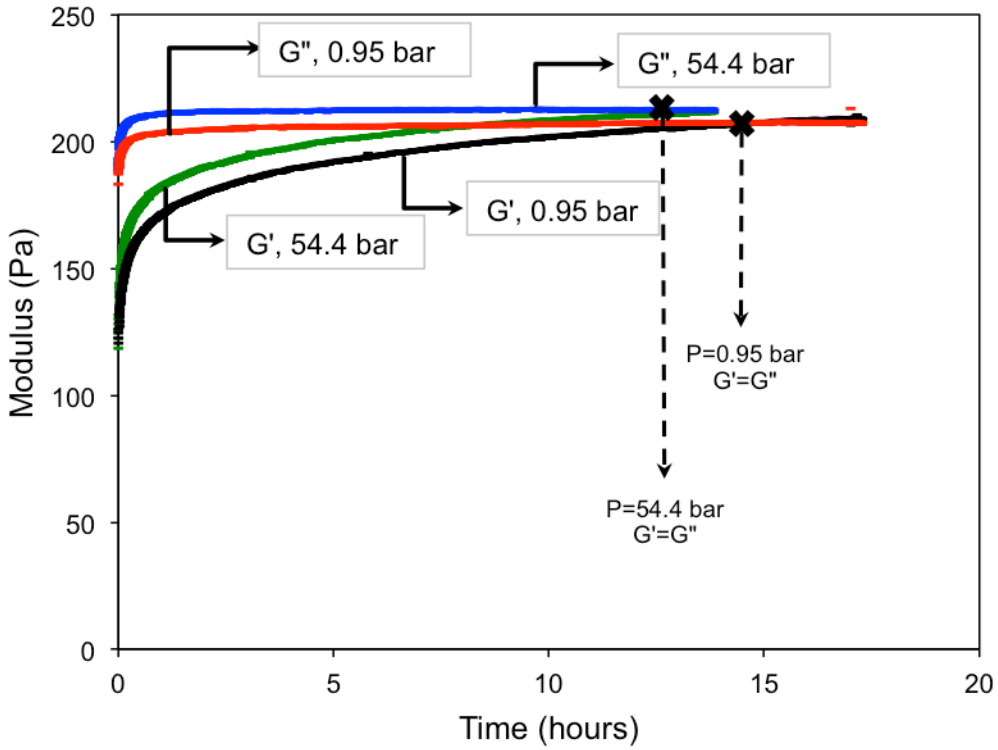

Figure 3-12. Thixotropic behavior explored by observation of recovery of moduli measured through oscillatory experiment (strain of 1%, angular frequency of 10 rad/s) following imposing a shear rate equal to 50 s^{-1} on Maya crude oil at 268 K.

3.4 Conclusions

The impacts of pressure on the viscosity of Maya crude oil were investigated. At fixed shear rate, the anticipated increase in viscosity with pressure was observed and the equivalence of the impact of temperature and pressure, two linked thermodynamic properties, was quantified. The non-Newtonian shear thinning behavior of Maya oil at temperatures lower than 313 K, previously attributed to structural and hydrodynamic properties of solid maltenes, was shown to persist at elevated pressure. Development and use of a non-Newtonian Index

revealed that high pressures not only lead to higher viscosities but they may also lead to more significant non-Newtonian behavior which must be addressed for adequate and reliable rheological property correlation, or industrial facility designs. Transient thixotropic effects, identified through small amplitude oscillatory shear measurements, reveal that thixotropy not only persists to higher pressures in Maya crude oil but that the recovery of the storage and loss moduli is faster at higher pressures than at lower pressures. Pressure accelerates the rebuilding of microstructures within Maya oil. Thus, processes operating at high pressure are more vulnerable kinetically to the impacts of thixotropy than low pressure processes during start up or restart.

3.5 References

1. FarouqAli, S. M., Heavy Oil—Evermore Mobile. *J. Pet. Sci. Eng.* 2003, 37, (1–2), 5-9.
2. Svrcek, W. Y.; Mehrotra, A. K., Gas Solubility, Viscosity and Density Measurements for Athabasca Bitumen. *J. Can. Pet. Technol.* 1982, 31-38.
3. Barrufet, M. A.; Setiadarma, A., Experimental Viscosities of Heavy Oil Mixtures up to 450 K and High Pressures using a Mercury Capillary Viscometer. *J. Pet. Sci. Eng.* 2003, 40, (1-2), 17-26.
4. Schramm, L. L. L.; Kwak, J. C. T., The Rheological Properties Of An Athabasca Bitumen And Some Bituminous Mixtures And Dispersions. *J. Can. Pet. Technol.* 1988, 27, (1).
5. Mehrotra, A. K.; Svrcek, W. Y., Viscosity, Density and Gas Solubility Data for Oil Sand Bitumens. Part I: Athabasca Bitumen Saturated with CO and C2H6. *AOSTRA J. Res.* 1985, 1, (4), 263-268.

6. A.Yazdani; Maini, B. B., Measurements and Modelling of Phase Behaviour and Viscosity of a Heavy Oil/Butane System. *J. Can. Pet. Technol.* 2010, (02), 9-14.

7. Guan, J. G.; Kariznovi, M.; Nourozieh, H.; Abedi, J., Density and Viscosity for Mixtures of Athabasca Bitumen and Aromatic Solvents. *J. Chem. Eng. Data* 2013, 58, (3), 611-624.

8. Bazyleva, A. B.; Hasan, M. A.; Fulem, M.; Becerra, M.; Shaw, J. M., Bitumen and Heavy Oil Rheological Properties: Reconciliation with Viscosity Measurements. *J. Chem. Eng. Data* 2010, 55, 1389-1397.

9. Hasan, M. D. A.; Fulem, M.; Bazyleva, A.; Shaw, J. M., Rheological Properties of Nanofiltered Athabasca Bitumen and Maya Crude Oil. *Energy Fuels* 2009, 23, (10), 5012-5021.

10. Evdokimov, I. N.; Losev, A. P., Thixotropy in Native Petroleum Emulsions. *J. Dispersion Sci. Technol.* 2011, 32, (8), 1206-1212.

11. Mortazavi-Manesh, S.; Shaw, J. M., Thixotropic Rheological Behavior of Maya Crude Oil. *Energy Fuels* 2014, 28, 972-979.

12. Novak, J. D.; Winer, W. O., The Effect of Pressure on the Non-Newtonian Behavior of Polymer Blended Petroleum Oils. *J. Lubr. Technol.* 1969, 91, (3), 459-462.

13. Hirst, W.; Moore, A. J., Elastohydrodynamic Lubrication at High Pressures. II. Non-Newtonian Behaviour. *Proceedings of the Royal Society of London. Series A, Mathematical and Physical Sciences* 1979, 365, (1723), 537-565.

14. Kioupis, L. I.; Maginn, E. J., Impact of Molecular Architecture on the High-Pressure Rheology of Hydrocarbon Fluids. *The Journal of Physical Chemistry B* 2000, 104, (32), 7774-7783.

15. Puttagunata, V. R.; Singh, B.; Miadonye, A., Correlation of Bitumen Viscosity with Temperature and Pressure. *The Canadian Journal of Chemical Engineering* 1993, 71, (3), 447-450.

16. Mehrotra, A. K.; Svrcek, W. Y., Viscosity of Compressed Athabasca Bitumen. *Can. J. Chem. Eng.* 1986, 64, (5), 844-847.

17. Mehrotra, A. K.; Svrcek, W. Y., Viscosity of Compressed Cold Lake Bitumen. *The Canadian Journal of Chemical Engineering* 1987, 65, (4), 672-675.

18. Khan, M. A. B.; Mehrotra, A. X.; Svrcek, W. Y., Viscosity Models For Gas-Free Athabasca Bitumen. *J. Can. Pet. Technol.* 1984, 23, (3).

19. Johnson, S. E.; Svrcek, W. Y.; Mehrotra, A. K., Viscosity Prediction of Athabasca Bitumen Using the Extended Principle of Corresponding States. *Industrial & Engineering Chemistry Research* 1987, 26, (11), 2290-2298.

20. Mewis, J., Thixotropy - a general review. *J. Non-Newtonian Fluid Mech.* 1979, 6, (1), 1-20.

21. Mewis, J.; Wagner, N. J., Thixotropy. *Adv. Colloid Interface Sci.* 2009, 147-148, 214-27.

22. Derksen, J. J., Agitation and Mobilization of Thixotropic Liquids. *AIChE J.* 2010, 2236-2247.

23. Derksen, J. J., Direct Flow Simulations of Thixotropic Liquids in Agitated Tanks. *Can. J. Chem. Eng.* 2011, 89, (4), 628-635.

24. Edwards, M. F.; Godfrey, J. C.; Kashani, M. M., Power Requirement for the Mixing of Thixotropic Liquids. *J. Non-Newtonian Fluid Mech.* 1976, 1, (4), 309-322.

25. Manriquez, L.; Moreno, A.; Tenorio, E. R.; Herrera, D., Guide to World Crudes: Four Mexican Crude Assays Updated. *Oil & Gas J.* 2000, 98, (20), 54-57.

26. Zhao, B.; Shaw, J. M., Composition and Size Distribution of Coherent Nanostructures in Athabasca Bitumen and Maya Crude Oil. *Energy Fuels* 2007, 21, 2795-2804.

27. Peleties, F.; Trusler, J. P. M., Viscosity of Liquid Di-isodecyl Phthalate at Temperatures Between (274 and 373) K and at Pressures up to 140 MPa. *J. Chem. Eng. Data* 2011, 56, (5), 2236-2241.

28. Cannon Instrument Company. http://www.cannoninstrument.com (Aug 1, 2014),

29. Abivin, P.; Henaut, I.; Argillier, J.-F.; Moan, M., Rheological Behavior of Foamy Oils. *Energy Fuels* 2008, 23, (3), 1316-1322.

30. Mehrotra, A. K.; Svrcek, W. Y., Viscosity, Density and Gas Solubility Data for Oil Sand Bitumens. Part II: Peace River Bitumen Saturated with N2, CO, CH4, CO2 and C2H6. *AOSTRA J. Res.* 1985, 1, (4), 269-279.

31. Mehrotra, A. K.; Svrcek, W. Y., Viscosity, Density and Gas Solubility Data for Oil Sand Bitumens. Part III: Wabasca Bitumen Saturated with N2, CO, CH4, CO2 and C2H6. *AOSTRA J. Res.* 1985, 2, (2), 83-93.

32. Barus, S., Isothermals, Isopiestics, and Isometrics Relatives to Viscosity. . *American Journal of Science* 1893, 45, 87-96.

33. Behzadfar, E.; Hatzikiriakos, S. G., Rheology of bitumen: Effects of temperature, pressure, CO2 concentration and shear rate. *Fuel* 2014, 116, (0), 578-587.

34. Fulem, M.; Becerra, M.; Hasan, M. D. A.; Zhao, B.; Shaw, J. M., Phase Behaviour of Maya Crude Oil Based on Calorimetry and Rheometry. *Fluid Phase Equilib.* 2008, 272, (1–2), 32-41.

35. Aerschot, E. V. d. Reologie van Reversiebel Geflocculeerde Dispersies PhD, Katholieke Universiteit Leuven, 1989.

36. Manley, S.; Davidovitch, B.; Davies, N. R.; Cipelletti, L.; Bailey, A. E.; Christianson, R. J.; Gasser, U.; Prasad, V.; Segre, P. N.; Doherty, M. P.; Sankaran, S.; Jankovsky, A. L.; Shiley, B.; Bowen, J.; Eggers, J.; Kurta, C.; Lorik, T.; Weitz, D. A., Time-Dependent Strength of Colloidal Gels. *Physical Review Letters* 2005, 95, (4), 048302.

37. Willenbacher, N., Unusual Thixotropic Properties of Aqueous Dispersions of Laponite RD. *Journal of Colloid and Interface Science* 1996, 182, (2), 501-510.

38. Mewis, J.; Spaull, A. J. B.; Helsen, J., Structural Hysteresis. *Nature* 1975, 253, (5493), 618-619.

39. Mewis, J.; Wagner, N. J., *Colloidal Suspension Rheology*. Cambridge University Press: New York, 2012.

40. Chhabra, R. P., Rheology of Complex Fluids, Chapter 1: Non-Newtonian Fluids. In Springer: New York, 2010.

Chapter 4 : Effect of Diluents on the Rheological Properties of Maya Crude Oil

4.1 Introduction

As conventional oil and gas reservoirs become depleted, other unconventional hydrocarbon sources are being exploited and produced, such as heavy oil and oil sands[1]. Heavy crude oils that typically result from a bacterial oxidation of conventional hydrocarbon resources inside the reservoir rock have much higher viscosity, higher heavy metals and higher sulfur and nitrogen contents[2]. The high viscosities of these resources pose challenges for their production, processing and transport. Mitigation strategies include heating, dilution, oil-in-water emulsion, upgrading and core annular flow as a method for lubricating the inner wall of the pipelines[2, 3]. Each strategy has its own benefits and drawbacks. Increasing the temperature decreases the viscosity considerably, however the energy consumption is significant. Preparation of oil-in-water emulsions typically yields viscosities in an acceptable range for pipelining but breaking the emulsion to recover the heavy oil, and water recycling are unresolved issues[2]. Among the treatment options for heavy hydrocarbon resources, dilution is one that has drawn much attention[4-6]. Many studies report experimental viscosity data of mixtures of bitumen or heavy oil with a light hydrocarbon or a non-hydrocarbon including but not limited to CO_2, methane, propane or butane[7-14]. Others have measured the viscosity of mixtures of bitumen or heavy oil + higher molar mass hydrocarbons

whether pure[15, 16] or mixtures of naphtha with or without additional organic solvents[6, 17]. Empirical models[18-22] and mixing rules[23, 24] have been developed for correlating the viscosity of mixtures of bitumen or heavy oil and solvents based on the available data in the literature. These studies do not incorporate the non-Newtonian behavior that bitumen and heavy oil exhibit at low temperatures[25-27]. The observed non-Newtonian behaviors include shear rate dependence (in the form of shear thinning behavior) and shear history dependence (in the form of thixotropic behavior[28, 29]) of viscosity values at fixed temperatures and pressures. Identification of the transition from Newtonian to non-Newtonian rheological behavior, and the magnitude of non-Newtonian effects at low temperatures in heavy hydrocarbon resources on their own and in mixtures with diluents are needed to create reliable and complete experimental data sets, for direct use or for the development of rheological models that take all of the rheological features of mixtures of these resources with diluents into account.

In this work, the effect that different types of chemical compounds have on the rheological properties of Maya crude oil is investigated. The focus is on rheological outcomes obtained using an aromatic solvent (toluene), an alkane (n-heptane) and a mixture of an aromatic solvent and a ketone (toluene + butanone 50/50 vol%). The shear rate dependence of viscosity for mixtures of Maya crude oil plus these diluents as functions of compositions and temperatures at steady state are studied for a fixed shear history. Transient thixotropic behaviors of these mixtures are also examined through start-up experiments, again with a common shear history. Key points of comparison including reduction of the non-

Newtonian behavior and viscosity values versus composition and relative to thermal treatment are also addressed.

4.2 Experimental Section

4.2.1 Materials

The heavy oil used in this work is Maya crude oil, which is a commercial heavy oil blend from Mexico. Detailed information about it is given in Chapter 2. Toluene (99.9%) and n-heptane (99.3%) were purchased from Fischer Scientific. Butanone (also know as methyl ethyl ketone or MEK, 99.9%) was purchased from Sigma-Aldrich. N-heptane and toluene were used as received, and a 50 vol. % mixture of toluene + butanone was also used as a diluent. Binary mixtures of Maya crude oil and these diluents were prepared by weighing each constituent in a vial. The uncertainty of the scale (Mettler Toledo AG285) is ± 0.112 mg. A magnet was then placed inside the vial and once sealed, the vial was put on a magnetic stirrer base at room temperature for at least one hour to ensure homogenous mixing. The vial was then reweighed to ensure that there was no mass loss. In all cases, the masses fell within the limits of measurement reproducibility - 0.03%.

4.2.2 Rheology measurements

The rheology experiments were performed using a stress-controlled rheometer (Physica MCR 301 Anton Paar) at atmospheric pressure and temperatures from (258 to 333) K using a double-gap cylinder geometry. The measuring bob internal

and external diameters are 21.03 and 23.04 mm respectively. The internal and external diameters of the measuring cup are 20.33 and 23.85 mm respectively. The amount of sample loaded for each test was 2.37 ml. Temperature gradients are negligible because of the small size of this geometry, which results in a thin layer of fluid inside the cup. Sample temperature is measured with a Pt100 DIN/IEC 751 sensor with a resolution of 0.01 K and controlled with an accuracy of ± 0.03 K. A peltier system (C-PTD200, Anton Paar), used to control the temperature of the sample in the rheometer, has a temperature operating range from (243 to 472) K. More detailed information about this rheometer is given in Chapter 2. The sample is loaded into the double-gap geometry inside the cell after performing a motor adjustment. Measurement quality was verified using Cannon certified viscosity standards. Detailed results are given in Chapter 3. Four standards were used with viscosities ranging from (0.2596 to 168.6) Pa.s. The largest relative deviations from these standards are 7.7 % at 260 K.

The same procedure was used for all of the experiments carried out in this work, in order to prevent the introduction of ambiguity into the results arising from the thixotropic behavior of Maya crude oil[28]. Samples were allowed to rest for 24 hours at 268 K once they were loaded into the rheometer and were then pre-sheared prior to performing rheological measurements. As a result, samples have shared thermal and shear histories.

All of the experiments were conducted in triplicate to confirm repeatability of the experiments. All of the data obtained are presented as tabulated supplemental data in Tables S10 to S18. These tables include standard uncertainties of the

measurements. The results are summarized in Figures 4.1 to 4.14. In these Figures, the error bars are smaller than the data-points in most cases and are not added to the figurers for clarity.

4.3 Results and Discussion

4.3.1 Steady shear experiments

The shear rate dependence of binary mixtures of Maya crude oil and diluent was examined over the temperature range (258 to 333) K at atmospheric pressure. N-heptane, toluene and toluene + butanone (50/50 vol.%) were used as diluents with weight fractions of 5, 10 and 20 % for n-heptane and toluene, and 13 % for toluene + butanone (50/50 vol.%). Shear rate ramps from (10 to 200) s^{-1} were imposed on the samples. For Maya crude oil + n-heptane (5.11 wt. %) and Maya crude oil + toluene (5.13 wt. %) at 258 K, the shear rate domain was from (5 to 40) s^{-1} and (5 to 105) s^{-1}, respectively. Prior to measurement, the samples were pre-sheared for 5 minutes at 40 s^{-1}. All of the measurements were performed isothermally. Each sample was sheared for 2 minutes at each shear rate, before making the shear stress measurement. As noted in Chapters 2 and 3, this step is intended to eliminate the thixotropic effects and to ensure that steady state shear stress values were obtained. The resulting flow curves at fixed composition are presented in Figures 4-1 through 4-7. As expected, diluent addition reduces mixture viscosity at all temperatures and the reduction is a strong function of diluent composition. However, shear thinning behavior continues to be observed in all cases at low temperatures. For n-heptane addition, the shear thinning to

Newtonian behavior transition drops from 313 K to values below 293 K and on to a plateau value exceeding 283 K, as the weight fraction increases from 0 to 0.0511, to 0.1003 and 0.2018. For toluene addition, the corresponding values are 313 K, ~ 283 K, ~ 278 K and ~ 273 K as toluene weight fraction is increased from 0 to 0.0513, 0.1002 and 0.2007. The transition with toluene + butanone (50/50 vol.%) arises at ~ 273 K for 0.1366 weight fraction.

Shear thinning behavior in Maya oil has been attributed to structural and hydrodynamic properties of solid maltenes (as explained in Chapter 2) that form below ~ 313 K. The observation that adding diluents decreases the upper temperature where shear thinning behavior occurs has two possible interpretations: diluents shift the liquid-solid phase boundary for maltene constituents to lower temperatures, or diluent molecules modify surface/structural and hydrodynamic properties, including particle interactions, of solid maltenes such that Newtonian behavior is observed at lower temperatures. Both attributions are plausible. Irrespective of the underlying cause, shifting the shear thinning to Newtonian behavior transition temperature by approximately 30 K is readily achieved. However, plateaus in the transition temperature with diluent weight fraction are evident and the transition to non-Newtonian behavior persists at industrially relevant conditions for storage and mixing applications, and for operating and shut in pipelines and production systems. The shear thinning behavior of mixtures of Maya crude oil + diluents, and by extension other heavy oil or bitumen + diluent mixtures should be included in equipment and system design calculations. This is not currently part of industrial practice.

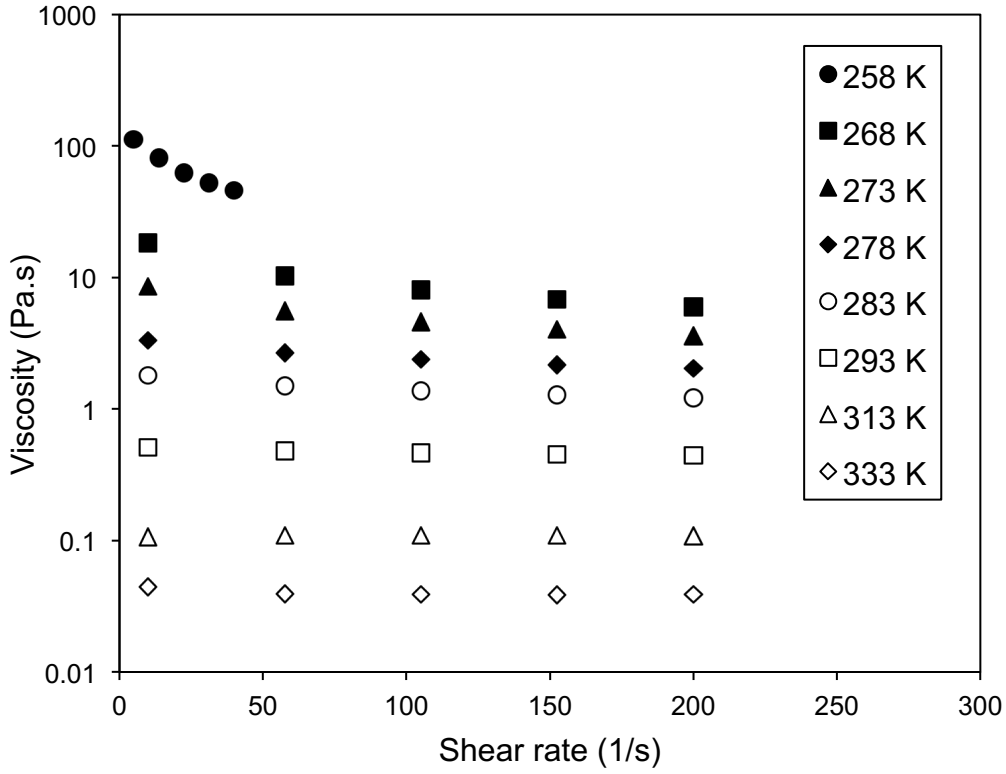

Figure 4-1. Flow curves for Maya crude oil + 5.11 wt% n-heptane. Temperature is a parameter.

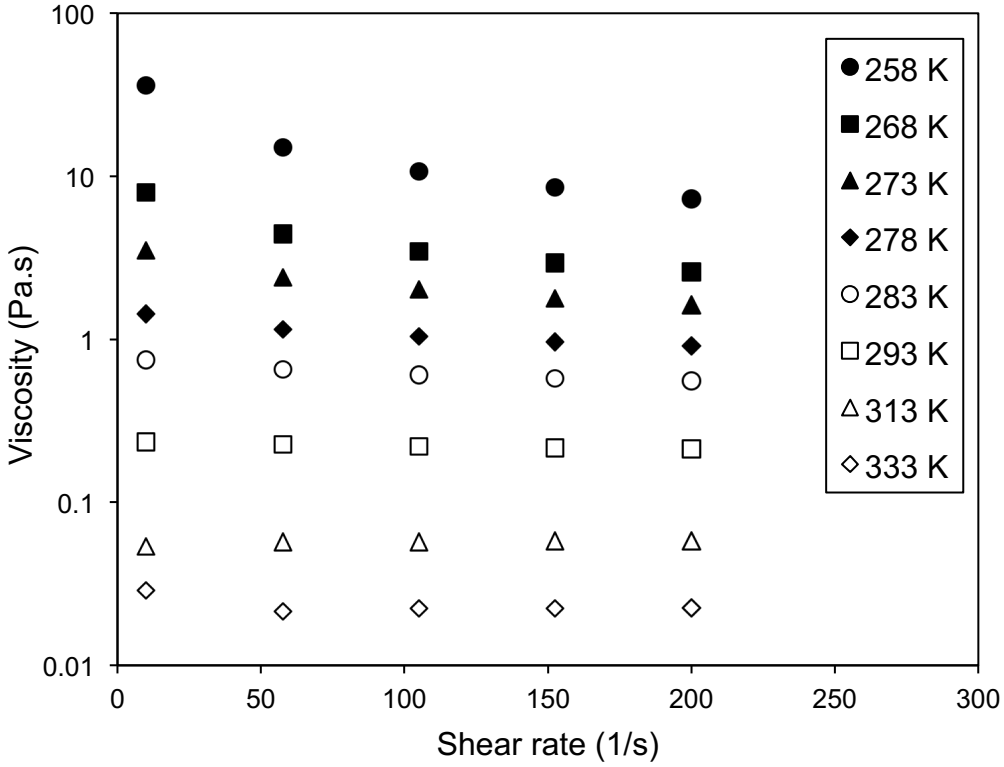

Figure 4-2. Flow curves for Maya crude oil + 10.03 wt% n-heptane. Temperature is a parameter.

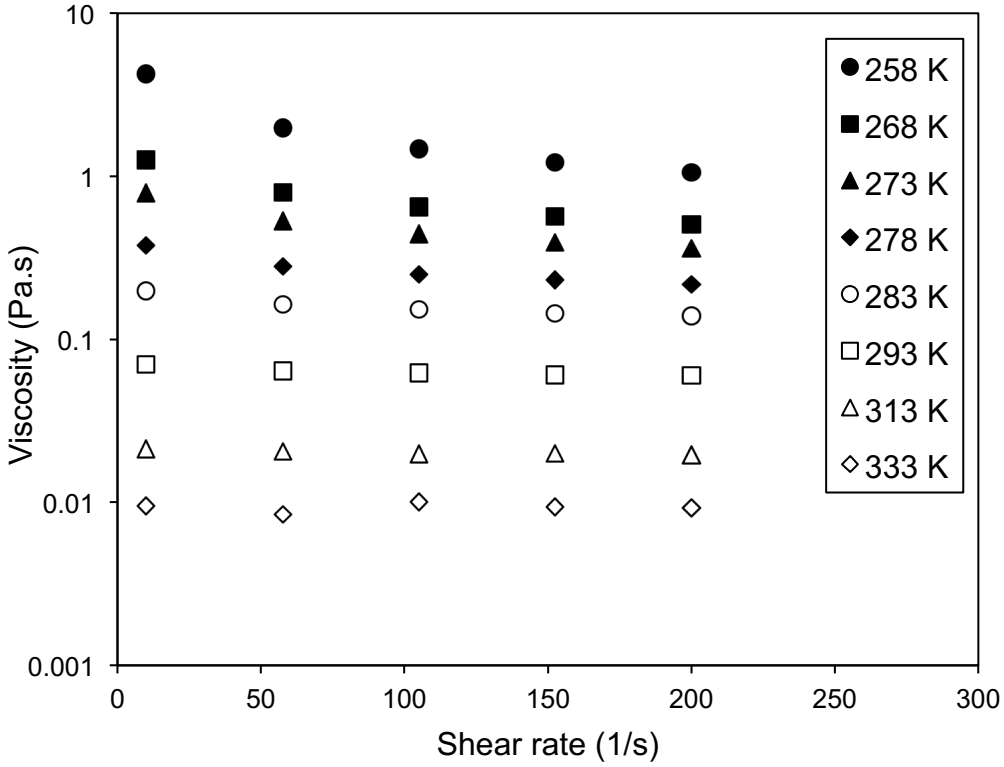

Figure 4-3. Flow curves for Maya crude oil + 20.18 wt% n-heptane. Temperature is a parameter.

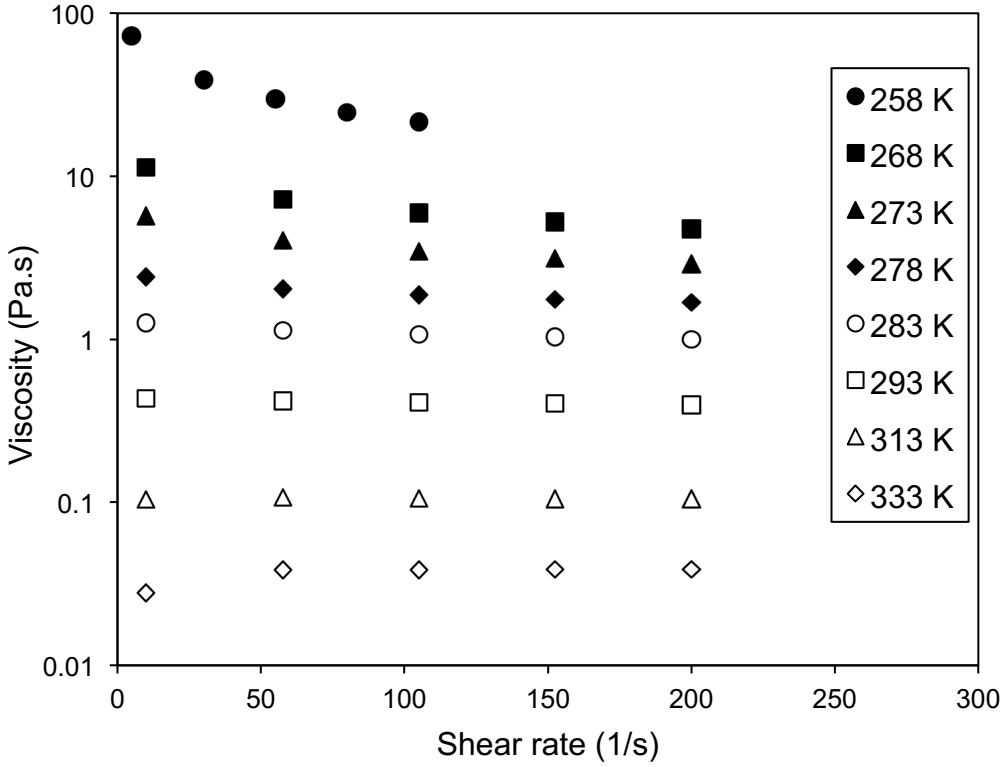

Figure 4-4. Flow curves for Maya crude oil + 5.13 wt% toluene. Temperature is a parameter.

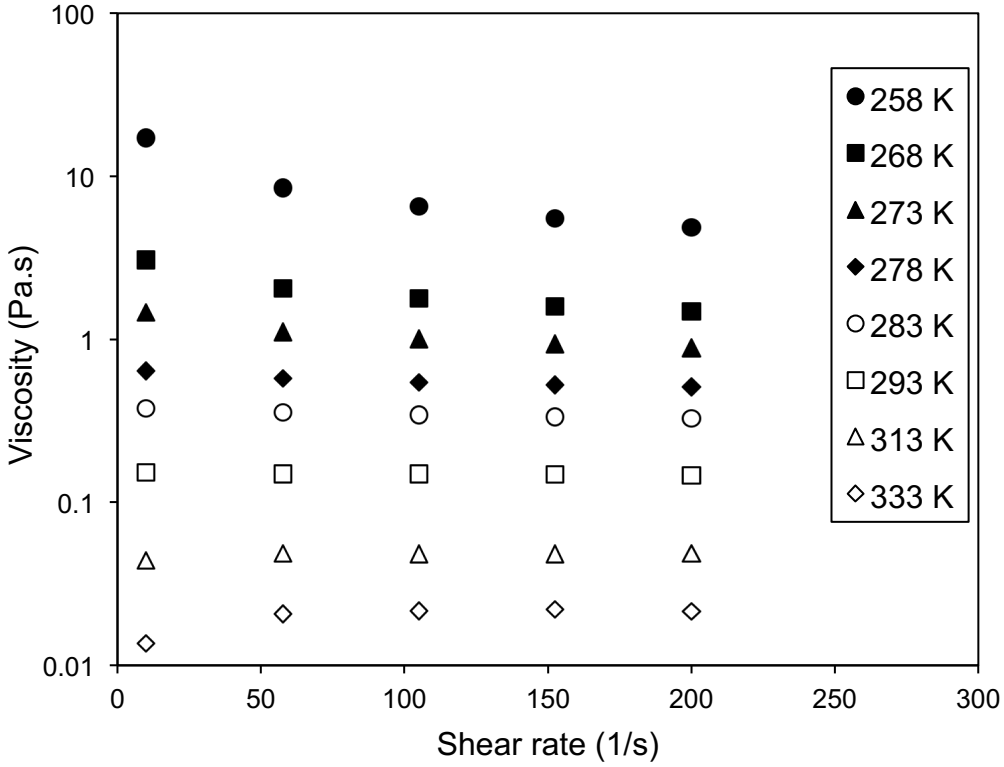

Figure 4-5. Flow curves for Maya crude oil + 10.02 wt% toluene. Temperature is a parameter.

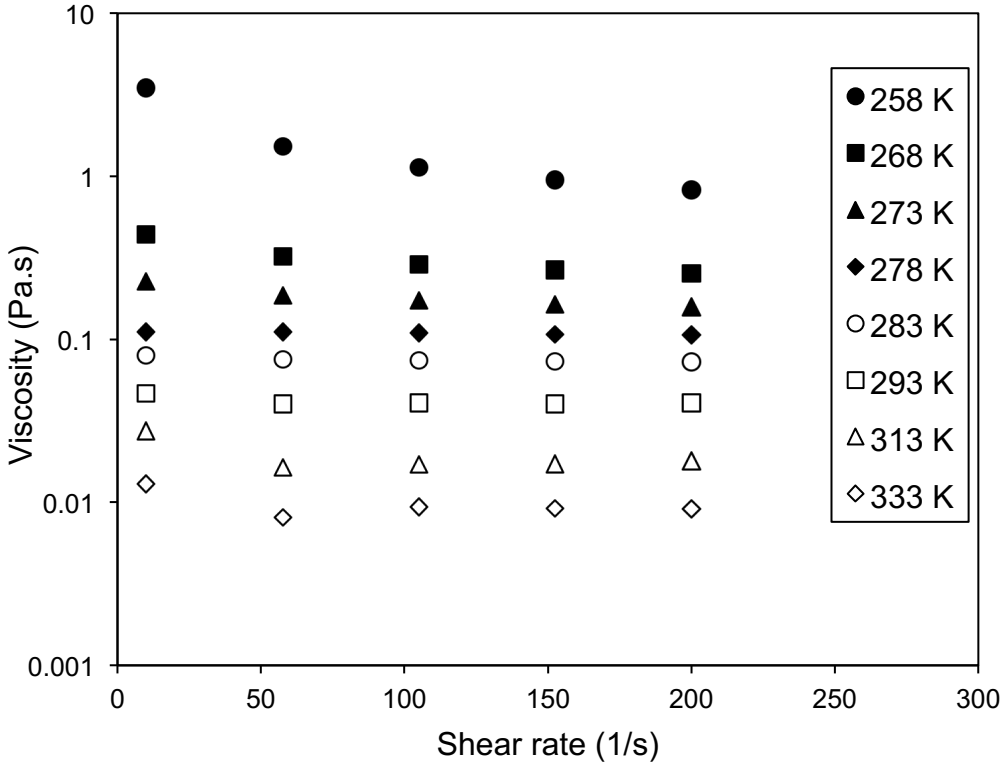

Figure 4-6. Flow curves for Maya crude oil + 20.07 wt% toluene. Temperature is a parameter.

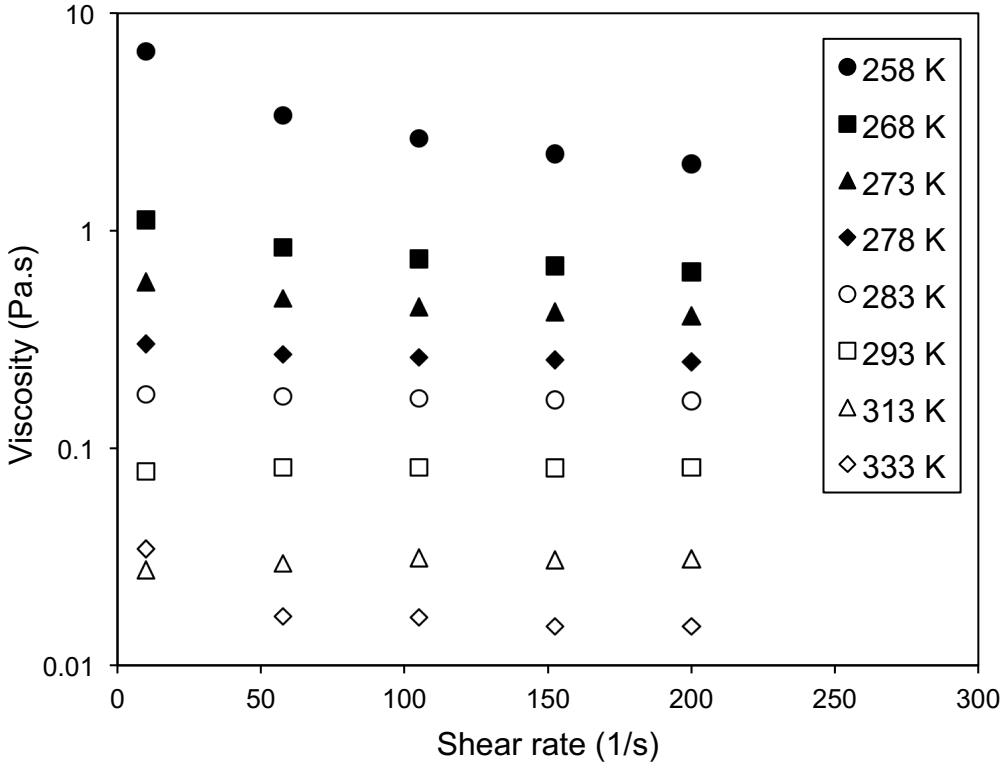

Figure 4-7. Flow curves for Maya crude oil + 13.66 wt% (toluene + butanone (50/50 vol%)). Temperature is a parameter.

4.3.2 Absolute and relative impacts of dilution on mixture viscosity at fixed temperature and fixed shear rate

The absolute and relative impacts of diluents on the viscosity of mixtures of Maya crude oil + n-heptane and Maya crude oil + toluene at a shear rate of 10 s^{-1} are shown in Figures 4-8 (a and b) and 4-9 (a and b), respectively. These results are also intended to be illustrative, particularly at low temperature where impacts are shear rate dependent. Viscosity values decrease exponentially with the weight fraction of diluent at constant temperature and shear rate – Figure 4-8a and Figure

4-9a. The relative viscosity, defined as the viscosity of the mixture divided by the viscosity of Maya oil measured at the same shear rate and temperature, are shown in Figure 4-8b and 4-9b. These relative viscosities also decrease exponentially with the weight fraction of diluent at constant temperature and shear rate. Further, the relative viscosities exhibit a variable temperature dependence. The order of experimental points does not possess a trend with temperature for either solvent. Thus the impact of dilution on viscosity can only be normalized in this way with significant uncertainty (~50%). While normalization in this way permits extrapolation and interpretation of sparse data, that is adequate for numerous applications, this latter finding complicates the development of high precision correlations for the impact of dilution on viscosity.

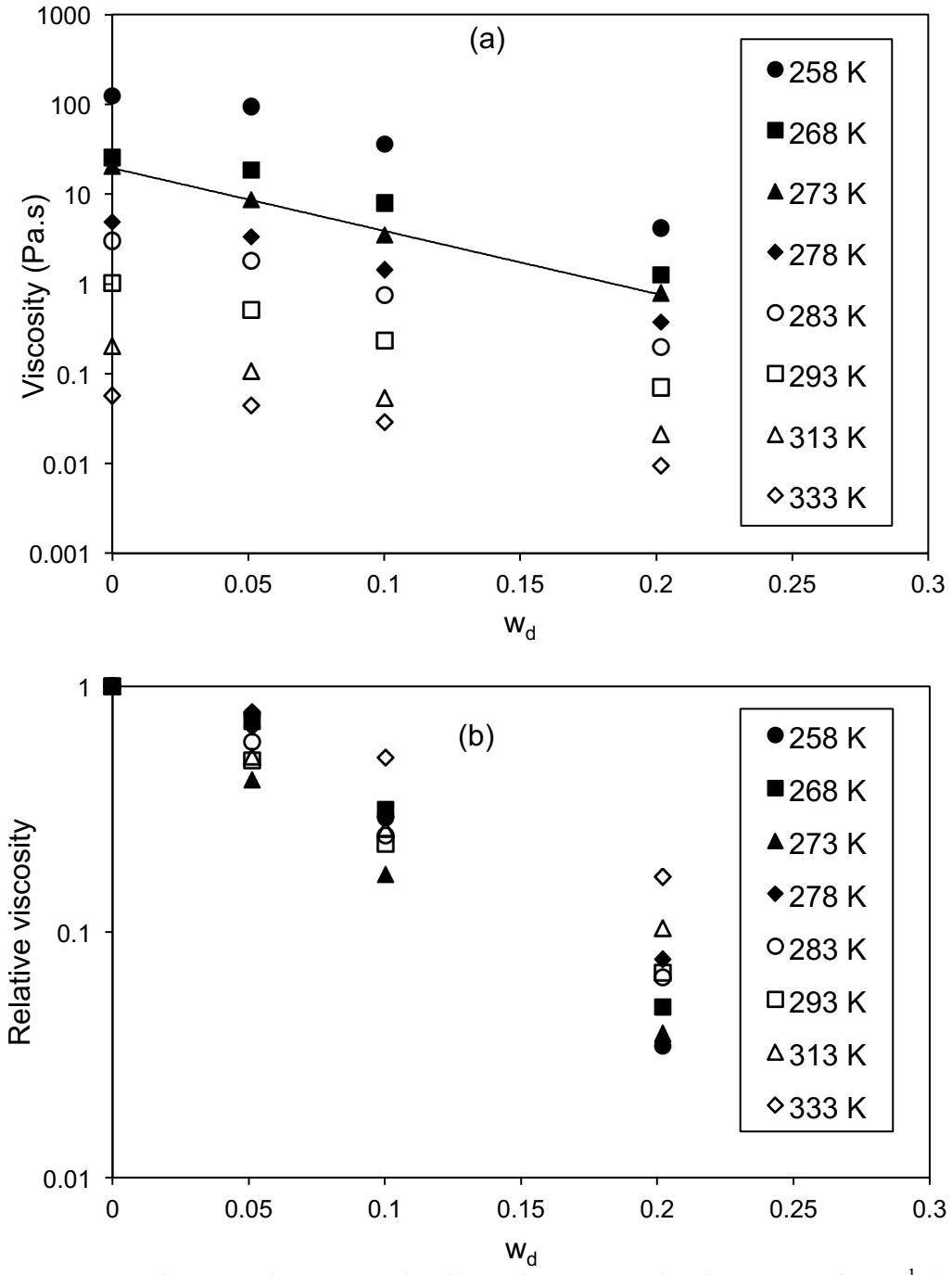

Figure 4-8. Mixtures of Maya crude oil + n-heptane at the shear rate of 10 s^{-1}. (a) Mixture viscosity versus the weight fraction of n-heptane (w_d). (b) Relative viscosity of the mixture versus n-heptane weight fraction. Temperature is a parameter. The line represents regression of the data based on Equation 4-3.

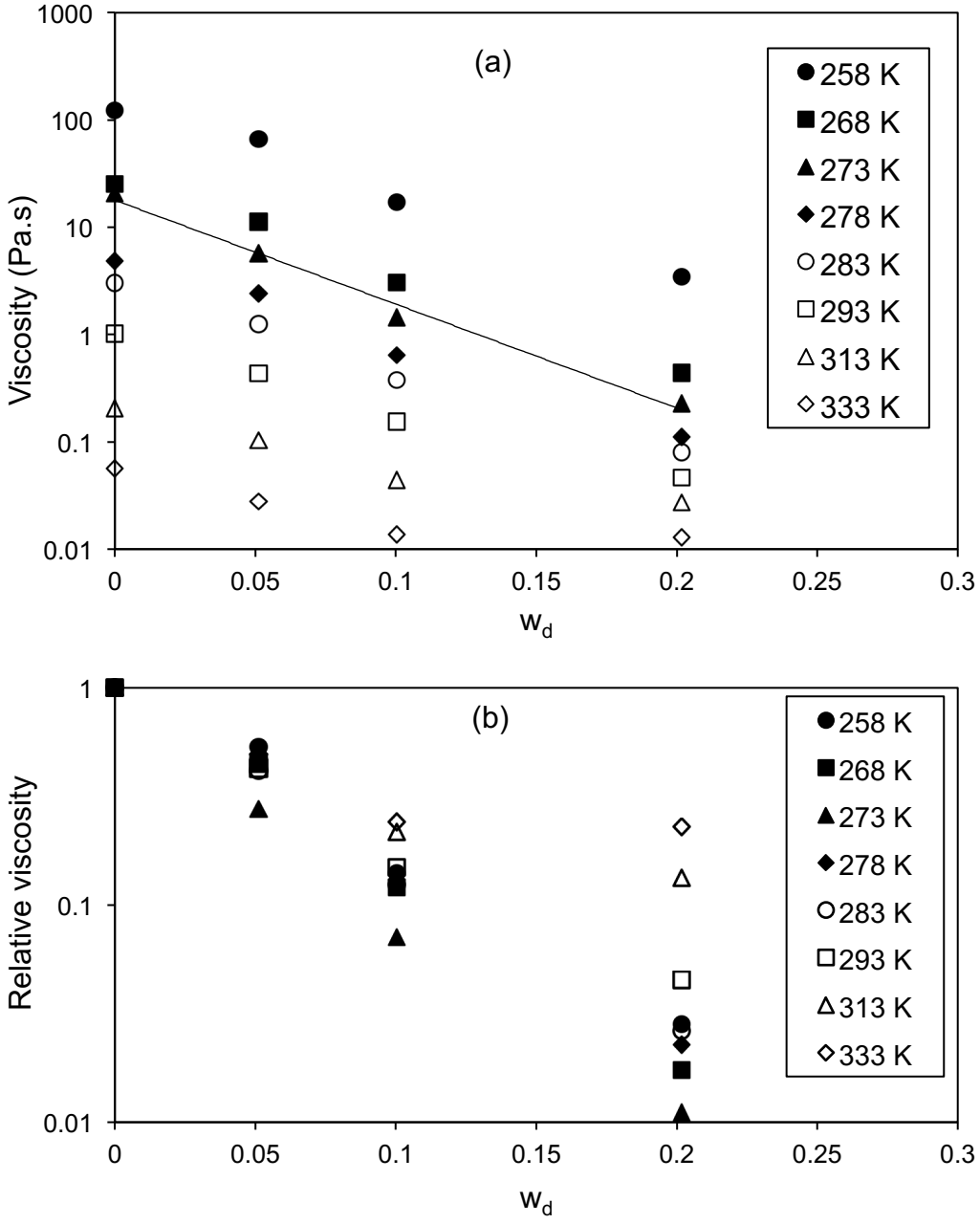

Figure 4-9. Mixtures of Maya crude oil and toluene at the shear rate of 10 s^{-1}. (a) Mixture viscosity versus the weight fraction of toluene (w_d). (b) Relative viscosity of the mixture versus toluene weight fraction. Temperature is a parameter. The line represents regression of the data based on Equation 4-4.

4.3.3 Quantifying impacts of diluent composition on non-Newtonian behavior

In order to look at the capability of the three diluents to reduce the impact of non-Newtonian behavior, the values of a Non-Newtonian Index (NN-Index), introduced in Chapter 3, were calculated at temperatures where shear thinning is observed. The NN-Index defined as:

$$\text{NN-Index} = \frac{\sqrt{\sum_{i=1}^{n}\left(\frac{\eta_i - \eta_{ref}}{\dot{\gamma}_i - \dot{\gamma}_{ref}}\right)^2}}{n} \tag{4-1}$$

where n is the number of data points at a fixed temperature, T; Σ is a summation over all of the data points at T; η_i is the viscosity associated with data point *i*; $\dot{\gamma}_i$ is the shear rate associated with data point *i*, subscript *ref* refers to a reference data point which is chosen to be the data point with the minimum value of shear rate at temperature T. The values of the Non-Newtonian Index for binary mixtures of Maya crude oil and diluent with diluent weight fractions of 0.1003, 0.1002 and 0.1366 for n-heptane, toluene and toluene + butanone (50/50 vol.%), respectively, are presented in Figure 4-10. Toluene + butanone (50/50 vol.%) addition to Maya crude oil induces the greatest reduction in shear thinning behavior irrespective of temperature; toluene addition is less impactful and n-heptane addition is least impactful.

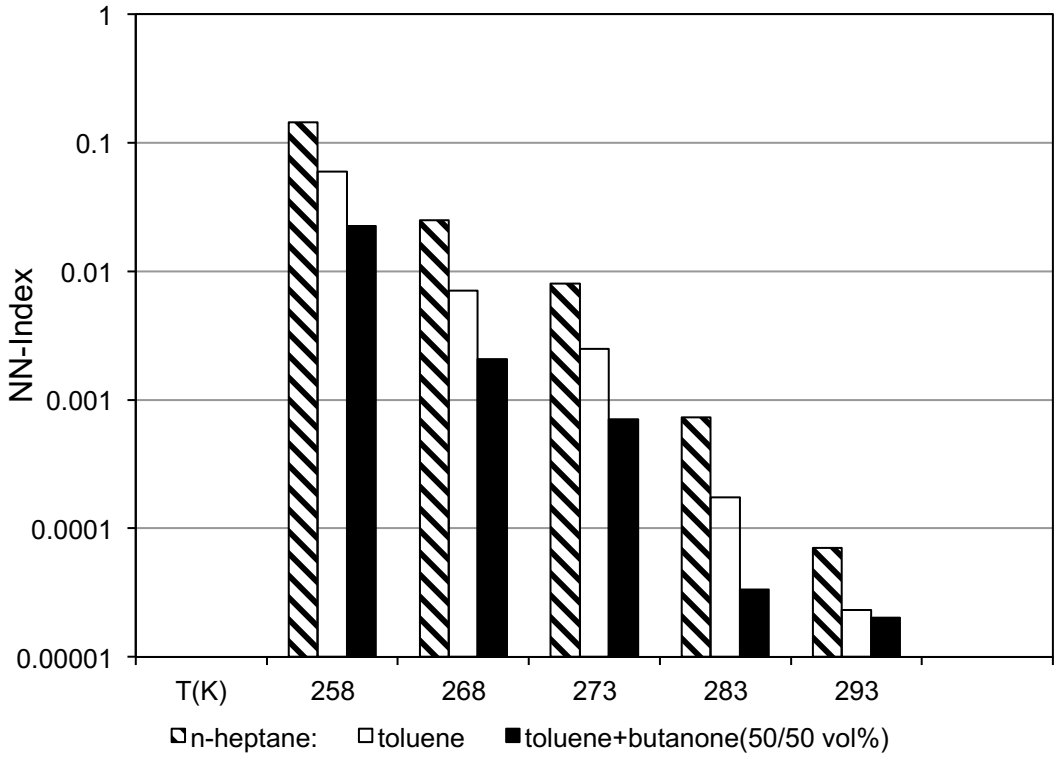

Figure 4-10. Effectiveness of diluents n-heptane, toluene and a mixture of toluene + butanone (50/50 vol.%) at reducing the Non-Newtonian Index (NN-Index) on addition to Maya crude oil.

The relative effectiveness of the three diluents in reducing the viscosity of Maya crude oil in comparison can also be evaluated relative to reductions obtained by heating. The comparison is exemplified by comparing the increase in temperature and the required addition of n-heptane, toluene or toluene + butanone (50/50 vol%) needed to decrease the viscosity at 273 K and a shear rate of 10 s^{-1} from 20.5 to a value of 0.5801 Pa.s. Viscosity data for Maya crude oil at a shear rate of 10 s^{-1}, for the temperature interval (254 to 338) K were correlated as:

$$\eta = 4.18205\times10^{-4}e^{6.05295\times10^{9}\left(\frac{1}{T}\right)^{3.6}} \quad (4\text{-}2)$$

where η is the viscosity in Pa.s at a shear rate of 10 s^{-1} and T is the absolute temperature in K. The results along with the relative deviation of the correlation are presented in Figures 4-11a and 4-11b, respectively. The average absolute relative deviation of the correlation is 12.6%. According to Equation 4-2, the temperature would need to be increased to 301 K, an increase of 28 K. If this reduction in viscosity were to be achieved by adding a diluent at 273 K, the required diluent fraction can be calculated from the viscosity of mixtures of Maya crude oil + diluents shown in Figures 4-8a and 4-9a by fitting an exponential function proposed previously for Athabasca bitumen[30]. The resulting correlations for n-heptane and toluene are respectively:

$$\eta = 19.493e^{-16.11w_d} \quad (4\text{-}3)$$

$$\eta = 17.857e^{-22.3w_d} \quad (4\text{-}4)$$

where η is the viscosity of the mixture of Maya crude oil and diluent in Pa.s and w_d is the weight fraction of diluent in the mixture. Dilution with 0.218 weight fraction n-heptane and 0.154 weight fraction toluene at 273 K provide an equal reduction in viscosity. For toluene + butanone (50/50 vol.%), the required weight fraction of diluent is 0.1366 – from Figure 4-7.

The order of effectiveness is clearly toluene + butanone (50/50 vol.%) followed by toluene and then n-heptane, the least effective diluent. Toluene is an aromatic compound and butanone is even more polar, whereas n-heptane is an alkane. The parity plot, Figure 4-12 shows how poor n-alkanes are from the perspective of

viscosity reduction vis-à-vis aromatics. Maya crude oil + toluene mixtures possess systematically lower viscosities than Maya crude oil + n-heptane mixtures when compared at the same temperature, shear rate and diluent weight fraction. As the density of toluene[31] is greater than the density of n-heptane[32], the comparison is worse on a volume fraction basis. This effect arises even though the viscosity of n-heptane[32] is lower than the viscosity of toluene[31]. Clearly, aromatic and polar diluents reduce the viscosity more effectively, than non-polar alkanes. These results provide directions for further research and are illustrative. Another recent study has shown that butanone addition to naphtha is a more effective additive than other polar compounds at reducing viscosity[6]. In any given industrial application, diluent availability and cost, and technical feasibility of separation etc. will play determining roles. However, the potential for design improvement for future pipeline projects, for example, is clear, as is the potential to improve the operation and capacity of existing infrastructure.

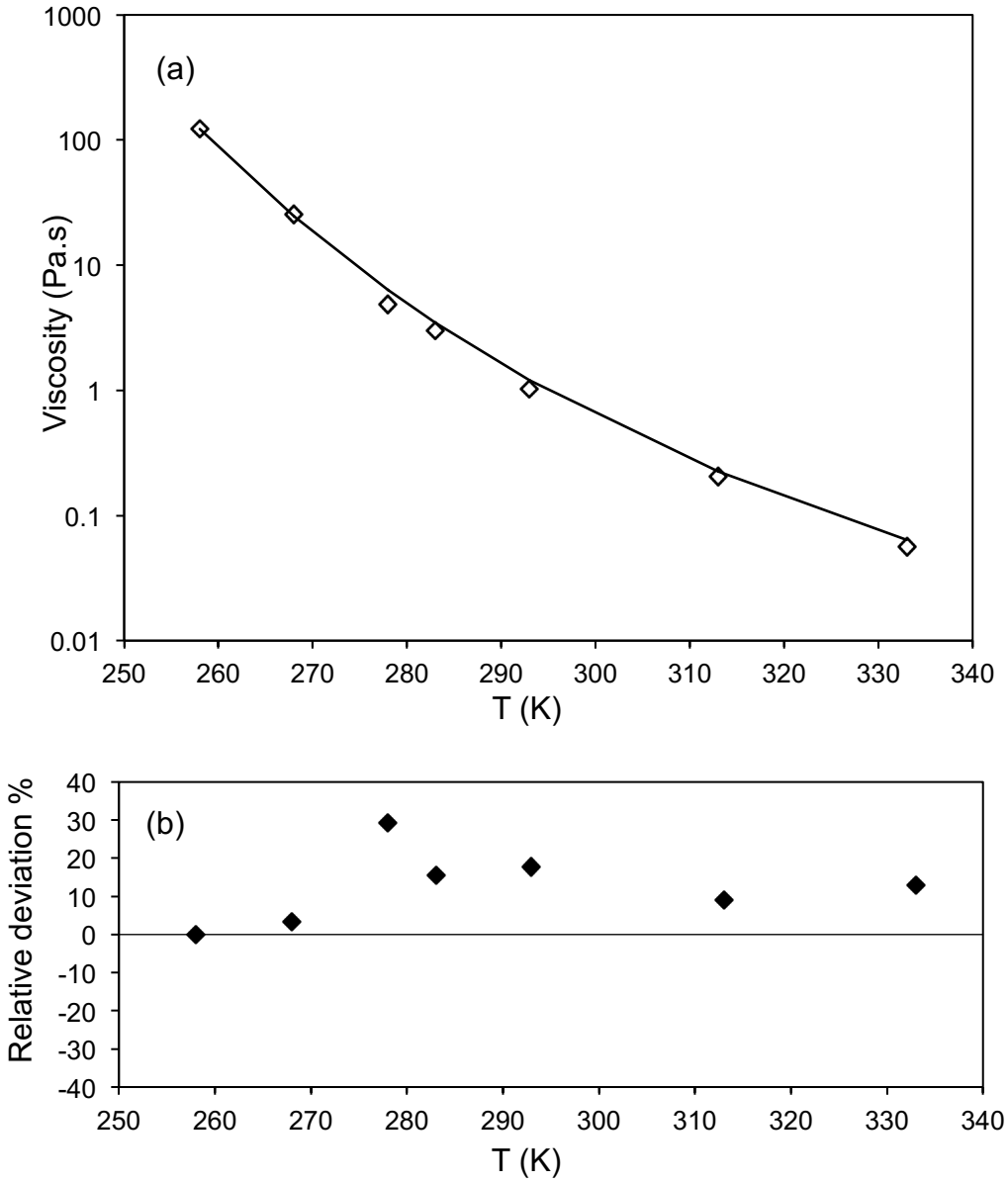

Figure 4-11. (a) Temperature dependence of the viscosity of Maya crude oil at the shear rate of 10 s^{-1}. The line represents regression of the data based on Equation 4-2. (b) Relative deviation of the correlated values from experimental values.

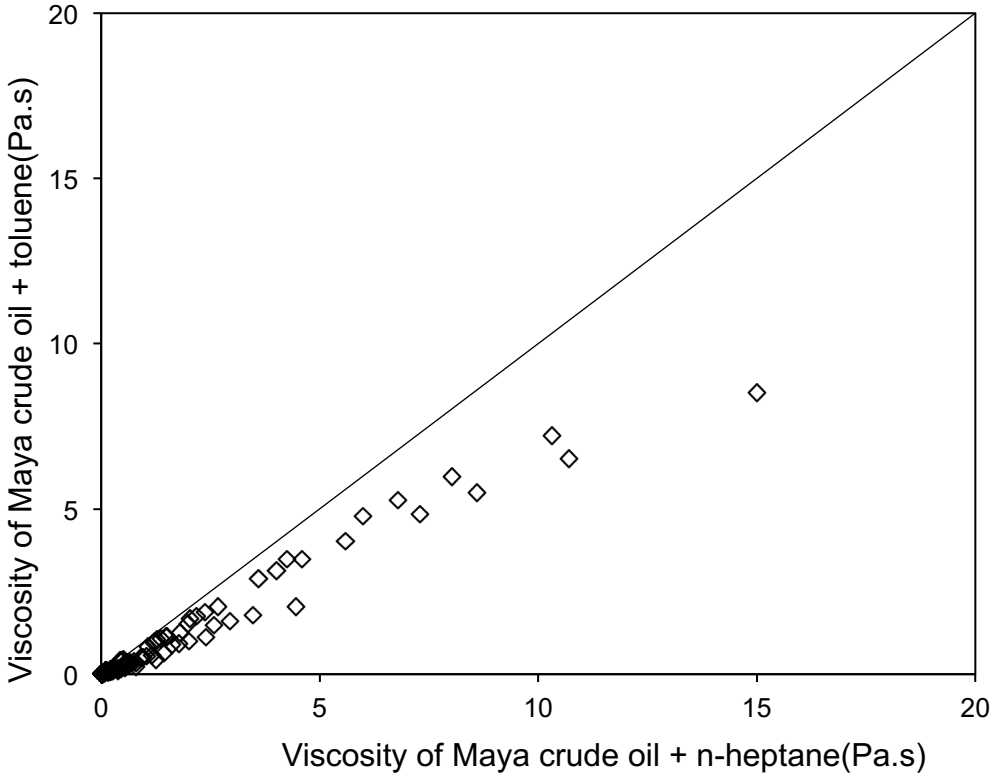

Figure 4-12. Parity plot comparing the viscosity of Maya crude oil + toluene with the viscosity of Maya crude oil + n-heptane at fixed temperature, shear rate and diluent weight fraction.

4.3.4 Thixotropic behavior

Maya crude oil exhibits thixotropic behavior at low temperatures. One of the techniques to study thixotropy is a start-up experiment, which clarifies the degree to which structuring occurs during rest and the effect of structure on the subsequent flow behavior under stress. The results obtained from this type of

experiment are especially helpful in understanding complications arising during heavy oil pipeline restart following a prolonged shutdown.

Mixtures of Maya crude oil and the diluent n-heptane, toluene and toluene + butanone (50/50 vol.%) were loaded into the rheometer. The samples were first pre-sheared at 40 s^{-1} for 5 minutes, then let rest for 120 minutes, and finally a start-up shear rate equal to 30 s^{-1} was imposed. The temperature was kept constant at 273 K during all of three steps. The shear stress values were monitored during the start-up step and the results obtained are presented in Figure 4-13 and 4-14. In all cases, the value of the shear stress during start-up decays with time, which is indicative of breakage of structures under shear that formed during rest. As was noted with shear thinning behavior, toluene + butanone (50/50 vol.%) is least impacted, and toluene less impacted than n-heptane by thixotropic behavior.

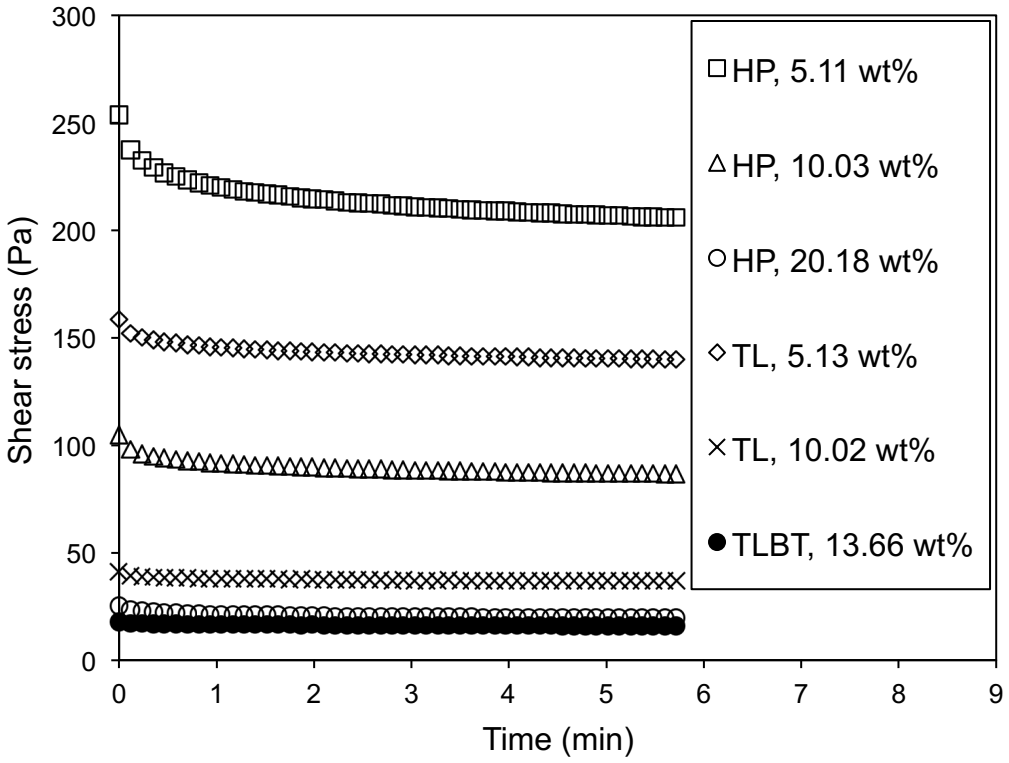

Figure 4-13. Transient shear stress arising during start-up experiment for mixtures of Maya crude oil + diluents at 273 K, where a 30 s^{-1} shear rate is imposed on samples formerly at rest. Diluent and diluent weight fraction are parameters. HP: n-heptane; TL: toluene; TLBT: toluene + butanone (50/50 vol.%).

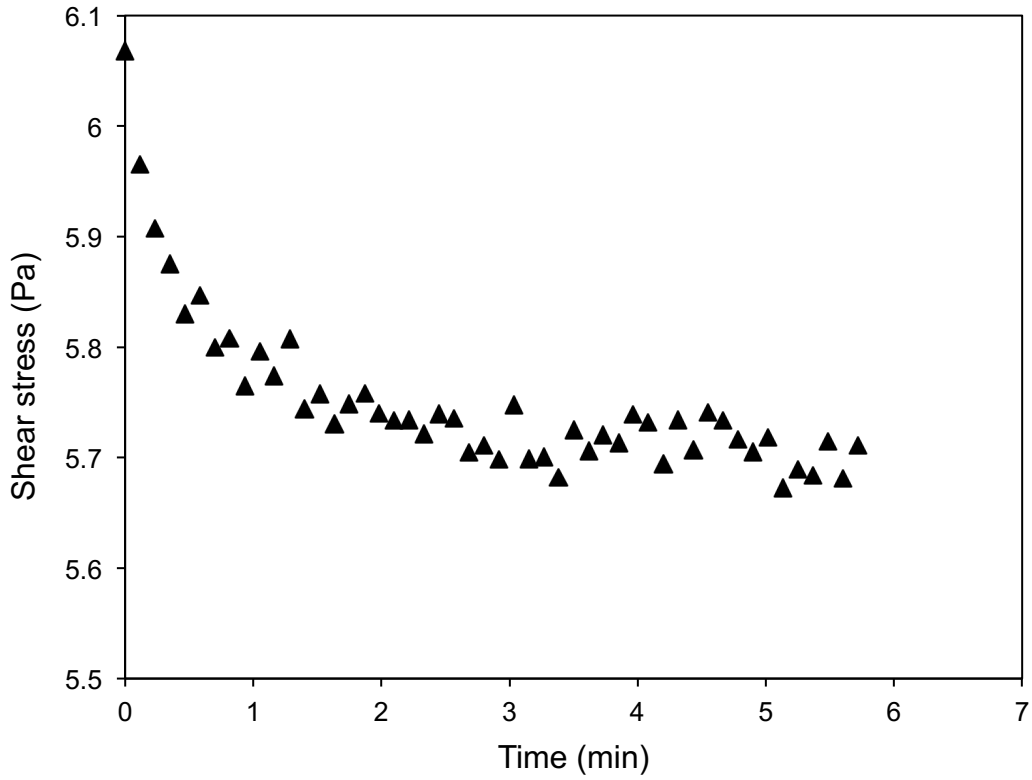

Figure 4-12. Transient shear stress arising during start-up experiment for Maya crude oil + 20.07 wt% toluene at 273 K, where a 30 s^{-1} shear rate is imposed on a sample formerly at rest.

4.4 Conclusions

The rheological properties of binary mixtures of Maya crude oil and three diluents (an aromatic solvent (toluene), an alkane (n-heptane) and a mixture of an aromatic solvent and a ketone (toluene + butanone 50/50 vol%)) were evaluated. The same experimental procedures and protocols were applied to each mixture to provide the same shear and thermal histories to all samples. Expected outcomes include that diluent addition reduces mixture viscosity at all temperatures, irrespective of shear conditions, and is a strong function of diluent composition.

More importantly, heptane is shown to be the least effective of the three diluents with respect to reducing viscosity on a mass or volume basis and all Maya oil + diluent samples continue to exhibit non-Newtonian shear thinning behavior, under steady shear, at low temperatures. The upper temperature, where shear thinning is observed does decrease as the diluent concentration is increased but the transition to non-Newtonian behavior remains above 273 K and continues to be relevant to blending, mixing, pipelining, and storage operations. Toluene + butanone (50/50 vol.%) addition to Maya crude oil induces the greatest reduction in viscosity and in shear thinning behavior at fixed shear rate, irrespective of temperature; toluene addition is less impactful and n-heptane addition is least impactful. Time dependent thixotropic behaviors of mixtures of Maya crude oil and these diluents arising on start-up or restart, follow a similar trend. N-heptane has the least impact on the value of the shear stress arising during start-up and mixtures of Maya oil + n-heptane exhibit the largest thixotropic effect. While local availability frequently dictates diluent choice, these results underscore the ranges of composition required to achieve a viscosity target at a given temperature in a given shear environment, and the sensitivity of rheological responses to variations of diluent composition, shear rate and to flow disruption. From a purely technical perspective, high polarity diluents are clearly preferred. However, optimization of diluent choice for specific applications is complex and reliable databases are needed for model development and evaluation under conditions where Newtonian and non-Newtonian behaviors are anticipated.

4.5 References

1. Hein, F., Heavy Oil and Oil (Tar) Sands in North America: An Overview & Summary of Contributions. *Nat Resour Res* 2006, 15, (2), 67-84.

2. Saniere, A.; Hénaut, I.; Argillier, J., F., Pipeline Transportation of Heavy Oils, a Strategic, Economic and Technological Challenge. *Oil & Gas Science and Technology - Rev. IFP* 2004, 59, (5), 455-466.

3. Bensakhria, A.; Peysson, Y.; Antonini, G., Experimental Study of the Pipeline Lubrication for Heavy Oil Transport. *Oil & Gas Science and Technology - Rev. IFP* 2004, 59, (5), 523-533.

4. Li, X.; Sun, W.; Wu, G.; He, L.; Li, H.; Sui, H., Ionic Liquid Enhanced Solvent Extraction for Bitumen Recovery from Oil Sands. *Energy Fuels* 2011, 25, (11), 5224-5231.

5. Hupka, J.; Miller, J. D.; Drelich, J., Water-Based Bitumen Recovery from Diluent-Conditioned Oil Sands. *The Canadian Journal of Chemical Engineering* 2004, 82, (5), 978-985.

6. Gateau, P.; Hénaut, I.; Barré, L.; Argillier, J., F., Heavy Oil Dilution. *Oil & Gas Science and Technology - Rev. IFP* 2004, 59, (5), 503-509.

7. A.Yazdani; Maini, B. B., Measurements and Modelling of Phase Behaviour and Viscosity of a Heavy Oil/Butane System. *J. Can. Pet. Technol.* 2010, (02), 9-14.

8. Bazyleva, A.; Akeredolu, B.; Liberatore, M. W., Viscosity of Alaska Heavy Oil Saturated with Methane. *Energy Fuels* 2013, 27, (2), 743-751.

9. Badamchi-Zadeh, A.; Yarranton, H. W.; Svrcek, W. Y.; Maini, B. B., Phase Behaviour and Physical Property Measurements for VAPEX Solvents: Part I. Propane and Athabasca Bitumen. 2009, (01), 54-61.

10. Badamchi-Zadeh, A.; Yarranton, H. W.; Maini, B. B.; Satyro, M. A., Phase Behaviour and Physical Property Measurements for VAPEX Solvents: Part II. Propane, Carbon Dioxide and Athabasca Bitumen. 2009, (03), 57-65.

11. Li, H.; Zheng, S.; Yang, D., Enhanced Swelling Effect and Viscosity Reduction of Solvents-CO2-Heavy Oil Systems. In *SPE Heavy Oil Conference and Exhibition 2011*, Society of Petroleum Engineers: Kuwait City, Kuwait, 2011; pp 196-217.

12. Mehrotra, A. K.; Svrcek, W. Y., Viscosity, Density and Gas Solubility Data for Oil Sand Bitumens. Part I: Athabasca Bitumen Saturated with CO and C2H6. *AOSTRA J. Res.* 1985, 1, (4), 263-268.

13. Mehrotra, A. K.; Svrcek, W. Y., Viscosity, Density and Gas Solubility Data for Oil Sand Bitumens. Part II: Peace River Bitumen Saturated with N2, CO, CH4, CO2 and C2H6. *AOSTRA J. Res.* 1985, 1, (4), 269-279.

14. Mehrotra, A. K.; Svrcek, W. Y., Viscosity, Density and Gas Solubility Data for Oil Sand Bitumens. Part III: Wabasca Bitumen Saturated with N2, CO, CH4, CO2 and C2H6. *AOSTRA J. Res.* 1985, 2, (2), 83-93.

15. Guan, J. G.; Kariznovi, M.; Nourozieh, H.; Abedi, J., Density and Viscosity for Mixtures of Athabasca Bitumen and Aromatic Solvents. *J. Chem. Eng. Data* 2013, 58, (3), 611-624.

16. Barrufet, M. A.; Setiadarma, A., Experimental Viscosities of Heavy Oil Mixtures up to 450 K and High Pressures using a Mercury Capillary Viscometer. *J. Pet. Sci. Eng.* 2003, 40, (1-2), 17-26.

17. Schramm, L. L. L.; Kwak, J. C. T., The Rheological Properties Of An Athabasca Bitumen And Some Bituminous Mixtures And Dispersions. *J. Can. Pet. Technol.* 1988, 27, (1).

18. Mehrotra, A. K.; Svrcek, W. Y., Correlations For Properties of Bitumen Saturated With CO2 , CH4 And N2 , And Experiments With Combustion Gas Mixtures. *J. Can. Pet. Technol.* 1982, 21, (6), 95-104.

19. Motahhari, H.; Schoeggl, F. F.; Satyro, M. A.; Yarranton, H. W., Prediction of the Viscosity of Solvent Diluted Live Bitumen at Temperatures up to 175C. In *Canadian Unconventional Resources Conference 2011*, Society of Petroleum Engineers: Alberta, Canada, 2011; Vol. 3, pp 2065-2083.

20. Miadonye, A.; Doyle, N. L.; Britten, A.; Latour, N.; Puttagunta, V. R., Modelling Viscosity and Mass Fraction of Bitumen-Diluent Mixtures. *J. Can. Pet. Technol.* 2001, 40, 52-57.

21. Novak, L. T., Entity-Based Eyring−NRTL Viscosity Model for Mixtures Containing Oils and Bitumens. *Industrial & Engineering Chemistry Research* 2006, 45, (21), 7329-7335.

22. Wen, Y.; Kantzas, A., Evaluation of Heavy Oil/Bitumen- Solvent Mixture Viscosity Models. *J. Can. Pet. Technol.* 2006, 45, 56-61.

23. Barrufet, M. A.; Setiadarma, A., Reliable Heavy Oil–Solvent Viscosity Mixing Rules for Viscosities up to 450K, Oil–Solvent Viscosity Ratios up to 4 × 105, and any Solvent Proportion. *Fluid Phase Equilib.* 2003, 213, (1-2), 65-79.

24. Mehrotra, A. K., A Mixing Rule Approach for Predicting the Viscosity of CO2-Saturated Cold Lake Bitumen and Bitumen Fractions. *J. Pet. Sci. Eng.* 1992, 6, (4), 289-299.

25. Hasan, M. D. A.; Fulem, M.; Bazyleva, A.; Shaw, J. M., Rheological Properties of Nanofiltered Athabasca Bitumen and Maya Crude Oil. *Energy Fuels* 2009, 23, (10), 5012-5021.

26. Bazyleva, A. B.; Hasan, M. A.; Fulem, M.; Becerra, M.; Shaw, J. M., Bitumen and Heavy Oil Rheological Properties: Reconciliation with Viscosity Measurements. *J. Chem. Eng. Data* 2010, 55, 1389-1397.

27. Pierre, C.; Barré, L.; Pina, A.; Moan, M., Composition and Heavy Oil Rheology. *Oil & Gas Science and Technology - Rev. IFP* 2004, 59, (5), 489-501.

28. Mortazavi-Manesh, S.; Shaw, J. M., Thixotropic Rheological Behavior of Maya Crude Oil. *Energy Fuels* 2014, 28, 972-979.

29. Evdokimov, I. N.; Losev, A. P., Thixotropy in Native Petroleum Emulsions. *J. Dispersion Sci. Technol.* 2011, 32, (8), 1206-1212.

30. Mehrotra, A. K.; Svrcek, W. Y., Viscosity of Compressed Athabasca Bitumen. *Can. J. Chem. Eng.* 1986, 64, (5), 844-847.

31. Avelino, H. M. T.; Fareleira, J. M. N. A.; Wakeham, W. A., Simultaneous Measurement of the Density and Viscosity of Compressed Liquid Toluene. *International Journal of Thermophysics* 2003, 24, (2), 323-336.

32. Sagdeev, D. I.; Fomina, M. G.; Mukhamedzyanov, G. K.; Abdulagatov, I. M., Experimental Study of the Density and Viscosity of n-Heptane at Temperatures from 298 K to 470 K and Pressure upto 245 MPa. *International Journal of Thermophysics* 2013, 34, (1), 1-33.

Chapter 5 : Conclusions and Recommendations for Future Work

5.1 Conclusions

In this work, the rheological behavior of Maya crude oil, with a focus on transitions between Newtonian and non-Newtonian behavior arising at low temperature, high pressure, or on addition of diluents has been investigated. The diversity of the conditions considered in this work both at steady state and during start-up or re-start operations reflect the diversity of processing conditions for heavy oils such as Maya crude oil that arise industrially.

Thixotropic behaviors of Maya crude oil that lead to time and shear history dependent viscosities have been explored over a wide range of temperatures with a focus on low temperatures. Maya crude oil shows shear thinning behavior at temperatures lower than 313 K that is consistent with its phase behavior, reported previously, and is attributed to structural and hydrodynamic properties of the maltene fraction. Solid maltenes are not present in Maya oil at temperatures higher than 313 K according to their phase behavior. The thixotropic behavior and the impact of rest time indicates the impact of shear history on the rheological response of Maya crude oil and the interplay between shear history and phase behavior. By neglecting the impact of shear history on laboratory measurements and the prediction of rheological properties in the field, poor operating practices or inadequate or inappropriate facility designs may arise. The data obtained

provide a simple and general benchmark for rheological response measurement and model development for heavy oils as well as a better understanding of the physical phenomena underlying the rheology. The roles of temperature, rest time, and shear rate are clearly delineated, using well-defined and well-established experimental protocols. The impacts of these variables for example on pipeline restart are explored. The relationships identified between rest time and other thixotropic parameters may facilitate reconciliation of rheological data in the literature. Furthermore, the impact of pressure on the rheological properties of Maya crude oil was examined closely over a wide range of temperatures. Again, particular attention was paid to low temperatures. It was concluded that the apparent values of viscosity of Maya crude oil increase with increasing pressure, at a given temperature and shear rate, which indicates raising pressure is equivalent to, and has an effect similar to, decreasing temperature from a thermodynamic perspective and therefore as viscosity increases with decreasing temperature, it would also increase with increasing pressure. Maya crude oil displays shear thinning behavior at temperatures lower than 313 K, which persists to higher pressures at this temperature range. Observation of shear thinning behavior at elevated pressures at the same temperature range may be an indication of the consistent structural and hydrodynamic roles of solid maltenes towards establishment of shear thinning properties in Maya crude oil up to high pressures. For the first time, non-Newtonian behavior was quantified by introducing a new parameter called NN-Index (Non-Newtonian Index). The magnitude of the non-Newtonian behavior increases with increasing the pressure, which in turn implies

that high pressures not only lead to higher viscosities but they may also lead to more significant non-Newtonian properties which needs to be taken into account in order for adequate and reliable facility designs. By investigating the effect of pressure on the recovery of structures within Maya oil at rest through SAOS (Small Amplitude Oscillatory Shear) experiments, it was revealed that thixotropy persists to higher pressures in Maya crude oil. The effect of pressure on thixotropic properties was unknown in the past. The recovery of the moduli is faster at higher pressure, which reflects the effect of pressure in speeding up the rebuilding process of microstructures within Maya oil.

Finally, the rheological properties of binary mixtures of Maya crude oil and three diluents (an aromatic solvent (toluene), an alkane (n-heptane) and a mixture of an aromatic solvent and a ketone (toluene + butanone 50/50 vol%)) were evaluated. Expected outcomes include that diluent addition reduces mixture viscosity at all temperatures, irrespective of shear conditions, and is a strong function of diluent composition. More importantly, n-heptane is shown to be the least effective of the three diluents with respect to reducing viscosity on a mass or volume basis and all Maya oil + diluent samples continue to exhibit non-Newtonian shear thinning behavior, under steady shear, at low temperatures. The upper temperature, where shear thinning is observed does decrease as the diluent concentration is increased but the transition to non-Newtonian behavior remains above 273 K and continues to be relevant to blending, mixing, pipelining, and storage operations. Toluene + butanone (50/50 vol.%) addition to Maya crude oil

induces the greatest reduction in viscosity and in shear thinning behavior at fixed shear rate, irrespective of temperature; toluene addition is less impactful and n-heptane addition is least impactful. Time dependent thixotropic behaviors of mixtures of Maya crude oil and these diluents arising on start-up or restart, follow a similar trend. N-heptane has the least impact on the value of the shear stress arising during start-up and mixtures of Maya oil + n-heptane exhibit the largest thixotropic effect. While local availability frequently dictates diluent choice, these results underscore the ranges of composition required to achieve a viscosity target at a given temperature in a given shear environment, and the sensitivity of rheological responses to variations of diluent composition, shear rate and to flow disruption. From a purely technical perspective, high polarity diluents are clearly preferred. However, optimization of diluent choice for specific applications is complex and reliable databases are needed for model development and evaluation under conditions where Newtonian and non-Newtonian behaviors are anticipated.

5.2 Recommendations for Future Work

Diverse production and processing environments are employed and are envisaged for heavy hydrocarbon resources. For production, cold flow, gas and diluent injection with and without heat, mining and steam injection, are employed. For transport, comingling with water and hydrocarbons is performed. In upgrading and refining, de-asphalting and other separation processes are required. Rheological properties of heavy hydrocarbon resources are necessary for adequate design of processes and equipment, selecting the most efficient diluent and

dealing with process shutdown challenges. The main objective of this project was to investigate the effect of temperature, particularly low temperatures, pressure, shear conditions, shear history and type and concentration of diluents on the rheological properties of heavy oil and to provide an accountable database over wide ranges of temperature, pressure and shear rate. Furthermore, an attempt was made to shed light on the physics behind the complex rheological properties of heavy oil through the phase behavior of the heavy oil constituents such as maltenes and asphaltenes. In this regard, development of rheological models that capture as much of the features observed experimentally in this project as possible would be necessary. Including thixotropic aspects of the rheological behavior of Maya crude oil in proper constitutive equations is very important. Furthermore, constitutive equations, which account for the effect of pressure on the non-Newtonian behavior is lacking in the literature and is worth looking at more closely. The effect of pressure on thixotropic properties was examined for the first time in this project. Further investigations can be followed up with respect to model development. In continuation of the path to a better understanding of the underlying physics for the complex rheological behavior of heavy oil and bitumen, it is recommended to further investigate the effects of heavy oil constituents such as maltenes and asphaltenes by performing Rheo-SAXS, which is a technique where Small Angle X-ray Scattering (SAXS) measurements are performed while the sample is under shear in the rheometer and this way, the interrelation between the structures within the sample and rheological properties can be closely investigated.

References

1. Gateau, P.; Hénaut, I.; Barré, L.; Argillier, J., F., Heavy Oil Dilution. *Oil & Gas Science and Technology - Rev. IFP* 2004, 59, (5), 503-509.

2. Pierre, C.; Barré, L.; Pina, A.; Moan, M., Composition and Heavy Oil Rheology. *Oil & Gas Science and Technology - Rev. IFP* 2004, 59, (5), 489-501.

3. Behzadfar, E.; Hatzikiriakos, S. G., Rheology of bitumen: Effects of temperature, pressure, CO2 concentration and shear rate. *Fuel* **2014,** 116, (0), 578-587.

4. Saniere, A.; Hénaut, I.; Argillier, J., F., Pipeline Transportation of Heavy Oils, a Strategic, Economic and Technological Challenge. *Oil & Gas Science and Technology - Rev. IFP* 2004, 59, (5), 455-466

5. Bensakhria, A.; Peysson, Y.; Antonini, G., Experimental Study of the Pipeline Lubrication for Heavy Oil Transport. *Oil & Gas Science and Technology - Rev. IFP* 2004, 59, (5), 523-533.

6. Li, X.; Sun, W.; Wu, G.; He, L.; Li, H.; Sui, H., Ionic Liquid Enhanced Solvent Extraction for Bitumen Recovery from Oil Sands. *Energy Fuels* 2011, 25, (11), 5224-5231.

7. Hupka, J.; Miller, J. D.; Drelich, J., Water-Based Bitumen Recovery from Diluent-Conditioned Oil Sands. *The Canadian Journal of Chemical Engineering* 2004, 82, (5), 978-985.

8. A.Yazdani; Maini, B. B., Measurements and Modelling of Phase Behaviour and Viscosity of a Heavy Oil/Butane System. *J. Can. Pet. Technol.* 2010, (02), 9-14.

9. Bazyleva, A.; Akeredolu, B.; Liberatore, M. W., Viscosity of Alaska Heavy Oil Saturated with Methane. *Energy Fuels* 2013, 27, (2), 743-751.

10. Badamchi-Zadeh, A.; Yarranton, H. W.; Svrcek, W. Y.; Maini, B. B., Phase Behaviour and Physical Property Measurements for VAPEX Solvents: Part I. Propane and Athabasca Bitumen. 2009, (01), 54-61.

11. Badamchi-Zadeh, A.; Yarranton, H. W.; Maini, B. B.; Satyro, M. A., Phase Behaviour and Physical Property Measurements for VAPEX Solvents: Part II. Propane, Carbon Dioxide and Athabasca Bitumen. 2009, (03), 57-65.

12. Li, H.; Zheng, S.; Yang, D., Enhanced Swelling Effect and Viscosity Reduction of Solvents-CO2-Heavy Oil Systems. In *SPE Heavy Oil Conference and Exhibition 2011*, Society of Petroleum Engineers: Kuwait City, Kuwait, 2011; pp 196-217.

13. Mehrotra, A. K.; Svrcek, W. Y., Viscosity, Density and Gas Solubility Data for Oil Sand Bitumens. Part I: Athabasca Bitumen Saturated with CO and C2H6. *AOSTRA J. Res.* 1985, 1, (4), 263-268.

14. Mehrotra, A. K.; Svrcek, W. Y., Viscosity, Density and Gas Solubility Data for Oil Sand Bitumens. Part II: Peace River Bitumen Saturated with N2, CO, CH4, CO2 and C2H6. *AOSTRA J. Res.* 1985, 1, (4), 269-279.

15. Mehrotra, A. K.; Svrcek, W. Y., Viscosity, Density and Gas Solubility Data for Oil Sand Bitumens. Part III: Wabasca Bitumen Saturated with N2, CO, CH4, CO2 and C2H6. *AOSTRA J. Res.* 1985, 2, (2), 83-93.

16. Guan, J. G.; Kariznovi, M.; Nourozieh, H.; Abedi, J., Density and Viscosity for Mixtures of Athabasca Bitumen and Aromatic Solvents. *J. Chem. Eng. Data* 2013, 58, (3), 611-624.

17. Barrufet, M. A.; Setiadarma, A., Experimental Viscosities of Heavy Oil Mixtures up to 450 K and High Pressures Using a Mercury Capillary Viscometer. *J. Pet. Sci. Eng.* 2003, 40, (1-2), 17-26.

18. Mehrotra, A. K.; Svrcek, W. Y., Correlations For Properties of Bitumen Saturated With CO2 , CH4 And N2 , And Experiments With Combustion Gas Mixtures. *J. Can. Pet. Technol.* 1982, 21, (6), 95-104.

19. Motahhari, H.; Schoeggl, F. F.; Satyro, M. A.; Yarranton, H. W., Prediction of the Viscosity of Solvent Diluted Live Bitumen at Temperatures up to 175C. In *Canadian Unconventional Resources Conference 2011*, Society of Petroleum Engineers: Alberta, Canada, 2011; Vol. 3, pp 2065-2083.

20. Miadonye, A.; Doyle, N. L.; Britten, A.; Latour, N.; Puttagunta, V. R., Modelling Viscosity and Mass Fraction of Bitumen-Diluent Mixtures. *J. Can. Pet. Technol.* 2001, 40, 52-57.

21. Novak, L. T., Entity-Based Eyring−NRTL Viscosity Model for Mixtures Containing Oils and Bitumens. *Industrial & Engineering Chemistry Research* 2006, 45, (21), 7329-7335.

22. Wen, Y.; Kantzas, A., Evaluation of Heavy Oil/Bitumen- Solvent Mixture Viscosity Models. *J. Can. Pet. Technol.* 2006, 45, 56-61.

23. Barrufet, M. A.; Setiadarma, A., Reliable Heavy Oil–Solvent Viscosity Mixing Rules for Viscosities up to 450K, Oil–Solvent Viscosity Ratios up to 4 × 105, and any Solvent Proportion. *Fluid Phase Equilib.* 2003, 213, (1-2), 65-79.

24. Mehrotra, A. K., A Mixing Rule Approach for Predicting the Viscosity of CO2-Saturated Cold Lake Bitumen and Bitumen Fractions. *J. Pet. Sci. Eng.* 1992, 6, (4), 289-299.

25. Chhabra, R. P., Rheology of Complex Fluids, Chapter 1: Non-Newtonian Fluids. In Springer: New York, 2010.

26. Barnes, H. A.; Hutton, J. F.; Walters, K., *An Introduction to Rheology*. Elsevier Science Publishers: Amsterdam, Netherlands, 1993.

27. Carreau, P. J. Ph.D. Thesis, University of Wisconsin, Madison, Wisc., 1968.

28. Carreau, P. J., Rheological Equations from Molecular Network Theories. *Transactions of The Society of Rheology (1957-1977)* 1972, 16, (1), 99-127.

29. Cross, M. M., Rheology of Non-Newtonian Fluids: A New Flow Equation for Pseudoplastic Systems. *J. Colloid Interface Sci.* 1965, 20, (5), 417-437.

30. Ellis, S. B. Thesis, Lafayette College, 1927.

31. Mezger, T. G., *The Rheology Handbook*. Vincentz Network: Hanover, 2011.

32. Bingham, E. C., An Investigation of the Laws of Elastic Flow. *Bull. U.S. Bur. of Standards* 1916.

33. Herschel, W. H. B., R., Measurement of Consistency as Applied to Rubber Benzene Solutions. *Proc. ASTM* 1925, 82.

34. Casson, N., *A Flow Equation for Pigment-Oil Suspensions of the Printing Ink Type, in: Rheology of Disperse Systems*. ed. C.C. Mill, Pergamon Press: New York, 1959.

35. McLeish, T. C. B.; Larson, R. G., Molecular Constitutive Equations for a Class of Branched Polymers: The Pom-Pom Polymer. *Journal of Rheology (1978-present)* 1998, 42, (1), 81-110.

36. Drozdov, A. D.; Jensen, E. A.; Christiansen, J. d. C., Thermo-Viscoelasticity of Polymer Melts: Experiments and Modeling. *Acta Mech* 2008, 197, (3-4), 211-245.

37. Mewis, J.; Wagner, N. J., Thixotropy. *Adv. Colloid Interface Sci.* 2009, 147-148, 214-27.

38. de Souza Mendes, P. R., Modeling the Thixotropic Behavior of Structured Fluids. *J. Non-Newtonian Fluid Mech.* 2009, 164, (1–3), 66-75.

39. de Souza Mendes, P. R., Thixotropic Elasto-Viscoplastic Model for Structured Fluids. *Soft Matter* 2011, 7, (6), 2471-2483.

40. Dullaert, K.; Mewis, J., A Structural Kinetics Model for Thixotropy. *J. Non-Newtonian Fluid Mech.* 2006, 139, (1-2), 21-30.

41. Quemada, D., Rheological Modelling of Complex Fluids: IV: Thixotropic and "thixoelastic" Behaviour. Start-up and Stress Relaxation, Creep Tests and Hysteresis Cycles. *Eur. Phys. J.: Appl. Phys.* 1999, 5, (02), 191-207.

42. Roussel, N.; Le Roy, R.; Coussot, P., Thixotropy Modelling at Local and Macroscopic Scales. *J. Non-Newtonian Fluid Mech.* 2004, 117, (2-3), 85-95.

43. Yziquel, F.; Carreau, P. J.; Moan, M.; Tanguy, P. A., Rheological Modeling of Concentrated Colloidal Suspensions. *J. Non-Newtonian Fluid Mech.* 1999, 86, (1–2), 133-155.

44. Dion, M. Modelling the Rheology of Complex Fluids: Cases of Bitumen and Heavy Oils at Low Temperatures. M.Sc. Thesis, University of Alberta, Edmonton, 2011.

45. Svrcek, W. Y.; Mehrotra, A. K., Gas Solubility, Viscosity and Density Measurements for Athabasca Bitumen. *J. Can. Pet. Technol.* 1982, 31-38.

46. Schramm, L. L. L.; Kwak, J. C. T., The Rheological Properties Of An Athabasca Bitumen And Some Bituminous Mixtures And Dispersions. *J. Can. Pet. Technol.* 1988, 27, (1).

47. Bazyleva, A. B.; Hasan, M. A.; Fulem, M.; Becerra, M.; Shaw, J. M., Bitumen and Heavy Oil Rheological Properties: Reconciliation with Viscosity Measurements. *J. Chem. Eng. Data* 2010, 55, 1389-1397.

48. Hasan, M. D. A.; Fulem, M.; Bazyleva, A.; Shaw, J. M., Rheological Properties of Nanofiltered Athabasca Bitumen and Maya Crude Oil. *Energy Fuels* 2009, 23, (10), 5012-5021.

49. Evdokimov, I. N.; Losev, A. P., Thixotropy in Native Petroleum Emulsions. *J. Dispersion Sci. Technol.* 2011, 32, (8), 1206-1212.

50. Mortazavi-Manesh, S.; Shaw, J. M., Thixotropic Rheological Behavior of Maya Crude Oil. *Energy Fuels* 2014.

51. Novak, J. D.; Winer, W. O., The Effect of Pressure on the Non-Newtonian Behavior of Polymer Blended Petroleum Oils. *J. Lubr. Technol.* 1969, 91, (3), 459-462.

52. Hirst, W.; Moore, A. J., Elastohydrodynamic Lubrication at High Pressures. II. Non-Newtonian Behaviour. *Proceedings of the Royal Society of London. Series A, Mathematical and Physical Sciences* 1979, 365, (1723), 537-565.

53. Kioupis, L. I.; Maginn, E. J., Impact of Molecular Architecture on the High-Pressure Rheology of Hydrocarbon Fluids. *The Journal of Physical Chemistry B* 2000, 104, (32), 7774-7783.

54. Puttagunata, V. R.; Singh, B.; Miadonye, A., Correlation of Bitumen Viscosity with Temperature and Pressure. *The Canadian Journal of Chemical Engineering* 1993, 71, (3), 447-450.

55. Mehrotra, A. K.; Svrcek, W. Y., Viscosity of Compressed Athabasca Bitumen. *Can. J. Chem. Eng.* 1986, 64, (5), 844-847.

56. Mehrotra, A. K.; Svrcek, W. Y., Viscosity of Compressed Cold Lake Bitumen. *The Canadian Journal of Chemical Engineering* 1987, 65, (4), 672-675.

57. Khan, M. A. B.; Mehrotra, A. X.; Svrcek, W. Y., Viscosity Models For Gas-Free Athabasca Bitumen. *J. Can. Pet. Technol.* 1984, 23, (3).

58. Johnson, S. E.; Svrcek, W. Y.; Mehrotra, A. K., Viscosity Prediction of Athabasca Bitumen Using the Extended Principle of Corresponding States. *Industrial & Engineering Chemistry Research* 1987, 26, (11), 2290-2298.

59. Nellensteyn, F. J. The Colloidal Structure of Bitumen. PhD Thesis, Delft Technical University, Delft, The Netherlands, 1923.

60. Hasan, M. D. A.; Shaw, J. M., Rheology of Reconstituted Crude Oils: Artifacts and Asphaltenes. *Energy Fuels* 2010, 24, (12), 6417-6427.

61. Jacobs, F. A.; Donnelly, J. K.; Stanislav, J., Viiscosity of Gas-saturated Bitumen. *J. Can. Pet. Technol.* 1980, 19, (4).

62. Dealy, J. M., Rheological Properties of Oil Sand Bitumens. *Can. J. Chem. Eng.* 1979, 57, (6), 677-683.

63. Bunger, J. W.; Thomas, K. P.; Dorrence, S. M., Compound Types and Properties of Utah and Athabasca Tar Sand Bitumens. *Fuel* 1979, 58, (3), 183-195.

64. Derksen, J. J., Agitation and Mobilization of Thixotropic Liquids. *AIChE J.* 2010, 2236-2247.

65. Derksen, J. J., Direct Flow Simulations of Thixotropic Liquids in Agitated Tanks. *Can. J. Chem. Eng.* 2011, 89, (4), 628-635.

66. Edwards, M. F.; Godfrey, J. C.; Kashani, M. M., Power Requirement for the Mixing of Thixotropic Liquids. *J. Non-Newtonian Fluid Mech.* 1976, 1, (4), 309-322.

67. Barnes, H. A., Thixotropy-a review. *J. Non-Newtonian Fluid Mech.* 1997, 70, 1-33.

68. Escudier, M. P.; Presti, F., Pipe Flow of a Thixotropic Liquid. *J. Non-Newtonian Fluid Mech.* 1996, 62, (2–3), 291-306.

69. Chang, C.; Nguyen, Q. D.; Rønningsen, H. P., Isothermal Start-up of Pipeline Transporting Waxy Crude Oil. *J. Non-Newtonian Fluid Mech.* 1999, 87, (2–3), 127-154.

70. Vinay, G.; Wachs, A.; Frigaard, I., Start-up Transients and Efficient Computation of Isothermal Waxy Crude Oil Flows. *J. Non-Newtonian Fluid Mech.* 2007, 143, (2–3), 141-156.

71. Negrão, C. O. R.; Franco, A. T.; Rocha, L. L. V., A Weakly Compressible Flow Model for the Restart of Thixotropic Drilling Fluids. *J. Non-Newtonian Fluid Mech.* 2011, 166, (23–24), 1369-1381.

72. Mewis, J., Thixotropy - a general review. *J. Non-Newtonian Fluid Mech.* 1979, 6, (1), 1-20.

73. Manriquez, L.; Moreno, A.; Tenorio, E. R.; Herrera, D., Guide to World Crudes: Four Mexican Crude Assays Updated. *Oil & Gas J.* 2000, 98, (20), 54-57.

74. Zhao, B.; Shaw, J. M., Composition and Size Distribution of Coherent Nanostructures in Athabasca Bitumen and Maya Crude Oil. *Energy Fuels* 2007, 21, 2795-2804.

75. http://www.cannoninstrument.com (Nov 14, 2013),

76. Heyer, P., Guidelines for the Pressure Cell. In Paar, A., Ed. 2007.

77. Fulem, M.; Becerra, M.; Hasan, M. D. A.; Zhao, B.; Shaw, J. M., Phase Behaviour of Maya Crude Oil Based on Calorimetry and Rheometry. *Fluid Phase Equilib.* 2008, 272, (1–2), 32-41.

78. Green, H.; Weltmann, R., Analysis of Thixotropy of Pigment-Vehicle Suspensions - Basic Principles of the Hysteresis Loop. *Ind. Eng. Chem., Anal. Ed.* 1943, 15, (3), 201-206.

79. Magda, J. J.; El-Gendy, H.; Oh, K.; Deo, M. D.; Montesi, A.; Venkatesan, R., Time-Dependent Rheology of a Model Waxy Crude Oil with Relevance to Gelled Pipeline Restart. *Energy Fuels* 2009, 23, (3), 1311-1315.

80. FarouqAli, S. M., Heavy Oil—Evermore Mobile. *J. Pet. Sci. Eng.* 2003, 37, (1–2), 5-9.

81. Abivin, P.; Henaut, I.; Argillier, J.-F.; Moan, M., Rheological Behavior of Foamy Oils. *Energy Fuels* 2008, 23, (3), 1316-1322.

82. Barus, S., Isothermals, Isopiestics, and Isometrics Relatives to Viscosity. . *American Journal of Science* 1893**,** 45, 87-96.

83. Aerschot, E. V. d. Reologie van Reversiebel Geflocculeerde Dispersies PhD, Katholieke Universiteit Leuven, 1989.

84. Manley, S.; Davidovitch, B.; Davies, N. R.; Cipelletti, L.; Bailey, A. E.; Christianson, R. J.; Gasser, U.; Prasad, V.; Segre, P. N.; Doherty, M. P.; Sankaran, S.; Jankovsky, A. L.; Shiley, B.; Bowen, J.; Eggers, J.; Kurta, C.; Lorik, T.; Weitz, D. A., Time-Dependent Strength of Colloidal Gels. *Physical Review Letters* 2005, 95, (4), 048302.

85. Willenbacher, N., Unusual Thixotropic Properties of Aqueous Dispersions of Laponite RD. *Journal of Colloid and Interface Science* 1996, 182, (2), 501-510.

86. Mewis, J.; Spaull, A. J. B.; Helsen, J., Structural Hysteresis. *Nature* 1975, 253, (5493), 618-619.

87. Mewis, J.; Wagner, N. J., *Colloidal Suspension Rheology*. Cambridge University Press: New York, 2012.

88. Hein, F., Heavy Oil and Oil (Tar) Sands in North America: An Overview & Summary of Contributions. *Nat Resour Res* 2006, 15, (2), 67-84.

89. Avelino, H. M. T.; Fareleira, J. M. N. A.; Wakeham, W. A., Simultaneous Measurement of the Density and Viscosity of Compressed Liquid Toluene. *International Journal of Thermophysics* 2003, 24, (2), 323-336.

90. Sagdeev, D. I.; Fomina, M. G.; Mukhamedzyanov, G. K.; Abdulagatov, I. M., Experimental Study of the Density and Viscosity of n-Heptane at Temperatures from 298 K to 470 K and Pressure upto 245 MPa. *International Journal of Thermophysics* 2013, 34, (1), 1-33.

Appendices

Appendix 1. Standard Operating Procedures of the Physica MCR 301 Anton Paar Rheometer

Scope

This standard operating procedure describes the methodology to follow when working with the high pressure Physica MCR 301 Anton Paar Rheometer and also highlights the main hazards involved in the process.

The high pressure Physica MCR 301 Anton Paar is a rotational rheometer system that imposes controlled shear stress or shear deformation on a sample and measures the flow properties such as shear viscosity, loss modulus and storage modulus through steady shear and oscillatory experiments.

Hazard Identification

✓ High temperature measurement → The pressure cell and the pressure cell head can become very hot; therefore precaution must be taken to avoid touching the external area of these units. Hand protection (thermal isolation gloves) must be worn when working.

✓ Low temperature measurements → The pressure cell and the pressure cell head can become very cold; therefore precaution must be taken to avoid touching the external area of these units. Hand protection (thermal isolation gloves) must be worn when working.

✓ High pressure measurements → The pressure in the pressure cell may be as high as 150 bar. The sudden discharge of pressure from the rupture disc attached to the pressure cell can occur at sonic velocity and cause violent noises. The user and any bystanders when handling the pressure cell must wear ear protection.

✓ The solvents used include, but are not limited to, toluene, pentane, tetrahydrofuran (THF), heptanes, etc. The MSDS for these solvents can be found in the MSDS Binder located in Lab 6-128. Care must be taken when working with solvents. Viton gloves are recommended when working with toluene and Silver Shield/4H laminated gloves when working with THF.

✓ Cleaning the rheometer after doing measurements → when cleaning the rheometer parts (e.g., plates, bob and cup, spatulas, etc.) with organic solvents such as toluene or THF, this must be done under the fume hood. When cleaning the rheometer (which cannot be moved to the fume hood area) the use of respiratory mask is mandatory and other researchers working in the vicinity must be alerted. The respiratory masks can be found in lab 6-133 in a drawer labeled "Masks Respirators".

Training Required

Proper training should be taken before using high pressure Physica MCR 301 Anton Paar rheometer, which can be instructed by the lab manager and/or the current researcher working with the unit.

Control/Protective Measures:

1. The use of lab coat, gloves, and safety glasses is mandatory.

2. Safety goggles and thermal isolation gloves must be worn when handling liquid nitrogen or touching hot or cold surfaces.

3. Safety gas mask should be used when cleaning rheometer outside the fume hood area.

4. The user and any bystanders when applying higher than atmospheric pressures must wear ear protection.

Emergency Procedures

The possible emergency situations that can be present are:

✓ If the high pressure air supplies present problems (e.g., the air compressor in the CME building stop working or is not working properly) the rheometer must be stopped and turned off. The rheometer bearing will be damaged if there is no air circulating through them. The pressure in the rheometer's pressure regulator must be ~ 5 bar.

✓ If when running analysis at high temperatures (e.g., T >200 °C), a strong smell is perceived in the lab, other researchers and/or members present in the lab must be alerted, so they will use air masks or leave the lab.

Step-by-Step Procedure of the Process

Rheology Procedures

1. The valve that connects the unit with the line of the compressed air must be open (Figure A-1). The pressure in the rheometer's regulator should be about 5 bar.

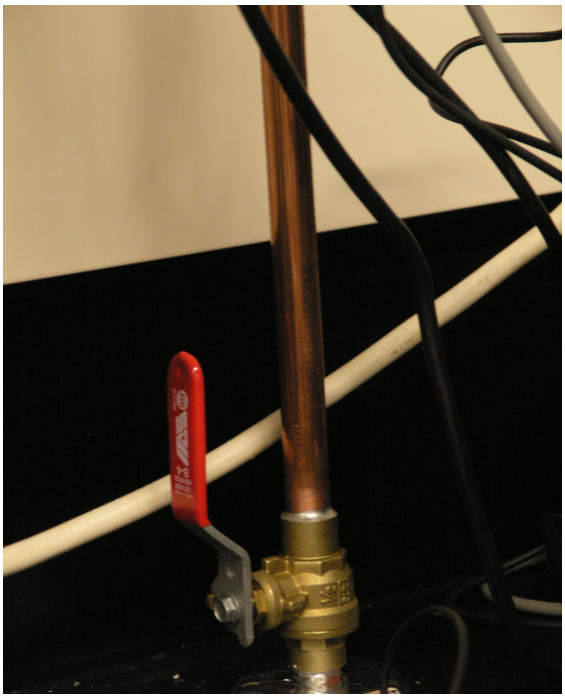

Figure A- 1. Compressed air line connected to the rheometer

Compressed air line connected to the rheometer

2. Turn on the rheometer

✓ If the Peltier system is in operation, turn on the cooling bath circulator and select the temperature according to the desired analysis (Figure A-2).

Figure A- 2. Cooling bath circulator

✓ If the electrical system is in operation, the cooling bath circulator is not connected to the system, so there is no need to turn it on. In this case, turn on the air cooler which is attached to the unit.

3. Attach the magnetic coupling to the rheometer head. Open the pressure head and attach the geometry that you are going to use (bob, double gap inside cylinder or plate) to the pressure head (Figures A-3 to A-7).

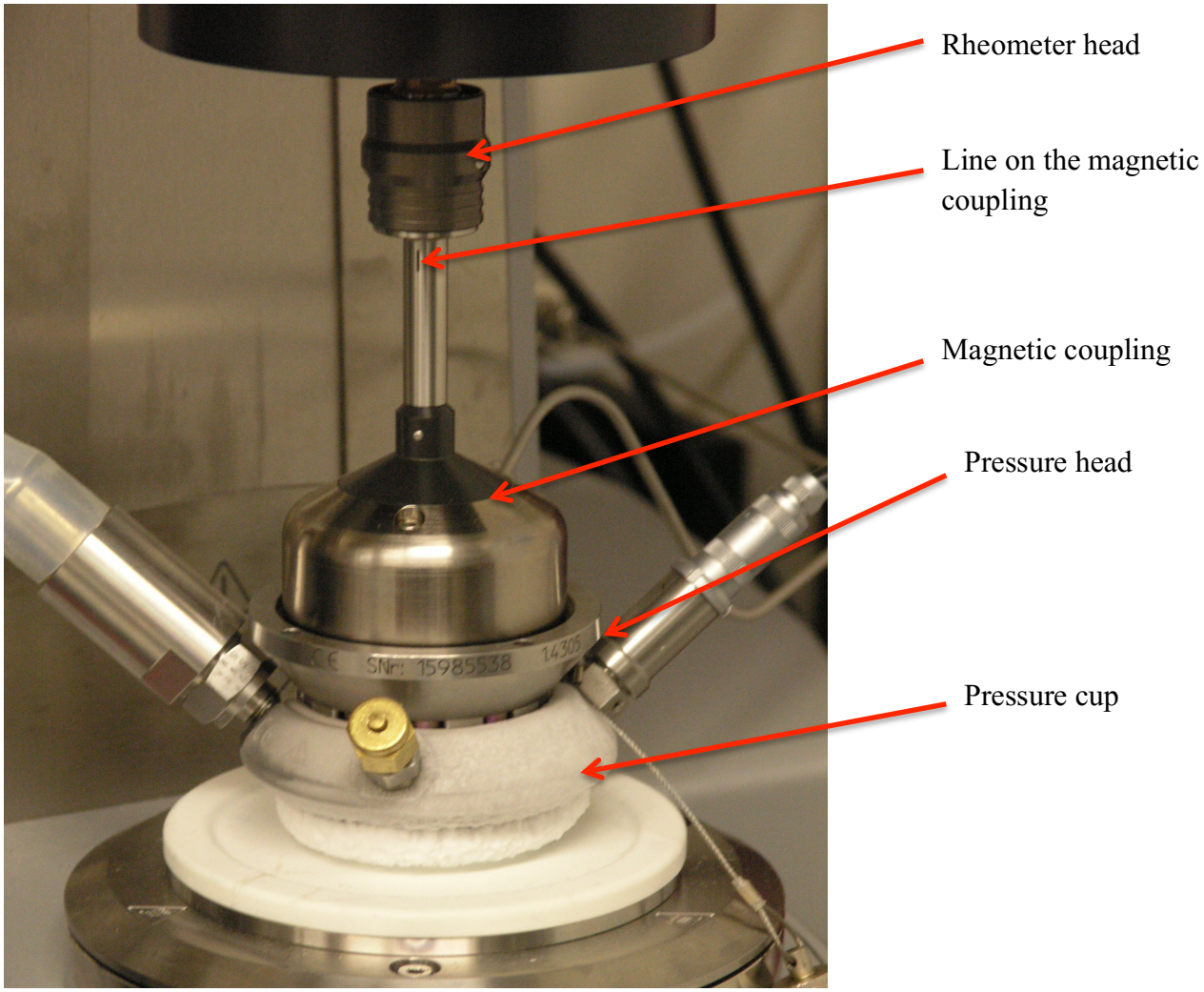

Figure A- 3. Rheometer parts

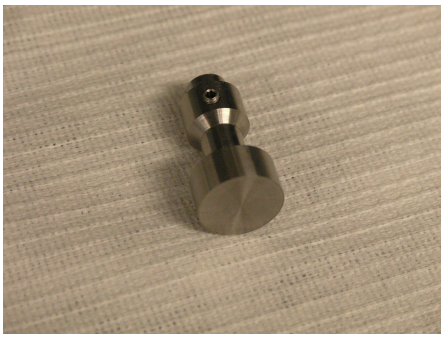

Figure A- 4. Upper plate of the parallel plate measuring system

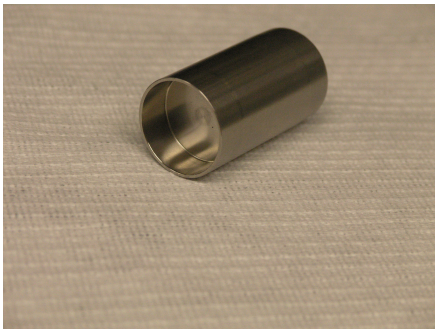

Figure A- 5. The cup of the parallel plate measuring system

Figure A- 6. Double gap cylinder geometry

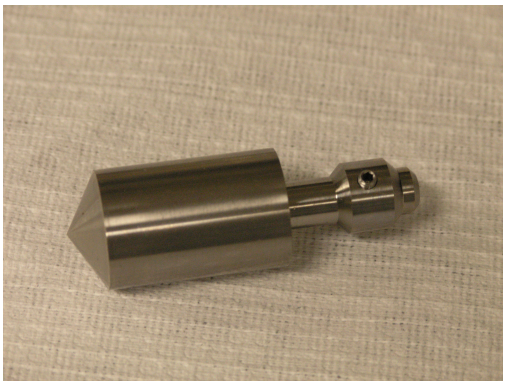

Figure A- 7. Bob of the concentric cylinder measuring system

✓ If you are using the parallel plate cup, take the pressure cup out and put the parallel plate cup inside the pressure cup and tighten it from the bottom of the pressure cup. Then mount the pressure cup again on the instrument. Mount the pressure head on the pressure cup and fasten it with the two hole turner.

✓ If you are using the concentric cylinder, put the cylinder cup inside the pressure cup. Mount the pressure head on the pressure cup and fasten it with the two hole turner.

✓ If you are using double gap cylinder, you should not put the cup inside the pressure cup in this stage. Mount the pressure head on the pressure cup and fasten it with the two hole turner.

Note: Apply some grease on the outer surface of any cup that you want to put inside the pressure cup.

4. Open the rheology software

✓ On the toolbar click on the “Device” and then on the “Control panel”.

✓ On the window that pops up click on the “initialize”.

✓ Go to “Configuration” tab and select the type of measuring system (CC25: Concentric cylinder, DG23.04: Double Gap cylinder, PP20&08: Parallel plate). Also select the heating system (C-ETD300 for Electrical or C-PTD200 for peltier) that you are using in the measuring cell section of the “Configuration” tab.

✓ Go to “Service” tab and click on the “Measuring system” in the “Inertia” section.

Note: For inertia check, the rheometer head is at the highest position.

✓ Go to the “Control panel” tab and click on “Reset normal force” and wait for a few seconds. The normal force shown on the rheometer screen and also on the rheometer software will be zero. (The rheometer head is still at the highest position.)

✓ On the “Control panel”, click on “measuring position”. The rheometer head will come down.

✓ On the rheometer push the “Online” button so that the light next to this button goes off (Figure A-8). Then with up and down buttons on the rheometer try to change the position of the rheometer head until the normal force shown on the rheometer screen becomes in the range of ±0.1 Nm. Then push “Online” again so that the light goes on again.

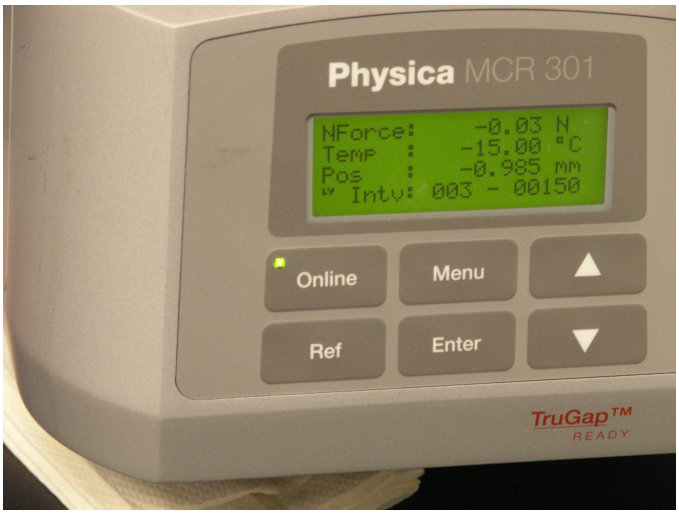

Figure A- 8. Rheometer screen

✓ Go to "Service" tab and click on "Motor adjustment". An air check can be performed to check the condition of the mechanical bearing in the pressure head. To do the air check, click on "New workbook" in the toolbar and then go to the "Support" tab and select "air check pressure cell". Then click on "Go to calibration position". Then follow the instructions given previously to make the normal force get in the range of ±0.1 Nm. Then click on "perform the air check".

In case you are using the double gap cylinder, insert the double gap cup into the pressure cup after performing the motor adjustment.

✓ At the end of motor adjustment, the magnetic coupling should not be disconnected from the pressure head. Disconnect the magnetic coupling from the rheometer head and go to the highest (reference) position[1]. Then open the pressure head together with the magnetic coupling to load the sample:

[1] Anton Paar, Technical Note, "Guidelines for the Pressure cell".

❖ For the double gap cylinder, load 2.37 ml of sample using a syringe into the rheometer.

❖ For the concentric cylinder, load 16 ml of sample using a syringe into the rheometer.

❖ For the parallel plate, load the sample on the upper plate OR make a mold from the sample and then put it in the parallel plate cup.

✓ Close the pressure head together with the magnetic coupling.

✓ On the software, in the control panel click on "Go to measuring position". Align the line on the rheometer head to the line on the magnetic coupling (Figure A-3).

✓ Follow the instructions given previously to make the normal force come in the range of ±0.1 Nm.

✓ On the control panel, set the desired temperature and wait until thermal equilibrium is reached.

✓ On the toolbar click on "New workbook" and select the kind of experiment you are going to perform.

✓ When the new workbook comes up, you can change the parameters related to steady shear and/or oscillatory experiment as well as temperature profile in the measurement window, which can be reached in the toolbar.

✓ According to the experiment selected, choose the temperature profile

- Isothermal
- Increasing or decreasing temperature
- Temperature profile

✓ It is recommended to let the sample reach thermal equilibrium for 30 minutes before starting the measurement.

✓ To start the experiment click on "Run" on the toolbar of the workbook.

Applying Pressure[2]

✓ As soon as the pressure head is mounted on the pressure cup, pressure can be supplied.

✓ Wear safety goggles and ear protection when applying pressure.

✓ Before applying pressure, the pressure cell has to be correctly filled and then tightly sealed.

✓ The gas for generating pressure should not react with the sample. Nitrogen gas or pressurized air is recommended.

✓ The pressure provided by the pressure bottle must not exceed 150 bar.

✓ The pressure bottle must permit releasing the pressure. Use e.g. a 3-way cock for applying and discharging pressure.

✓ To apply pressure, the valve that connects the pressure line of the pressure cell to the forced leading-off pressure outlet (Outlet valve) must be closed first and then the valve that connects the pressure bottle to the rheometer (Inlet valve) must be opened (Figure A-9). Then open the pressure regulator valve on the pressure bottle (Figure A-10).

✓ At the end of a measurement the pressure must always be released before opening the pressure cell. The cell or the pressure connection may be opened only

[2] Anton Paar, Instruction manual, pressure cell.

if the overpressure inside the cell has been completely discharged, so it equals the atmospheric pressure. To release the pressure, the pressure regulator valve on the pressure bottle must be closed. Then the valve that connects the pressure line of the pressure cell to the forced leading-off pressure outlet must be opened carefully and very slowly. At the end, the valve that connects the pressure bottle to the rheometer must be closed.

- ✓ The maximum allowable pressure that can be applied is 150 bar.

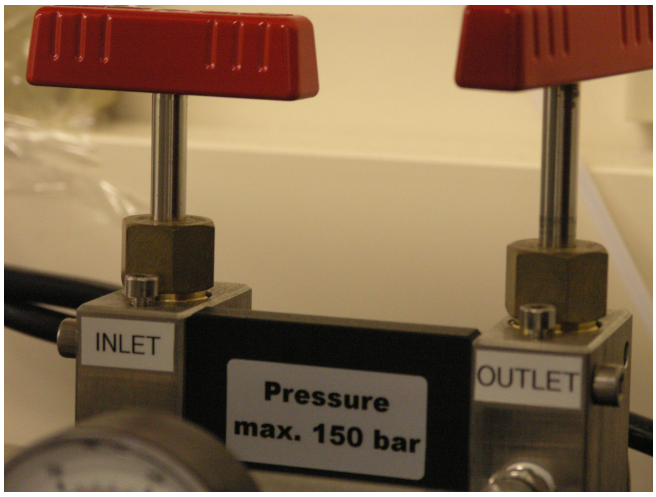

Figure A- 9. Inlet and outlet pressure valves on the rheometer

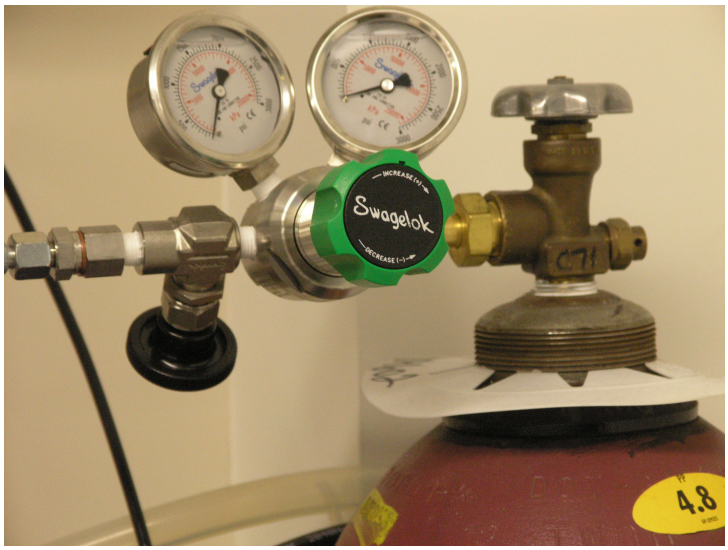

Figure A- 10. Pressure regulator on the pressure bottle (compressed liquid Nitrogen)

Hazardous Waste Disposal Procedures

✓ Organic waste such as toluene, crude oil samples, etc., must be disposed in the organic waste bottle located inside the fume hood. When the bottle is full, report to the lab manager (Mildred Becerra, Labs 6-128 & 6-133) who will submit a request to the Environmental, Health and Safety Department – Hazardous Waste Disposal, for its disposal.

✓ Disposable syringes after use must be disposed in the plastic/needle container. When the container is full, report to the lab manager (Mildred Becerra, Labs 6-128 & 6-133) who will submit a request to the Environmental, Health and Safety Department – Hazardous Waste Disposal, for its disposal.

Equipment Maintenance Procedures

✓ The filter on the dry-point membrane drier must be exchanged every year or when the indicator on the drier shows warning, whichever happens earlier. The contact information of Anton Paar is:

www.anton-paar.com

E-mail: info.de@anton-paar.com OR jean-francois.tremblay@anton-paar.com

✓ The friction resulting from the mechanical bearing in the pressure head needs to be checked regularly (a daily check is recommended) through "Motor adjustment" and "Air check" which is explained in detail in the previous sections. If the results of the torque measurements are values more than ±150 μNm, then the ball bearings inside the pressure head need to be changed.

✓ Under normal conditions the rupture disc attached to the pressure head must be replaced every year. Extreme measuring conditions may require a more frequent period of changing[3].

✓ The O-ring gasket between the pressure cup and the pressure head has to be checked before every measurement for intact condition and correct seat in the groove. If it shows signs of wear, it must be replaced.

✓ The cooling bath circulator refrigerant level must be monitored. In case more liquid is needed a solution 50/50 volume% ethylene glycol/distillated water must be added.

✓ The rheometer's parts (magnetic coupling, concentric cylinder, double gap cylinder, parallel plates, screwdriver, etc.) must be placed back in their respective cases.

[3] Anton Paar, Instruction manual, pressure cell.

Appendix 2. Supplementary Data

Table S- 1. Shear thinning behavior of Maya oil[a].

T = 254 K		T = 258 K		T = 263 K	
$\dot{\gamma}$ /s^{-1}	μ/(Pa.s)	$\dot{\gamma}$ /s^{-1}	μ/(Pa.s)	$\dot{\gamma}$ /s^{-1}	μ/(Pa.s)
2.67	882	2.57	482	10	106
3.15	769	3.12	425	15.3	80.5
3.61	689	3.65	383	20.6	67.7
4.01	641	4.18	350	25.9	59.2
		4.71	322	31.2	53.2
		5.24	299	36.5	48.8
		5.76	283	41.8	45.2
		6.29	267	47.1	42.3
		6.82	254	52.4	39.9
		7.35	240	57.6	37.9
		7.88	227	62.9	36.1
		8.41	218	68.2	34.5
		8.94	208	73.5	33.1
		9.47	199	78.8	31.7
		10	194		
T = 268 K		T = 273 K		T = 278 K	
$\dot{\gamma}$ /s^{-1}	μ/(Pa.s)	$\dot{\gamma}$ /s^{-1}	μ/(Pa.s)	$\dot{\gamma}$ /s^{-1}	μ/(Pa.s)
10	49.5	10	20.5	10	8.5
15.3	39.3	15.3	17.4	15.3	7.64
20.6	34	20.6	15.6	20.6	7.13
25.9	30.3	25.9	14.3	25.9	6.74
31.2	27.6	31.2	13.4	31.2	6.44
36.5	25.6	36.5	12.6	36.5	6.19
41.8	23.9	41.8	12	41.8	5.98
47.1	22.6	47.1	11.5	47.1	5.80
52.4	21.5	52.4	11	52.4	5.63
57.6	20.5	57.6	10.6	57.6	5.49
62.9	19.7	62.9	10.3	62.9	5.36
68.2	18.9	68.2	9.95	68.2	5.24
73.5	18.2	73.5	9.67	73.5	5.13
78.8	17.6	78.8	9.41	78.8	5.03
84.1	17.1	84.1	9.18	84.1	4.94
89.4	16.5	89.4	8.96	89.4	4.85
94.7	16.1	94.7	8.76	94.7	4.77
100	15.7	100	8.58	100	4.70
144	13.4	144	8.55	144	4.27
189	11.8	189	7.56	189	3.96
		233	6.83	233	3.7
		278	6.25	278	3.48
		322	5.78	322	3.3
		367	5.38	367	3.13
		411	5.04	411	2.99
		456	4.74	456	2.86
		500	4.48	500	2.75
T = 283 K		T = 288 K		T = 293 K	
$\dot{\gamma}$ /s^{-1}	μ/(Pa.s)	$\dot{\gamma}$ /s^{-1}	μ/(Pa.s)	$\dot{\gamma}$ /s^{-1}	μ/(Pa.s)
10	3.7	10	1.58	10	0.997
15.3	3.47	15.3	1.57	15.3	0.986

20.6	3.32	20.6	1.54	20.6	0.979
25.9	3.21	25.9	1.53	25.9	0.97
31.2	3.12	31.2	1.52	31.2	0.96
36.5	3.05	36.5	1.51	36.5	0.955
41.8	2.99	41.8	1.5	41.8	0.945
47.1	2.93	47.1	1.49	47.1	0.942
52.4	2.88	52.4	1.48	52.4	0.933
57.6	2.84	57.6	1.47	57.6	0.929
62.9	2.8	62.9	1.46	62.9	0.923
68.2	2.76	68.2	1.46	68.2	0.919
73.5	2.72	73.5	1.45	73.5	0.915
78.8	2.69	78.8	1.44	78.8	0.911
84.1	2.66	84.1	1.43	84.1	0.908
89.4	2.63	89.4	1.43	89.4	0.903
94.7	2.6	94.7	1.42	94.7	0.899
100	2.57	100	1.41	100	0.896
144	2.42	144	1.36	144	0.871
189	2.29	189	1.32	189	0.852
233	2.18	233	1.28	233	0.833
278	2.09	278	1.25	278	0.817
322	2.01	322	1.22	322	0.803
367	1.93	367	1.19	367	0.789
411	1.87	411	1.16	411	0.776
456	1.81	456	1.14	456	0.763
500	1.75	500	1.11	500	0.752

T = 298 K		T = 303 K		T = 308 K	
$\dot{\gamma}$ /s^{-1}	μ/(Pa.s)	$\dot{\gamma}$ /s^{-1}	μ/(Pa.s)	$\dot{\gamma}$ /s^{-1}	μ/(Pa.s)
10	0.689	10	0.375	10	0.259
15.3	0.672	15.3	0.378	15.3	0.263
20.6	0.669	20.6	0.377	20.6	0.264
25.9	0.663	25.9	0.377	25.9	0.264
31.2	0.657	31.2	0.377	31.2	0.265
36.5	0.655	36.5	0.376	36.5	0.264
41.8	0.65	41.8	0.376	41.8	0.264
47.1	0.644	47.1	0.374	47.1	0.266
52.4	0.642	52.4	0.375	52.4	0.263
57.6	0.639	57.6	0.375	57.6	0.263
62.9	0.636	62.9	0.373	62.9	0.264
68.2	0.632	68.2	0.373	68.2	0.263
73.5	0.629	73.5	0.373	73.5	0.263
78.8	0.627	78.8	0.372	78.8	0.263
84.1	0.625	84.1	0.371	84.1	0.262
89.4	0.622	89.4	0.371	89.4	0.264
94.7	0.619	94.7	0.371	94.7	0.263
100	0.617	100	0.371	100	0.262
144	0.602	144	0.366	144	0.261
189	0.59	189	0.363	189	0.259
233	0.579	233	0.359	233	0.257
278	0.569	278	0.357	278	0.255
322	0.56	322	0.354	322	0.254
367	0.552	367	0.351	367	0.253
411	0.544	411	0.349	411	0.251
456	0.537	456	0.346	456	0.25
500	0.53	500	0.344	500	0.249

T = 313 K		T = 318 K		T = 323 K	
$\dot{\gamma}$ /s^{-1}	μ/(Pa.s)	$\dot{\gamma}$ /s^{-1}	μ/(Pa.s)	$\dot{\gamma}$ /s^{-1}	μ/(Pa.s)
10	0.183	10	0.134	10	0.108
15.3	0.186	15.3	0.138	15.3	0.104
20.6	0.188	20.6	0.14	20.6	0.105

25.9	0.188	25.9	0.138	25.9	0.103
31.2	0.188	31.2	0.138	31.2	0.104
36.5	0.189	36.5	0.14	36.5	0.105
41.8	0.189	41.8	0.139	41.8	0.104
47.1	0.19	47.1	0.142	47.1	0.106
52.4	0.19	52.4	0.14	52.4	0.107
57.6	0.189	57.6	0.139	57.6	0.106
62.9	0.189	62.9	0.139	62.9	0.105
68.2	0.189	68.2	0.14	68.2	0.105
73.5	0.189	73.5	0.14	73.5	0.105
78.8	0.189	78.8	0.14	78.8	0.105
84.1	0.189	84.1	0.14	84.1	0.106
89.4	0.189	89.4	0.139	89.4	0.106
94.7	0.19	94.7	0.139	94.7	0.106
100	0.189	100	0.139	100	0.106
144	0.188	144	0.139	144	0.105
189	0.187	189	0.139	189	0.106
233	0.187	233	0.139	233	0.105
278	0.186	278	0.139	278	0.105
322	0.185	322	0.138	322	0.105
367	0.184	367	0.138	367	0.105
411	0.184	411	0.138	411	0.105
456	0.183	456	0.137	456	0.105
500	0.183	500	0.137	500	0.104
T = 328 K		T = 333 K		T = 338 K	
$\dot{\gamma}$ /s^{-1}	μ/(Pa.s)	$\dot{\gamma}$ /s^{-1}	μ/(Pa.s)	$\dot{\gamma}$ /s^{-1}	μ/(Pa.s)
10	0.0772	10	0.0564	10	0.0428
15.3	0.0759	15.3	0.0589	15.3	0.0456
20.6	0.0794	20.6	0.0587	20.6	0.0516
25.9	0.078	25.9	0.0604	25.9	0.0512
31.2	0.0792	31.2	0.0598	31.2	0.051
36.5	0.0796	36.5	0.061	36.5	0.0491
41.8	0.0801	41.8	0.0611	41.8	0.05
47.1	0.0806	47.1	0.0627	47.1	0.0497
52.4	0.0806	52.4	0.0624	52.4	0.0506
57.6	0.0809	57.6	0.0628	57.6	0.0498
62.9	0.0804	62.9	0.063	62.9	0.051
68.2	0.0804	68.2	0.0636	68.2	0.0513
73.5	0.0808	73.5	0.0636	73.5	0.0501
78.8	0.0812	78.8	0.0631	78.8	0.0516
84.1	0.0809	84.1	0.0632	84.1	0.0504
89.4	0.0812	89.4	0.0637	89.4	0.0502
94.7	0.0809	94.7	0.0632	94.7	0.0505
100	0.0812	100	0.0642	100	0.0507
144	0.0812	144	0.0635	144	0.0508
189	0.0808	189	0.0636	189	0.0508
233	0.081	233	0.0633	233	0.0508
278	0.0811	278	0.0635	278	0.0509
322	0.081	322	0.0637	322	0.0508
367	0.0808	367	0.0635	367	0.0509
411	0.0808	411	0.0636	411	0.0509
456	0.0807	456	0.0636	456	0.0508
500	0.0807	500	0.0635	500	0.0509

[a] Standard uncertainties u: u(T) = 0.02 K, u($\dot{\gamma}$) = 0.003$\dot{\gamma}$, u(μ) = 0.03 μ.

Table S- 2. Temperature dependence of reduced enclosed area for Maya oil obtained from the hysteresis technique measurements[a].

T /K	$\bar{A}$ /Pa
308	0.08
303	0.42
298	0.85
293	2.32
288	4.93
283	14.79
278	30.95
273	58.30
268	138.91
263	228.41
258	310.69

[a] Standard uncertainty: $u(T) = 0.02$ K, Combined standard uncertainty: $u_c(\bar{A}) = 0.004\ \bar{A}$.

Table S- 3. Impact of rest period on hysteresis area for Maya oil at 278 K[a].

Rest time (hr)	A/(Pa/s)
0.25	4,594
0.5	4,697
1	5,018
3	7459
20	8,465
24	8,252
120	11140
600	12204

[a] Combined standard uncertainty: $u_c(A) = 0.003\ A$.

Table S- 4. Build-up behavior of Maya oil after a step-down in shear rate from (40 to 10) s^{-1} [a].

T = 278 K		T = 273 K		T = 268 K	
Time (sec)	□/Pa	Time (sec)	□/Pa	Time (sec)	□/Pa
0.00	31.72	0.00	67.58	0.00	140.6
0.33	32.14	0.33	69.38	0.33	147.5
0.67	32.24	0.67	70.08	0.67	150.1
1.00	32.35	1.00	70.51	1.00	151.8
1.33	32.38	1.33	70.87	1.33	153.1
1.67	32.5	1.67	71.13	1.67	154.1
2.00	32.53	2.00	71.42	2.00	154.9
2.33	32.61	2.33	71.58	2.33	155.6
2.67	32.59	2.67	71.79	2.67	156.2
3.00	32.64	3.00	71.9	3.00	156.8
3.33	32.64	3.33	72.04	3.33	157.3
3.67	32.68	3.67	72.17	3.67	157.7
4.00	32.72	4.00	72.38	4.00	158.1
4.33	32.72	4.33	72.48	4.33	158.5
4.67	32.77	4.67	72.51	4.67	158.9
5.00	32.75	5.00	72.64	5.00	159.2
5.33	32.81	5.33	72.73	5.33	159.5
5.67	32.8	5.67	72.82	5.67	159.7
6.00	32.83	6.00	72.87	6.00	160.1

6.33	32.85	6.33	72.98	6.33	160.3
6.67	32.87	6.67	73.02	6.67	160.6
7.00	32.84	7.00	73.11	7.00	160.8
7.33	32.84	7.33	73.14	7.33	161.1
7.67	32.89	7.67	73.21	7.67	161.4
8.00	32.87	8.00	73.3	8.00	161.4
8.33	32.92	8.33	73.32	8.33	161.6
8.67	32.92	8.67	73.38	8.67	161.7
9.00	32.97	9.00	73.4	9.00	162
9.33	32.96	9.33	73.52	9.33	162.1
9.67	32.98	9.67	73.52	9.67	162.3
10.00	33	10.00	73.64	10.00	162.4
10.33	32.96	10.33	73.63	10.33	162.6
10.67	32.97	10.67	73.67	10.67	162.8
11.00	32.96	11.00	73.73	11.00	163
11.33	32.99	11.33	73.74	11.33	163
11.67	32.97	11.67	73.79	11.67	163.2
12.00	33.02	12.00	73.83	12.00	163.3
12.33	33	12.33	73.89	12.33	163.4
12.67	33.01	12.67	73.88	12.67	163.6
13.00	33.01	13.00	73.95	13.00	163.7
13.33	33.01	13.33	73.95	13.33	163.8
13.67	33.01	13.67	74	13.67	163.9
14.00	33.14	14.00	74.01	14.00	164.1
14.33	33.18	14.33	74.07	14.33	164.2
14.67	33.1	14.67	74.1	14.67	164.3
15.00	33.09	15.00	74.14	15.00	164.4
15.33	33.07	15.33	74.17	15.33	164.5
15.67	33.13	15.67	74.16	15.67	164.6
16.00	33.13	16.00	74.26	16.00	164.8
16.33	33.13	16.33	74.28	16.33	164.9
16.67	33.1	16.67	74.3	16.67	164.9
17.00	33.14	17.00	74.28	17.00	165
17.33	33.14	17.33	74.33	17.33	165
17.67	33.22	17.67	74.38	17.67	165.2
18.00	33.14	18.00	74.44	18.00	165.2
18.33	33.12	18.33	74.43	18.33	165.4
18.67	33.19	18.67	74.42	18.67	165.4
19.00	33.2	19.00	74.44	19.00	165.5
19.33	33.2	19.33	74.43	19.33	165.6
19.67	33.16	19.67	74.48	19.67	165.7
20.00	33.17	20.00	74.47	20.00	165.8
20.33	33.2	20.33	74.52	20.33	165.8
20.67	33.19	20.67	74.53	20.67	165.9
21.00	33.23	21.00	74.58	21.00	166
21.33	33.18	21.33	74.56	21.33	166.1
21.67	33.19	21.67	74.56	21.67	166.2
22.00	33.21	22.00	74.58	22.00	166.2
22.33	33.22	22.33	74.62	22.33	166.3
22.67	33.19	22.67	74.62	22.67	166.3
23.00	33.26	23.00	74.65	23.00	166.4
23.33	33.22	23.33	74.7	23.33	166.5
23.67	33.36	23.67	74.72	23.67	166.6
24.00	33.22	24.00	74.76	24.00	166.6
24.33	33.22	24.33	74.8	24.33	166.7
24.67	33.21	24.67	74.85	24.67	166.7
25.00	33.19	25.00	74.84	25.00	166.8
25.33	33.23	25.33	74.83	25.33	166.9
25.67	33.21	25.67	74.82	25.67	166.9
26.00	33.21	26.00	74.82	26.00	167
26.33	33.19	26.33	74.9	26.33	167

26.67	33.26	26.67	74.92	26.67	167.1
27.00	33.24	27.00	74.88	27.00	167.1
27.33	33.25	27.33	74.86	27.33	167.2
27.67	33.28	27.67	74.97	27.67	167.3
28.00	33.28	28.00	74.96	28.00	167.4
28.33	33.27	28.33	75.03	28.33	167.3
28.67	33.28	28.67	75	28.67	167.5
29.00	33.28	29.00	75.01	29.00	167.5
29.33	33.32	29.33	75	29.33	167.5
29.67	33.42	29.67	74.99	29.67	167.6
30.00	33.37	30.00	75.04	30.00	167.7
30.33	33.32	30.33	75.04	30.33	167.7
30.67	33.31	30.67	75.07	30.67	167.7
31.00	33.39	31.00	75.1	31.00	167.8
31.33	33.5	31.33	75.09	31.33	167.8
31.67	33.26	31.67	75.14	31.67	167.9
32.00	33.29	32.00	75.18	32.00	167.9
32.33	33.25	32.33	75.15	32.33	168
32.67	33.29	32.67	75.15	32.67	168
33.00	33.28	33.00	75.17	33.00	168.1
33.33	33.31	33.33	75.15	33.33	168.1
33.67	33.28	33.67	75.2	33.67	168.1
34.00	33.29	34.00	75.21	34.00	168.3
34.33	33.29	34.33	75.22	34.33	168.3
34.67	33.28	34.67	75.22	34.67	168.3
35.00	33.31	35.00	75.23	35.00	168.3
35.33	33.31	35.33	75.22	35.33	168.4
35.67	33.39	35.67	75.27	35.67	168.4
36.00	33.3	36.00	75.28	36.00	168.5
36.33	33.34	36.33	75.31	36.33	168.5
36.67	33.29	36.67	75.33	36.67	168.5
37.00	33.33	37.00	75.3	37.00	168.6
37.33	33.31	37.33	75.32	37.33	168.6
37.67	33.34	37.67	75.36	37.67	168.7
38.00	33.32	38.00	75.36	38.00	168.7
38.33	33.33	38.33	75.33	38.33	168.7
38.67	33.36	38.67	75.34	38.67	168.8
39.00	33.33	39.00	75.37	39.00	168.9
39.33	33.37	39.33	75.38	39.33	169
39.67	33.39	39.67	75.41	39.67	168.9
40.00	33.35	40.00	75.44	40.00	168.9
40.33	33.32	40.33	75.42	40.33	169
40.67	33.35	40.67	75.38	40.67	169
41.00	33.34	41.00	75.47	41.00	169
41.33	33.39	41.33	75.41	41.33	169.2
41.67	33.45	41.67	75.45	41.67	169.1
42.00	33.38	42.00	75.51	42.00	169.2
42.33	33.39	42.33	75.51	42.33	169.1
42.67	33.52	42.67	75.49	42.67	169.2
43.00	33.42	43.00	75.49	43.00	169.2
43.33	33.39	43.33	75.5	43.33	169.3
43.67	33.39	43.67	75.57	43.67	169.3
44.00	33.55	44.00	75.59	44.00	169.3
44.33	33.35	44.33	75.53	44.33	169.4
44.67	33.34	44.67	75.55	44.67	169.4
45.00	33.37	45.00	75.58	45.00	169.5
45.33	33.44	45.33	75.56	45.33	169.5
45.67	33.43	45.67	75.65	45.67	169.5
46.00	33.42	46.00	75.56	46.00	169.5
46.33	33.38	46.33	75.58	46.33	169.6
46.67	33.39	46.67	75.57	46.67	169.6

47.00	33.37	47.00	75.63	47.00	169.7
47.33	33.43	47.33	75.56	47.33	169.7
47.67	33.37	47.67	75.63	47.67	169.6
48.00	33.4	48.00	75.58	48.00	169.7
48.33	33.39	48.33	75.62	48.33	169.7
48.67	33.4	48.67	75.62	48.67	169.8
49.00	33.42	49.00	75.64	49.00	169.8
49.33	33.41	49.33	75.64	49.33	169.9
49.67	33.43	49.67	75.62	49.67	169.8
50.00	33.4	50.00	75.65	50.00	169.9
50.33	33.43	50.33	75.64	50.33	169.9
50.67	33.41	50.67	75.75	50.67	169.9
51.00	33.47	51.00	75.7	51.00	170
51.33	33.4	51.33	75.7	51.33	170
51.67	33.42	51.67	75.74	51.67	170
52.00	33.42	52.00	75.7	52.00	170.1
52.33	33.41	52.33	75.69	52.33	170.1
52.67	33.43	52.67	75.78	52.67	170.1
53.00	33.42	53.00	75.78	53.00	170.2
53.33	33.42	53.33	75.79	53.33	170.2
53.67	33.41	53.67	75.73	53.67	170.2
54.00	33.42	54.00	75.72	54.00	170.2
54.33	33.48	54.33	75.8	54.33	170.2
54.67	33.38	54.67	75.78	54.67	170.3
55.00	33.4	55.00	75.83	55.00	170.3
55.33	33.38	55.33	75.82	55.33	170.4
55.67	33.4	55.67	75.79	55.67	170.3
56.00	33.4	56.00	75.76	56.00	170.4
56.33	33.39	56.33	75.79	56.33	170.4
56.67	33.41	56.67	75.81	56.67	170.4
57.00	33.38	57.00	75.79	57.00	170.4
57.33	33.39	57.33	75.82	57.33	170.5
57.67	33.41	57.67	75.8	57.67	170.5
58.00	33.43	58.00	75.87	58.00	170.5
58.33	33.39	58.33	75.8	58.33	170.5
58.67	33.37	58.67	75.85	58.67	170.6
59.00	33.4	59.00	75.82	59.00	170.6
59.33	33.38	59.33	75.84	59.33	170.6
59.67	33.4	59.67	75.85	59.67	170.7
60.00	33.44	60.00	75.99	60.00	170.6
60.33	33.58	60.33	75.89	60.33	170.7
60.67	33.54	60.67	75.89	60.67	170.7
61.00	33.51	61.00	75.91	61.00	170.8
61.33	33.49	61.33	75.85	61.33	170.8
61.67	33.51	61.67	75.91	61.67	170.7
62.00	33.48	62.00	75.89	62.00	170.9
62.33	33.48	62.33	75.91	62.33	170.8
62.67	33.49	62.67	75.98	62.67	170.9
63.00	33.5	63.00	75.93	63.00	170.8
63.33	33.46	63.33	76.01	63.33	170.9
63.67	33.49	63.67	75.99	63.67	170.9
64.00	33.51	64.00	75.95	64.00	171
64.33	33.52	64.33	76	64.33	170.9
64.67	33.48	64.67	75.99	64.67	171
65.00	33.49	65.00	75.98	65.00	171.1
65.33	33.47	65.33	75.99	65.33	171
65.67	33.48	65.67	75.97	65.67	171.1
66.00	33.47	66.00	76.02	66.00	171
66.33	33.48	66.33	75.98	66.33	171.1
66.67	33.5	66.67	76	66.67	171.1
67.00	33.44	67.00	76	67.00	171.1

67.33	33.47	67.33	76.02	67.33	171.1
67.67	33.44	67.67	76.03	67.67	171.2
68.00	33.47	68.00	76.02	68.00	171.2
68.33	33.43	68.33	76.03	68.33	171.2
68.67	33.47	68.67	76.03	68.67	171.2
69.00	33.46	69.00	76.08	69.00	171.2
69.33	33.46	69.33	76.1	69.33	171.4
69.67	33.46	69.67	76.09	69.67	171.3
70.00	33.47	70.00	76.08	70.00	171.3
70.33	33.5	70.33	76.05	70.33	171.3
70.67	33.45	70.67	76.04	70.67	171.3
71.00	33.49	71.00	76.07	71.00	171.3
71.33	33.46	71.33	76.08	71.33	171.4
71.67	33.49	71.67	76.06	71.67	171.4
72.00	33.47	72.00	76.09	72.00	171.4
72.33	33.49	72.33	76.06	72.33	171.4
72.67	33.49	72.67	76.1	72.67	171.4
73.00	33.54	73.00	76.04	73.00	171.5
73.33	33.61	73.33	76.1	73.33	171.4
73.67	33.51	73.67	76.09	73.67	171.5
74.00	33.52	74.00	76.11	74.00	171.5
74.33	33.51	74.33	76.12	74.33	171.6
74.67	33.54	74.67	76.11	74.67	171.5
75.00	33.51	75.00	76.14	75.00	171.6
75.33	33.55	75.33	76.08	75.33	171.6
75.67	33.61	75.67	76.14	75.67	171.6
76.00	33.57	76.00	76.11	76.00	171.6
76.33	33.55	76.33	76.15	76.33	171.7
76.67	33.56	76.67	76.11	76.67	171.7
77.00	33.53	77.00	76.11	77.00	171.7
77.33	33.55	77.33	76.14	77.33	171.7
77.67	33.6	77.67	76.14	77.67	171.7
78.00	33.55	78.00	76.15	78.00	171.7
78.33	33.58	78.33	76.17	78.33	171.7
78.67	33.59	78.67	76.2	78.67	171.8
79.00	33.56	79.00	76.15	79.00	171.8
79.33	33.58	79.33	76.18	79.33	171.8
79.67	33.6	79.67	76.19	79.67	171.8
80.00	33.61	80.00	76.24	80.00	171.8
80.33	33.58	80.33	76.23	80.33	171.8
80.67	33.57	80.67	76.2	80.67	171.8
81.00	33.53	81.00	76.17	81.00	171.9
81.33	33.6	81.33	76.2	81.33	171.8
81.67	33.5	81.67	76.21	81.67	171.9
82.00	33.59	82.00	76.18	82.00	172
82.33	33.59	82.33	76.23	82.33	172
82.67	33.62	82.67	76.25	82.67	172
83.00	33.55	83.00	76.25	83.00	172

[a] Standard uncertainties u: u(T) = 0.03 K, u(□) = 0.0005 □

Table S- 4. Continued.

T = 263 K		T = 258 K	
Time (sec)	□/Pa	Time (sec)	□/Pa
0.00	301.3	0.00	543.9
0.33	323.9	0.33	595.8
0.67	331.9	0.67	599.2
1.00	337.2	1.00	616.1
1.33	341	1.33	628.2
1.67	343.9	1.67	637.7
2.00	346.3	2.00	644.7

2.33	348.2	2.33	650.4
2.67	350	2.67	655.2
3.00	351.4	3.00	659.2
3.33	353	3.33	662.9
3.67	354	3.67	666
4.00	355.2	4.00	668.9
4.33	356.1	4.33	671.4
4.67	356.9	4.67	673.8
5.00	357.8	5.00	676
5.33	358.6	5.33	677.9
5.67	359.3	5.67	679.8
6.00	360	6.00	681.5
6.33	360.7	6.33	683.2
6.67	361.2	6.67	684.7
7.00	361.9	7.00	686.2
7.33	362.4	7.33	687.5
7.67	363	7.67	688.8
8.00	363.4	8.00	690.1
8.33	363.9	8.33	691.2
8.67	364.5	8.67	692.3
9.00	364.8	9.00	693.3
9.33	365.3	9.33	694.3
9.67	365.6	9.67	695.3
10.00	366	10.00	696.2
10.33	366.4	10.33	697.1
10.67	366.8	10.67	698
11.00	367.1	11.00	698.8
11.33	367.5	11.33	699.6
11.67	367.8	11.67	700.3
12.00	368.1	12.00	701.1
12.33	368.4	12.33	701.8
12.67	368.7	12.67	702.5
13.00	369	13.00	703.1
13.33	369.2	13.33	703.8
13.67	369.5	13.67	704.5
14.00	369.8	14.00	705.1
14.33	370.1	14.33	705.7
14.67	370.3	14.67	706.2
15.00	370.6	15.00	706.8
15.33	370.8	15.33	707.4
15.67	371	15.67	707.9
16.00	371.3	16.00	708.5
16.33	371.5	16.33	709
16.67	371.7	16.67	709.5
17.00	371.9	17.00	710
17.33	372.1	17.33	710.5
17.67	372.3	17.67	711
18.00	372.6	18.00	711.4
18.33	372.7	18.33	711.9
18.67	372.9	18.67	712.4
19.00	373.1	19.00	712.9
19.33	373.3	19.33	713.3
19.67	373.5	19.67	713.8
20.00	373.7	20.00	714
20.33	373.8	20.33	714.5
20.67	373.9	20.67	714.9
21.00	374.2	21.00	715.2
21.33	374.3	21.33	715.6
21.67	374.5	21.67	715.9
22.00	374.7	22.00	716.3
22.33	374.8	22.33	716.7

22.67	375.1	22.67	716.9
23.00	375.1	23.00	717.2
23.33	375.2	23.33	717.7
23.67	375.4	23.67	717.9
24.00	375.6	24.00	718.2
24.33	375.6	24.33	718.6
24.67	375.8	24.67	718.8
25.00	375.9	25.00	719.2
25.33	376.1	25.33	719.5
25.67	376.2	25.67	719.8
26.00	376.3	26.00	720
26.33	376.4	26.33	720.3
26.67	376.6	26.67	720.6
27.00	376.8	27.00	721
27.33	376.8	27.33	721.1
27.67	377	27.67	721.4
28.00	377.1	28.00	721.7
28.33	377.3	28.33	721.9
28.67	377.4	28.67	722.2
29.00	377.5	29.00	722.4
29.33	377.5	29.33	722.7
29.67	377.6	29.67	723
30.00	377.8	30.00	723.3
30.33	377.8	30.33	723.5
30.67	378	30.67	723.7
31.00	378.1	31.00	724
31.33	378.2	31.33	724.3
31.67	378.3	31.67	724.5
32.00	378.5	32.00	724.7
32.33	378.5	32.33	724.9
32.67	378.6	32.67	725.2
33.00	378.7	33.00	725.4
33.33	378.8	33.33	725.6
33.67	378.9	33.67	725.9
34.00	379	34.00	726
34.33	379.1	34.33	726.3
34.67	379.1	34.67	726.5
35.00	379.3	35.00	726.7
35.33	379.3	35.33	726.8
35.67	379.5	35.67	727
36.00	379.6	36.00	727.2
36.33	379.6	36.33	727.4
36.67	379.7	36.67	727.6
37.00	379.8	37.00	727.8
37.33	379.9	37.33	728
37.67	379.9	37.67	728.2
38.00	380.1	38.00	728.4
38.33	380.1	38.33	728.6
38.67	380.2	38.67	728.7
39.00	380.3	39.00	729
39.33	380.4	39.33	729.1
39.67	380.4	39.67	729.3
40.00	380.5	40.00	729.5
40.33	380.6	40.33	729.6
40.67	380.7	40.67	729.8
41.00	380.8	41.00	730
41.33	380.9	41.33	730.3
41.67	380.9	41.67	730.5
42.00	380.9	42.00	730.6
42.33	381.1	42.33	730.8
42.67	381.1	42.67	731

43.00	381.2	43.00	731.2
43.33	381.3	43.33	731.3
43.67	381.3	43.67	731.4
44.00	381.4	44.00	731.6
44.33	381.5	44.33	731.7
44.67	381.5	44.67	732
45.00	381.6	45.00	732.1
45.33	381.7	45.33	732.3
45.67	381.7	45.67	732.4
46.00	381.9	46.00	732.5
46.33	381.9	46.33	732.7
46.67	381.9	46.67	732.8
47.00	382	47.00	733
47.33	382	47.33	733.2
47.67	382.1	47.67	733.3
48.00	382.2	48.00	733.4
48.33	382.3	48.33	733.6
48.67	382.3	48.67	733.7
49.00	382.5	49.00	733.9
49.33	382.4	49.33	733.9
49.67	382.5	49.67	734.1
50.00	382.6	50.00	734.3
50.33	382.6	50.33	734.4
50.67	382.7	50.67	734.6
51.00	382.7	51.00	734.7
51.33	382.8	51.33	734.8
51.67	382.9	51.67	734.9
52.00	382.9	52.00	735
52.33	382.9	52.33	735.2
52.67	383	52.67	735.3
53.00	383.1	53.00	735.4
53.33	383.2	53.33	735.5
53.67	383.1	53.67	735.6
54.00	383.2	54.00	735.8
54.33	383.4	54.33	735.9
54.67	383.3	54.67	735.9
55.00	383.4	55.00	736.1
55.33	383.4	55.33	736.2
55.67	383.5	55.67	736.4
56.00	383.5	56.00	736.4
56.33	383.6	56.33	736.5
56.67	383.6	56.67	736.6
57.00	383.7	57.00	736.8
57.33	383.7	57.33	736.8
57.67	383.7	57.67	737
58.00	383.8	58.00	737.1
58.33	383.8	58.33	737.2
58.67	383.9	58.67	737.4
59.00	383.9	59.00	737.5
59.33	384	59.33	737.6
59.67	384	59.67	737.7
60.00	384.1	60.00	737.8
60.33	384.1	60.33	737.8
60.67	384.2	60.67	738
61.00	384.2	61.00	738.1
61.33	384.3	61.33	738.2
61.67	384.3	61.67	738.2
62.00	384.4	62.00	738.4
62.33	384.4	62.33	738.5
62.67	384.4	62.67	738.6
63.00	384.6	63.00	738.7

63.33	384.5	63.33	738.8
63.67	384.6	63.67	738.9
64.00	384.6	64.00	739
64.33	384.7	64.33	739.2
64.67	384.8	64.67	739.3
65.00	384.7	65.00	739.3
65.33	384.8	65.33	739.5
65.67	384.8	65.67	739.6
66.00	385	66.00	739.6
66.33	384.9	66.33	739.7
66.67	385	66.67	739.9
67.00	385	67.00	739.9
67.33	385.1	67.33	740.1
67.67	385	67.67	740.1
68.00	385.1	68.00	740.2
68.33	385.2	68.33	740.3
68.67	385.2	68.67	740.5
69.00	385.4	69.00	740.5
69.33	385.3	69.33	740.6
69.67	385.4	69.67	740.7
70.00	385.3	70.00	740.9
70.33	385.5	70.33	740.9
70.67	385.5	70.67	741
71.00	385.5	71.00	741.2
71.33	385.5	71.33	741.3
71.67	385.5	71.67	741.4
72.00	385.6	72.00	741.4
72.33	385.6	72.33	741.5
72.67	385.7	72.67	741.7
73.00	385.7	73.00	741.7
73.33	385.7	73.33	741.8
73.67	385.7	73.67	741.9
74.00	385.9	74.00	742
74.33	385.9	74.33	742.1
74.67	385.9	74.67	742.2
75.00	385.9	75.00	742.3
75.33	386	75.33	742.3
75.67	386	75.67	742.4
76.00	386	76.00	742.4
76.33	386	76.33	742.6
76.67	386	76.67	742.6
77.00	386.1	77.00	742.7
77.33	386.1	77.33	742.8
77.67	386.2	77.67	742.9
78.00	386.2	78.00	743
78.33	386.3	78.33	743
78.67	386.3	78.67	743.1
79.00	386.3	79.00	743.1
79.33	386.4	79.33	743.2
79.67	386.4	79.67	743.2
80.00	386.4	80.00	743.3
80.33	386.4	80.33	743.3
80.67	386.5	80.67	743.3
81.00	386.5	81.00	743.5
81.33	386.6	81.33	743.6
81.67	386.5	81.67	743.5
82.00	386.6	82.00	743.6
82.33	386.6	82.33	743.7
82.67	386.7	82.67	743.7
83.00	386.7	83.00	743.8

Table S- 5. Change of transient shear stress over time during start-up measurements at 273 K, where a 30 s^{-1} shear rate was imposed on a Maya oil sample formerly at rest. Rest time prior to start-up is a parameter. All samples were pre-sheared at 50 s^{-1} for 5 min[a].

Rest time = 5 min		Rest time = 15 min		Rest time = 30 min	
Time (min)	□/Pa	Time (min)	□/Pa	Time (min)	□/Pa
5.12	460.7	15.12	483.6	30.12	501.9
5.23	439.2	15.23	455.3	30.23	470.9
5.35	432.5	15.35	447.4	30.35	461.7
5.47	428.5	15.47	442.1	30.47	455.6
5.58	425.7	15.58	438.5	30.58	451.3
5.7	423.6	15.7	435.7	30.7	448
5.82	422	15.82	433.3	30.82	445.3
5.93	420.6	15.93	431.5	30.93	443.1
6.05	419.5	16.05	429.8	31.05	441.1
6.17	418.5	16.17	428.4	31.17	439.5
6.28	417.6	16.28	427.2	31.28	438
6.4	416.8	16.4	426.1	31.4	436.7
6.52	416.2	16.52	425.2	31.52	435.5
6.63	415.5	16.63	424.2	31.63	434.4
6.75	414.9	16.75	423.4	31.75	433.4
6.87	414.5	16.87	422.6	31.87	432.5
6.98	414	16.98	421.9	31.98	431.6
7.1	413.5	17.1	421.3	32.1	430.8
7.22	413.1	17.22	420.7	32.22	430.1
7.33	412.7	17.33	420	32.33	429.3
7.45	412.3	17.45	419.5	32.45	428.8
7.57	412	17.57	419	32.57	428.1
7.68	411.6	17.68	418.5	32.68	427.5
7.8	411.3	17.8	418	32.8	426.9
7.92	411	17.92	417.7	32.92	426.4
8.03	410.8	18.03	417.2	33.03	425.9
8.15	410.4	18.15	416.8	33.15	425.4
8.27	410.2	18.27	416.4	33.27	424.9
8.38	410	18.38	416.1	33.38	424.5
8.5	409.7	18.5	415.7	33.5	424
8.62	409.5	18.62	415.4	33.62	423.6
8.73	409.3	18.73	415	33.73	423.2
8.85	409	18.85	414.7	33.85	422.8
8.97	408.8	18.97	414.5	33.97	422.4
9.08	408.6	19.08	414.1	34.08	422.1
9.2	408.4	19.2	413.9	34.2	421.7
9.32	408.2	19.32	413.5	34.32	421.3
9.43	408	19.43	413.3	34.43	421
9.55	407.8	19.55	413	34.55	420.7
9.67	407.6	19.67	412.8	34.67	420.4
9.78	407.4	19.78	412.5	34.78	420.1
9.9	407.3	19.9	412.3	34.9	419.8
10.02	407.1	20.02	412.1	35.02	419.5
10.13	406.9	20.13	411.8	35.13	419.3
10.25	406.8	20.25	411.6	35.25	418.9
10.37	406.6	20.37	411.4	35.37	418.7
10.48	406.5	20.48	411.2	35.48	418.4
10.6	406.2	20.6	411	35.6	418.2
10.72	406.1	20.72	410.7	35.72	417.9
10.83	405.9	20.83	410.5	35.83	417.7

[a] Standard uncertainties: u(□) = 0.0005 □

Table S- 5. Continued

Rest time = 1 hr		Rest time = 2 hr	
Time (min)	□/Pa	Time (min)	□/Pa
60.12	516.1	120.1	517
60.23	483.9	120.2	481.5
60.35	473	120.4	470.9
60.47	466.3	120.5	464
60.58	461.6	120.6	459
60.7	457.8	120.7	455.1
60.82	454.8	120.8	451.9
60.93	452.3	120.9	449.2
61.05	450.1	121.1	447
61.17	448.2	121.2	444.9
61.28	446.5	121.3	443.1
61.4	445	121.4	441.4
61.52	443.7	121.5	440
61.63	442.4	121.6	438.7
61.75	441.2	121.8	437.5
61.87	440.2	121.9	436.3
61.98	439.2	122	435.2
62.1	438.3	122.1	434.2
62.22	437.4	122.2	433.3
62.33	436.7	122.3	432.4
62.45	435.9	122.5	431.6
62.57	435.2	122.6	430.8
62.68	434.5	122.7	430.1
62.8	433.9	122.8	429.4
62.92	433.2	122.9	428.7
63.03	432.7	123	428
63.15	432	123.2	427.4
63.27	431.6	123.3	426.9
63.38	431	123.4	426.3
63.5	430.5	123.5	425.8
63.62	430.1	123.6	425.2
63.73	429.6	123.7	424.7
63.85	429.1	123.9	424.2
63.97	428.7	124	423.8
64.08	428.3	124.1	423.3
64.2	427.8	124.2	422.9
64.32	427.5	124.3	422.4
64.43	427.1	124.4	422
64.55	426.7	124.6	421.6
64.67	426.3	124.7	421.3
64.78	426	124.8	420.8
64.9	425.6	124.9	420.4
65.02	425.3	125	420.1
65.13	425	125.1	419.8
65.25	424.7	125.3	419.4
65.37	424.3	125.4	419.1
65.48	424.1	125.5	418.8
65.6	423.7	125.6	418.4
65.72	423.5	125.7	418.1
65.83	423.2	125.8	417.8

Table S- 6. Effect of rest time on stress decay during start-up experiments, where shear rate of 30 s^{-1} was imposed on samples formerly at rest. All samples were pre-sheared at 50 s^{-1} for 5 min. Temperature is a parameter[a].

T = 258 K		T = 263 K		T = 268 K	
Rest time (min)	□□Pa	Rest time (min)	□□Pa	Rest time (min)	□□Pa
5	431	5	414	5	169.3
15	577	15	549	15	227
30	745	30	640	30	264
60	787	60	732	60	296
120	923	120	818	120	327

T = 273 K		T = 278 K	
Rest time (min)	□□Pa	Rest time (min)	□□Pa
5	54.8	5	16
15	73.1	15	20.6
30	84.2	30	23
60	92.9	60	28.3
120	99.2	120	30.62

[a] Standard uncertainties u: u(T) = 0.03 K, u(□□) = 0.0005 □□.

Table S- 7. Apparent viscosity values of Maya oil at different T, P and shear rates[a].

T = 258 K, P = 0.95 bar		T = 258 K, P = 20.5 bar		T = 258 K, P = 40.5 bar	
$\dot{\gamma}$ /s^{-1}	□/(Pa.s)	$\dot{\gamma}$ /s^{-1}	□/(Pa.s)	$\dot{\gamma}$ /s^{-1}	□/(Pa.s)
2.6	238.5	2.6	253	2.6	263
4.45	201.7	4.45	214	4.45	221.6
6.3	165.5	6.3	180.9	6.3	183.3
8.15	140.1	8.15	157.8	8.15	159
10	123.1	10	143.5	10	144.5

T = 258 K, P = 61 bar		T = 258 K, P = 76.5 bar		T = 258 K, P = 99.5 bar	
$\dot{\gamma}$ /s^{-1}	□/(Pa.s)	$\dot{\gamma}$ /s^{-1}	□/(Pa.s)	$\dot{\gamma}$ /s^{-1}	□/(Pa.s)
2.6	278	2.6	289.5	2.6	306.7
4.45	234.8	4.45	244.1	4.45	260.6
6.3	195	6.3	201.4	6.3	217.5
8.15	172.1	8.15	175.2	8.15	190.1
10	158.4	10	163.5	10	170.4

T = 258 K, P = 121.5 bar		T = 258 K, P = 140.5 bar		T = 268 K, P = 0.95 bar	
$\dot{\gamma}$ /s^{-1}	□/(Pa.s)	$\dot{\gamma}$ /s^{-1}	□/(Pa.s)	$\dot{\gamma}$ /s^{-1}	□/(Pa.s)
4.45	286.8	4.45	310.9	9.998	25.45
6.3	234	6.3	257.7	32.5	20.19
8.15	207	8.15	229.8	55	16.95
10	189.7	10	205.1	77.5	15.39
				100	14.2

T = 268 K, P = 20.6 bar		T = 268 K, P = 40.4 bar		T = 268 K, P = 62.4 bar	
$\dot{\gamma}$ /s^{-1}	□/(Pa.s)	$\dot{\gamma}$ /s^{-1}	□/(Pa.s)	$\dot{\gamma}$ /s^{-1}	□/(Pa.s)
9.998	26.49	9.998	27.25	9.998	28.9
32.5	21.7	32.5	22.25	32.5	23.42

55	18.81	55	19.4	55	20.28
77.5	16.79	77.5	17.44	77.5	18.01
100	15.08	100	15.88	100	16.52
T = 268 K, P = 81.8 bar		T = 268 K, P = 103.7 bar		T = 268 K, P = 126.5 bar	
$\dot{\gamma}$ /s^{-1}	η/(Pa.s)	$\dot{\gamma}$ /s^{-1}	η/(Pa.s)	$\dot{\gamma}$ /s^{-1}	η/(Pa.s)
9.998	30.12	9.995	29.62	9.995	30.99
32.5	24.29	32.5	25.19	32.5	26.3
55	20.91	55	21.96	55.01	22.88
77.5	18.96	77.5	20.11	77.5	20.92
100	17.1	100	18.02	100	19.15
T = 268 K, P = 139 bar		T = 278 K, P = 0.95 bar		T = 278 K, P = 20.8 bar	
$\dot{\gamma}$ /s^{-1}	η/(Pa.s)	$\dot{\gamma}$ /s^{-1}	η/(Pa.s)	$\dot{\gamma}$ /s^{-1}	η/(Pa.s)
9.998	34.04	9.999	4.891	9.999	5.114
32.5	27.19	57.5	4.204	57.5	4.519
55	23.35	105	3.847	105	4.214
77.5	21.23	152.5	3.561	152.5	3.98
100	19.17	200	3.184	200	3.794
T = 278 K, P = 41.1 bar		T = 278 K, P = 61.4 bar		T = 278 K, P = 81.3 bar	
$\dot{\gamma}$ /s^{-1}	η/(Pa.s)	$\dot{\gamma}$ /s^{-1}	η/(Pa.s)	$\dot{\gamma}$ /s^{-1}	η/(Pa.s)
9.999	5.348	9.999	5.614	9.999	5.899
57.5	4.717	57.5	4.938	57.5	5.177
105	4.394	105	4.593	105	4.808
152.5	4.147	152.5	4.329	152.5	4.523
200	3.936	200	4.103	200	4.282
T = 278 K, P = 102.3 bar		T = 278 K, P = 126 bar		T = 278 K, P = 147 bar	
$\dot{\gamma}$ /s^{-1}	η/(Pa.s)	$\dot{\gamma}$ /s^{-1}	η/(Pa.s)	$\dot{\gamma}$ /s^{-1}	η/(Pa.s)
9.999	6.225	9.999	6.629	9.999	7.117
57.5	5.449	57.5	5.771	57.5	6.15
105	5.051	105	5.335	105	5.651
152.5	4.743	152.5	5	152.5	5.269
200	4.484	200	4.716	200	4.953
T = 283 K, P = 0.95 bar		T = 283 K, P = 21.5 bar		T = 283 K, P = 41.9 bar	
$\dot{\gamma}$ /s^{-1}	η/(Pa.s)	$\dot{\gamma}$ /s^{-1}	η/(Pa.s)	$\dot{\gamma}$ /s^{-1}	η/(Pa.s)
9.999	3.011	9.999	3.357	9.999	3.493
57.5	2.521	57.5	2.825	57.5	2.939
105	2.339	105	2.584	105	2.684
152.5	2.186	152.5	2.42	152.5	2.509
200	2.046	200	2.292	200	2.374
T = 283 K, P = 61.6 bar		T = 283 K, P = 81.9 bar		T = 283 K, P = 105.5 bar	
$\dot{\gamma}$ /s^{-1}	η/(Pa.s)	$\dot{\gamma}$ /s^{-1}	η/(Pa.s)	$\dot{\gamma}$ /s^{-1}	η/(Pa.s)
9.999	3.659	9.999	3.822	9.999	4.138
57.5	3.07	57.5	3.209	57.5	3.425
105	2.799	105	2.921	105	3.091
152.5	2.614	152.5	2.727	152.5	2.862
200	2.47	200	2.576	200	2.683
T = 283 K, P = 123 bar		T = 283 K, P = 160.5 bar		T = 293 K, P = 0.95 bar	
$\dot{\gamma}$ /s^{-1}	η/(Pa.s)	$\dot{\gamma}$ /s^{-1}	η/(Pa.s)	$\dot{\gamma}$ /s^{-1}	η/(Pa.s)
9.999	4.677	9.999	5.064	9.999	1.024
57.5	3.673	57.5	3.962	57.5	0.9361
105	3.266	105	3.533	105	0.8967

152.5	3.001	152.5	3.261	152.5	0.8664
200	2.805	200	3.063	200	0.8424

T = 293 K, P = 22.5 bar		T = 293 K, P = 43 bar		T = 293 K, P = 63.8 bar	
$\dot{\gamma}$ /s^{-1}	η/(Pa.s)	$\dot{\gamma}$ /s^{-1}	η/(Pa.s)	$\dot{\gamma}$ /s^{-1}	η/(Pa.s)
9.999	1.048	9.999	1.08	9.999	1.127
57.5	0.9602	57.5	1.003	57.5	1.049
105	0.9224	105	0.9619	105	1.005
152.5	0.8937	152.5	0.9314	152.5	0.9729
200	0.8711	200	0.9063	200	0.9465

T = 293 K, P = 83.5 bar		T = 293 K, P = 102.9 bar		T = 293 K, P = 127 bar	
$\dot{\gamma}$ /s^{-1}	η/(Pa.s)	$\dot{\gamma}$ /s^{-1}	η/(Pa.s)	$\dot{\gamma}$ /s^{-1}	η/(Pa.s)
9.999	1.182	9.999	1.254	9.999	1.318
57.5	1.099	57.5	1.162	57.5	1.215
105	1.05	105	1.104	105	1.158
152.5	1.016	152.5	1.064	152.5	1.118
200	0.9877	200	1.033	200	1.087

T = 293 K, P = 149 bar		T = 313 K, P = 0.88 bar		T = 313 K, P = 21.2 bar	
$\dot{\gamma}$ /s^{-1}	η/(Pa.s)	$\dot{\gamma}$ /s^{-1}	η/(Pa.s)	$\dot{\gamma}$ /s^{-1}	η/(Pa.s)
9.999	1.406	9.998	0.2047	9.999	0.1997
57.5	1.29	57.51	0.1995	57.51	0.1986
105	1.226	105	0.1995	105	0.1967
152.5	1.182	152.5	0.1984	152.5	0.1959
200	1.147	200	0.1956	200	0.1946

T = 313 K, P = 38.2 bar		T = 313 K, P = 61.7 bar		T = 313 K, P = 82.8 bar	
$\dot{\gamma}$ /s^{-1}	η/(Pa.s)	$\dot{\gamma}$ /s^{-1}	η/(Pa.s)	$\dot{\gamma}$ /s^{-1}	η/(Pa.s)
9.999	0.2009	9.999	0.214	9.999	0.2276
57.51	0.2053	57.51	0.2138	57.51	0.2231
105	0.2042	105	0.2121	105	0.2216
152.5	0.2028	152.5	0.2105	152.5	0.2198
200	0.2021	200	0.2092	200	0.2181

T = 313 K, P = 102.7 bar		T = 313 K, P = 127.1 bar		T = 313 K, P = 151.5 bar	
$\dot{\gamma}$ /s^{-1}	η/(Pa.s)	$\dot{\gamma}$ /s^{-1}	η/(Pa.s)	$\dot{\gamma}$ /s^{-1}	η/(Pa.s)
9.999	0.2404	9.999	0.248	9.999	0.266
57.51	0.2342	57.51	0.2464	57.51	0.264
105	0.2312	105	0.2438	105	0.261
152.5	0.2288	152.5	0.2412	152.5	0.2572
200	0.2271	200	0.2391	200	0.2546

T = 333 K, P = 0.95 bar		T = 333 K, P = 20.5 bar		T = 333 K, P = 41.6 bar	
$\dot{\gamma}$ /s^{-1}	η/(Pa.s)	$\dot{\gamma}$ /s^{-1}	η/(Pa.s)	$\dot{\gamma}$ /s^{-1}	η/(Pa.s)
57.52	0.06908	57.52	0.07046	57.52	0.07125
105	0.06834	105	0.07038	105	0.07141
152.5	0.07136	152.5	0.06975	152.5	0.07154
200	0.07041	200	0.06977	200	0.07116

T = 333 K, P = 62.3 bar		T = 333 K, P = 81 bar		T = 333 K, P = 101.3 bar	
$\dot{\gamma}$ /s^{-1}	η/(Pa.s)	$\dot{\gamma}$ /s^{-1}	η/(Pa.s)	$\dot{\gamma}$ /s^{-1}	η/(Pa.s)
57.52	0.07346	57.52	0.07595	57.52	0.08131
105	0.07395	105	0.07732	105	0.07884
152.5	0.07396	152.5	0.07636	152.5	0.07953
200	0.07423	200	0.07642	200	0.07902

T = 333 K, P = 124.5 bar		T = 333 K, P = 149.6 bar	
$\dot{\gamma}$ /s^{-1}	□/(Pa.s)	$\dot{\gamma}$ /s^{-1}	□/(Pa.s)
57.52	0.08545	57.51	0.08861
105	0.08331	105	0.08803
152.5	0.08199	152.5	0.08752
200	0.08223	200	0.08733

[a] Standard uncertainties u: u(T) = 0.02 K, u(P) = 0.01 bar, u($\dot{\gamma}$) = 0.003$\dot{\gamma}$, u(□) = 0.03 □.

Table S- 8. Comparison between the equivalent effects of pressure and temperature. The viscosity at T_{ref} and P is the same as the viscosity at P_{atm} and T. Shear rate is 10 s^{-1}. * Shear rate: 57.52 s^{-1} [a].

T_{ref} = 258 K		T_{ref} = 268 K		T_{ref} = 278 K		T_{ref} = 283 K	
T_{ref} - T (K)	P - P_{atm} (Pa)	T_{ref} - T (K)	P - P_{atm} (Pa)	T_{ref} - T (K)	P - P_{atm} (Pa)	T_{ref} - T (K)	P - P_{atm} (Pa)
0	0	0	0	0.2801	0	0	0
0.9331	19.55	0.2637	19.65	0.5607	19.85	1.1367	20.55
0.9752	39.55	0.4496	39.45	0.8644	40.15	1.5494	40.95
1.5307	60.05	0.8351	61.45	1.1736	60.45	2.0304	60.65
1.7218	75.55	1.1057	80.85	1.5086	80.35	2.4804	80.95
1.9706	98.55	0.9962	102.75	1.8993	101.35	3.2970	104.55
2.6143	120.55	1.2916	125.55	2.3392	125.05	4.5463	122.05
3.0806	139.55	1.9029	138.05	0.2801	146.05	5.3515	159.55

T_{ref} = 293 K		T_{ref} = 313 K		T_{ref} = 333 K*	
T_{ref} - T (K)	P - P_{atm} (Pa)	T_{ref} - T (K)	P - P_{atm} (Pa)	T_{ref} - T (K)	P - P_{atm} (Pa)
0	0	0	0	0	0
0.2222	21.55	-0.3285	20.32	0.3964	19.55
0.5102	42.05	-0.2489	37.32	0.6194	40.65
0.9171	62.85	0.5885	60.82	1.2288	61.35
1.3710	82.55	1.4010	81.92	1.8914	80.05
1.9322	101.95	2.1190	101.82	3.2386	100.35
2.4030	126.05	2.5259	126.22	4.2128	123.55
3.0120	148.05	3.4381	150.62	4.9215	148.65

[a] Standard uncertainties u: u(T) = 0.03 K, u(P) = 0.01 bar.

Table S- 9. Pressure dependence of the non-Newtonian index (NN-Index) at different temperatures[a].

T = 258 K		T = 268 K		T = 278 K	
P(bar)	NN-Index/(Pa.s^2)	P(bar)	NN-Index/(Pa.s^2)	P(bar)	NN-Index/(Pa.s^2)
0.95	9.1600	0.95	0.089496	0.95	0.005578
20.5	9.1424	20.6	0.083352	20.8	0.004732
40.5	9.9195	40.4	0.085470	41.1	0.005022
61	10.2280	62.4	0.093857	61.4	0.005377
76.5	10.8491	81.8	0.099144	81.3	0.005748
99.5	11.1321	103.7	0.080690	102.3	0.006183
121.5	13.2741	126.5	0.084943	126	0.006818
140.5	13.6251	139	0.115219	147	0.007707

T = 283 K		T = 293 K		T = 313 K	
P(bar)	NN-Index/(Pa.s^2)	P(bar)	NN-Index/(Pa.s^2)	P(bar)	NN-Index/(Pa.s^2)
0.95	0.003672	0.95	0.000678	0.88	3.466E-05

21.5	0.004080	22.5	0.000671	21.2	1.361E-05
41.9	0.004264	43	0.000617	38.2	2.500E-05
61.6	0.004532	63.8	0.000633	61.7	1.018E-05
81.9	0.004734	83.5	0.000679	82.8	3.396E-05
105.5	0.005509	102.9	0.000765	102.7	4.869E-05
123	0.007512	127	0.000829	127.1	2.174E-05
160.5	0.008174	149	0.000931	151.5	2.734E-05

T = 333 K	
P(bar)	NN-Index/(Pa.s^2)
0.95	1.003E-05
20.5	3.022E-06
41.6	1.530E-06
62.3	4.261E-06
81	9.787E-06
101.3	1.919E-05
124.5	2.073E-05
149.6	6.339E-06

[a] Standard uncertainties u: u(T) = 0.02 K, u(P) = 0.01 bar.

Table S- 10. Apparent viscosity values for Maya crude oil + 5.11 wt% n-heptane at different T and shear rates[a].

T = 258 K		T = 268 K		T = 273 K	
$\dot{\gamma}$ /s^{-1}	η/(Pa.s)	$\dot{\gamma}$ /s^{-1}	η/(Pa.s)	$\dot{\gamma}$ /s^{-1}	η/(Pa.s)
5	112	9.997	18.36	9.998	8.551
13.75	81.35	57.51	10.32	57.5	5.594
22.5	63	105	8.028	105	4.598
31.25	52.69	152.5	6.797	152.5	4.009
40	45.88	200	5.986	200	3.603

T = 278 K		T = 283 K		T = 293 K	
$\dot{\gamma}$ /s^{-1}	η/(Pa.s)	$\dot{\gamma}$ /s^{-1}	η/(Pa.s)	$\dot{\gamma}$ /s^{-1}	η/(Pa.s)
9.999	3.348	9.999	1.795	9.999	0.5104
57.5	2.669	57.5	1.505	57.51	0.4817
105	2.374	105	1.376	105	0.4648
152.5	2.181	152.5	1.288	152.5	0.453
200	2.036	200	1.221	200	0.4429

T = 313 K		T = 333 K	
$\dot{\gamma}$ /s^{-1}	η/(Pa.s)	$\dot{\gamma}$ /s^{-1}	η/(Pa.s)
9.998	0.1065	9.999	0.04455
57.51	0.1097	57.52	0.03956
105	0.1095	105	0.03899
152.5	0.1086	152.5	0.03847
200	0.1079	200	0.03878

[a] Standard uncertainties u: u(T) = 0.02 K, u($\dot{\gamma}$) = 0.003$\dot{\gamma}$, u(η) = 0.03 η.

Table S- 11. Apparent viscosity values for Maya crude oil + 10.03 wt% n-heptane at different T and shear rates[a].

T = 258 K		T = 268 K		T = 273 K	
$\dot{\gamma}$ /s^{-1}	η/(Pa.s)	$\dot{\gamma}$ /s^{-1}	η/(Pa.s)	$\dot{\gamma}$ /s^{-1}	η/(Pa.s)
9.996	36.11	9.998	8	9.998	3.506

57.52	15.01	57.51	4.449	57.5	2.398
105	10.7	105	3.471	105	2.013
152.5	8.606	152.5	2.94	152.5	1.784
200	7.306	200	2.594	200	1.623
T = 278 K		*T* = 283 K		*T* = 293 K	
$\dot{\gamma}$ /s^{-1}	η/(Pa.s)	$\dot{\gamma}$ /s^{-1}	η/(Pa.s)	$\dot{\gamma}$ /s^{-1}	η/(Pa.s)
9.998	8	9.999	0.746	9.999	0.2348
57.51	4.449	57.5	0.6514	57.51	0.2266
105	3.471	105	0.6061	105	0.2213
152.5	2.94	152.5	0.5752	152.5	0.2163
200	2.594	200	0.5517	200	0.2128
T = 313 K		*T* = 333 K			
$\dot{\gamma}$ /s^{-1}	η/(Pa.s)	$\dot{\gamma}$ /s^{-1}	η/(Pa.s)		
9.999	0.05365	9.999	0.02896		
57.52	0.05733	57.52	0.02139		
105	0.05733	105	0.02234		
152.5	0.05771	152.5	0.02242		
200	0.05774	200	0.02251		

[a] Standard uncertainties u: u(T) = 0.02 K, u($\dot{\gamma}$) = 0.003$\dot{\gamma}$, u(η) = 0.03 η.

Table S- 12. Apparent viscosity values for Maya crude oil + 20.18 wt% n-heptane at different T and shear rates[a].

T = 258 K		*T* = 268 K		*T* = 273 K	
$\dot{\gamma}$ /s^{-1}	η/(Pa.s)	$\dot{\gamma}$ /s^{-1}	η/(Pa.s)	$\dot{\gamma}$ /s^{-1}	η/(Pa.s)
9.997	4.237	9.998	1.261	9.998	0.7926
57.51	1.987	57.51	0.7968	57.51	0.533
105	1.474	105	0.6467	105	0.4452
152.5	1.219	152.5	0.5638	152.5	0.3951
200	1.06	200	0.5088	200	0.3614
T = 278 K		*T* = 283 K		*T* = 293 K	
$\dot{\gamma}$ /s^{-1}	η/(Pa.s)	$\dot{\gamma}$ /s^{-1}	η/(Pa.s)	$\dot{\gamma}$ /s^{-1}	η/(Pa.s)
9.999	0.3775	9.998	0.1977	9.998	0.06989
57.51	0.2806	57.51	0.164	57.52	0.064
105	0.2499	105	0.1525	105	0.06249
152.5	0.2306	152.5	0.1446	152.5	0.06085
200	0.2169	200	0.1389	200	0.05992
T = 313 K		*T* = 333 K			
$\dot{\gamma}$ /s^{-1}	η/(Pa.s)	$\dot{\gamma}$ /s^{-1}	η/(Pa.s)		
9.999	0.02117	9.999	0.009485		
57.52	0.02049	57.52	0.008443		
105	0.01969	105	0.01003		
152.5	0.02003	152.5	0.009377		
200	0.01958	200	0.009234		

[a] Standard uncertainties u: u(T) = 0.02 K, u($\dot{\gamma}$) = 0.003$\dot{\gamma}$, u(η) = 0.03 η.

Table S- 13. Apparent viscosity values for Maya crude oil + 5.13 wt% toluene at different T and shear rates[a].

T = 258 K		T = 268 K		T = 273 K	
$\dot{\gamma}$ /s^{-1}	η/(Pa.s)	$\dot{\gamma}$ /s^{-1}	η/(Pa.s)	$\dot{\gamma}$ /s^{-1}	η/(Pa.s)
5	72.61	9.998	11.31	9.999	5.686
30	39.24	57.5	7.229	57.5	4.032
55.01	29.78	105	5.984	105	3.48
80.01	24.78	152.5	5.266	152.5	3.133
105	21.53	200	4.773	200	2.886
T = 278 K		T = 283 K		T = 293 K	
$\dot{\gamma}$ /s^{-1}	η/(Pa.s)	$\dot{\gamma}$ /s^{-1}	η/(Pa.s)	$\dot{\gamma}$ /s^{-1}	η/(Pa.s)
9.999	2.427	9.999	1.258	9.999	0.4335
57.5	2.042	57.5	1.135	57.51	0.4187
105	1.878	105	1.075	105	0.4105
152.5	1.768	152.5	1.033	152.5	0.4041
200	1.684	200	0.9994	200	0.3984
T = 313 K		T = 333 K			
$\dot{\gamma}$ /s^{-1}	η/(Pa.s)	$\dot{\gamma}$ /s^{-1}	η/(Pa.s)		
9.998	0.1042	9.999	0.02786		
57.51	0.1066	57.52	0.0386		
105	0.1057	105	0.03847		
152.5	0.1052	152.5	0.03877		
200	0.105	200	0.03891		

[a] Standard uncertainties u: u(T) = 0.02 K, u($\dot{\gamma}$) = 0.003$\dot{\gamma}$, u(η) = 0.03 η.

Table S- 14. Apparent viscosity values for Maya crude oil + 10.02 wt% toluene at different T and shear rates[a].

T = 258 K		T = 268 K		T = 273 K	
$\dot{\gamma}$ /s^{-1}	η/(Pa.s)	$\dot{\gamma}$ /s^{-1}	η/(Pa.s)	$\dot{\gamma}$ /s^{-1}	η/(Pa.s)
9.998	17.19	9.999	3.06	9.999	1.46
57.51	8.513	57.5	2.058	57.5	1.115
105	6.532	105	1.773	105	1.004
152.5	5.5	152.5	1.602	152.5	0.9348
200	4.841	200	1.485	200	0.8847
T = 278 K		T = 283 K		T = 293 K	
$\dot{\gamma}$ /s^{-1}	η/(Pa.s)	$\dot{\gamma}$ /s^{-1}	η/(Pa.s)	$\dot{\gamma}$ /s^{-1}	η/(Pa.s)
9.999	0.6412	9.999	0.376	9.999	0.1527
57.5	0.5732	57.51	0.3545	57.51	0.1493
105	0.5437	105	0.3424	105	0.1488
152.5	0.5244	152.5	0.3339	152.5	0.1483
200	0.5096	200	0.328	200	0.1474
T = 313 K		T = 333 K			
$\dot{\gamma}$ /s^{-1}	η/(Pa.s)	$\dot{\gamma}$ /s^{-1}	η/(Pa.s)		
9.998	0.0442	9.998	0.01362		
57.52	0.04881	57.52	0.02059		
105	0.04833	105	0.02151		
152.5	0.04827	152.5	0.0219		
200	0.04865	200	0.02132		

[a] Standard uncertainties u: u(T) = 0.02 K, u($\dot{\gamma}$) = 0.003$\dot{\gamma}$, u(η) = 0.03 η.

Table S- 15. Apparent viscosity values for Maya crude oil + 20.07 wt% toluene at different T and shear rates[a].

T = 258 K		T = 268 K		T = 273 K	
$\dot{\gamma}$ /s^{-1}	η/(Pa.s)	$\dot{\gamma}$ /s^{-1}	η/(Pa.s)	$\dot{\gamma}$ /s^{-1}	η/(Pa.s)
9.999	3.474	9.999	0.4404	9.999	0.2268
57.5	1.536	57.51	0.3225	57.51	0.1861
105	1.137	105	0.2862	105	0.1725
152.5	0.9448	152.5	0.2663	152.5	0.1641
200	0.8307	200	0.2533	200	0.1588
T = 278 K		T = 283 K		T = 293 K	
$\dot{\gamma}$ /s^{-1}	η/(Pa.s)	$\dot{\gamma}$ /s^{-1}	η/(Pa.s)	$\dot{\gamma}$ /s^{-1}	η/(Pa.s)
9.998	0.1111	9.999	0.07969	9.999	0.04647
57.51	0.1109	57.52	0.07569	57.52	0.03999
105	0.1091	105	0.07403	105	0.04088
152.5	0.1073	152.5	0.07357	152.5	0.04008
200	0.1058	200	0.07296	200	0.04069
T = 313 K		T = 333 K			
$\dot{\gamma}$ /s^{-1}	η/(Pa.s)	$\dot{\gamma}$ /s^{-1}	η/(Pa.s)		
9.999	0.02726	9.998	0.01292		
57.52	0.0164	57.52	0.008073		
105	0.01717	105	0.009303		
152.5	0.01732	152.5	0.009188		
200	0.01786	200	0.009083		

[a] Standard uncertainties u: u(T) = 0.02 K, u($\dot{\gamma}$) = 0.003$\dot{\gamma}$, u(η) = 0.03 η.

Table S- 16. Apparent viscosity values for mixture of 13.66 wt% (toluene + butanone (50/50 vol%)) in Maya crude oil at different T and shear rates[a].

T = 258 K		T = 268 K		T = 273 K	
$\dot{\gamma}$ /s^{-1}	η/(Pa.s)	$\dot{\gamma}$ /s^{-1}	η/(Pa.s)	$\dot{\gamma}$ /s^{-1}	η/(Pa.s)
9.998	6.657	9.999	1.125	9.999	0.5801
57.5	3.395	57.5	0.8366	57.51	0.4856
105	2.647	105	0.7416	105	0.4465
152.5	2.259	152.5	0.6869	152.5	0.4224
200	2.02	200	0.648	200	0.4049
T = 278 K		T = 283 K		T = 293 K	
$\dot{\gamma}$ /s^{-1}	η/(Pa.s)	$\dot{\gamma}$ /s^{-1}	η/(Pa.s)	$\dot{\gamma}$ /s^{-1}	η/(Pa.s)
9.999	0.3014	9.999	0.1758	9.999	0.07809
57.51	0.2706	57.51	0.1721	57.52	0.08128
105	0.2613	105	0.1691	105	0.08148
152.5	0.2542	152.5	0.1673	152.5	0.08104
200	0.2491	200	0.1649	200	0.0812
T = 313 K		T = 333 K			
$\dot{\gamma}$ /s^{-1}	η/(Pa.s)	$\dot{\gamma}$ /s^{-1}	η/(Pa.s)		
9.998	0.02749	9.998	0.03429		
57.52	0.02936	57.52	0.01671		
105	0.03122	105	0.01664		
152.5	0.03067	152.5	0.01509		
200	0.0309	200	0.01515		

[a] Standard uncertainties u: u(T) = 0.02 K, u($\dot{\gamma}$) = 0.003$\dot{\gamma}$, u(η) = 0.03 η.

Table S- 17. Effectiveness of different diluents in decreasing the Non-Newtonian Index (NN-Index) at constant temperatures for mixtures of Maya crude oil and diluents[a].

	NN-Index ($Pa.s^2$)		
	n-heptane	toluene	toluene + butanone (50/50 vol%)
T (K)	w_d = 10.03 wt%	w_d = 10.03 wt%	w_d = 10.03 wt%
9.998	6.657	9.999	1.125
57.5	3.395	57.5	0.8366
105	2.647	105	0.7416
152.5	2.259	152.5	0.6869
200	2.02	200	0.648

[a] Standard uncertainties u: u(T) = 0.02 K, u(m) = 0.112 mg; m: mass of diluent in Maya oil.

Table S- 18. Transient shear stress arising during start-up experiment for mixtures of diluent and Maya crude oil at 273 K, where a 30 s^{-1} shear rate is imposed on samples formerly at rest for 120 minutes. All samples were pre-sheared at 40 s^{-1} for 5 minutes. Type of diluent and its weight fraction in the mixture is a parameter[a].

n-heptane, w_d = 5.11 wt%		n-heptane, w_d = 10.03 wt%		n-heptane, w_d = 20.18 wt%	
Time (min)	□(Pa)	Time (min)	□(Pa)	Time (min)	□(Pa)
0.0000	253.59	0.0000	104.7	0.0000	25.183
0.1167	237.62	0.1167	98.228	0.1167	23.582
0.2333	232.46	0.2333	96.175	0.2333	22.902
0.3500	229.23	0.3500	95.015	0.3500	22.621
0.4667	226.8	0.4667	94.086	0.4667	22.167
0.5833	224.95	0.5833	93.464	0.5833	21.968
0.7000	223.37	0.7000	92.902	0.7000	21.785
0.8167	222.14	0.8167	92.471	0.8167	21.605
0.9333	220.92	0.9333	91.991	0.9333	21.469
1.0500	220.04	1.0500	91.69	1.0500	21.336
1.1667	219.01	1.1667	91.324	1.1667	21.371
1.2833	218.21	1.2833	91.107	1.2833	21.113
1.4000	217.49	1.4000	90.804	1.4000	21.063
1.5167	216.84	1.5167	90.585	1.5167	20.981
1.6333	216.32	1.6333	90.33	1.6333	21.007
1.7500	215.64	1.7500	90.117	1.7500	20.905
1.8667	215.05	1.8667	89.935	1.8667	20.753
1.9833	214.6	1.9833	89.736	1.9833	20.722
2.1000	214.15	2.1000	89.624	2.1000	20.718
2.2167	213.63	2.2167	89.403	2.2167	20.573
2.3333	213.21	2.3333	89.261	2.3333	20.565
2.4500	212.86	2.4500	89.067	2.4500	20.567
2.5667	212.45	2.5667	89.044	2.5667	20.446
2.6833	212.08	2.6833	88.839	2.6833	20.46
2.8000	211.68	2.8000	88.658	2.8000	20.436
2.9167	211.34	2.9167	88.511	2.9167	20.409
3.0333	211.12	3.0333	88.443	3.0333	20.228
3.1500	210.7	3.1500	88.289	3.1500	20.224
3.2667	210.51	3.2667	88.228	3.2667	20.116

3.3833	210.18	3.3833	88.043	3.3833	20.148
3.5000	209.88	3.5000	87.959	3.5000	20.038
3.6167	209.58	3.6167	87.896	3.6167	20.073
3.7333	209.34	3.7333	87.809	3.7333	20.014
3.8500	209.06	3.8500	87.67	3.8500	19.962
3.9667	208.85	3.9667	87.572	3.9667	19.94
4.0833	208.59	4.0833	87.493	4.0833	19.891
4.2000	208.36	4.2000	87.443	4.2000	19.89
4.3167	208.14	4.3167	87.378	4.3167	19.884
4.4333	207.97	4.4333	87.279	4.4333	19.815
4.5500	207.78	4.5500	87.218	4.5500	19.775
4.6667	207.54	4.6667	87.151	4.6667	19.77
4.7833	207.35	4.7833	87.073	4.7833	19.742
4.9000	207.11	4.9000	86.97	4.9000	19.742
5.0167	206.96	5.0167	87.004	5.0167	19.714
5.1333	206.76	5.1333	86.924	5.1333	19.672
5.2500	206.58	5.2500	86.826	5.2500	19.626
5.3667	206.37	5.3667	86.842	5.3667	19.675
5.4833	206.23	5.4833	86.722	5.4833	19.59
5.6000	206.05	5.6000	86.589	5.6000	19.583
5.7167	205.89	5.7167	86.562	5.7167	19.527

toluene, w_d = 5.13 wt%		toluene, w_d = 10.02 wt%		toluene, w_d = 20.07 wt%	
Time (min)	□(Pa)	Time (min)	□(Pa)	Time (min)	□(Pa)
0.0000	158.74	0.0000	41.012	0.0000	6.0679
0.1167	151.98	0.1167	39.393	0.1167	5.9651
0.2333	150.17	0.2333	38.816	0.2333	5.9073
0.3500	148.95	0.3500	38.638	0.3500	5.8748
0.4667	148.12	0.4667	38.431	0.4667	5.8301
0.5833	147.46	0.5833	38.263	0.5833	5.8465
0.7000	146.83	0.7000	38.22	0.7000	5.7997
0.8167	146.29	0.8167	37.976	0.8167	5.8079
0.9333	145.89	0.9333	37.985	0.9333	5.7652
1.0500	145.52	1.0500	37.797	1.0500	5.7964
1.1667	145.23	1.1667	37.875	1.1667	5.7738
1.2833	144.88	1.2833	37.734	1.2833	5.8075
1.4000	144.56	1.4000	37.734	1.4000	5.7442
1.5167	144.36	1.5167	37.636	1.5167	5.7576
1.6333	144.12	1.6333	37.679	1.6333	5.7303
1.7500	144.02	1.7500	37.548	1.7500	5.7488
1.8667	143.69	1.8667	37.731	1.8667	5.7578
1.9833	143.45	1.9833	37.531	1.9833	5.7403
2.1000	143.23	2.1000	37.569	2.1000	5.7337
2.2167	143.13	2.2167	37.527	2.2167	5.7341
2.3333	142.91	2.3333	37.545	2.3333	5.7215
2.4500	142.86	2.4500	37.424	2.4500	5.7394
2.5667	142.56	2.5667	37.477	2.5667	5.7355
2.6833	142.46	2.6833	37.357	2.6833	5.7046
2.8000	142.36	2.8000	37.283	2.8000	5.7109
2.9167	142.3	2.9167	37.361	2.9167	5.6981
3.0333	142.01	3.0333	37.233	3.0333	5.7477
3.1500	142	3.1500	37.268	3.1500	5.6989
3.2667	141.91	3.2667	37.241	3.2667	5.7009
3.3833	141.78	3.3833	37.353	3.3833	5.682
3.5000	141.63	3.5000	37.107	3.5000	5.7252
3.6167	141.46	3.6167	37.28	3.6167	5.706
3.7333	141.36	3.7333	37.147	3.7333	5.7205
3.8500	141.26	3.8500	37.213	3.8500	5.7136
3.9667	141.29	3.9667	37.022	3.9667	5.7387
4.0833	141.04	4.0833	37.197	4.0833	5.732
4.2000	140.97	4.2000	36.98	4.2000	5.6946

4.3167	140.85	4.3167	37.035	4.3167	5.7341
4.4333	140.77	4.4333	37.013	4.4333	5.7073
4.5500	140.69	4.5500	36.951	4.5500	5.7405
4.6667	140.6	4.6667	36.919	4.6667	5.7338
4.7833	140.54	4.7833	36.895	4.7833	5.7163
4.9000	140.5	4.9000	36.882	4.9000	5.7054
5.0167	140.37	5.0167	36.811	5.0167	5.7178
5.1333	140.37	5.1333	36.849	5.1333	5.6721
5.2500	140.26	5.2500	36.788	5.2500	5.6889
5.3667	140.16	5.3667	36.822	5.3667	5.6837
5.4833	140.12	5.4833	36.815	5.4833	5.7146
5.6000	139.99	5.6000	36.857	5.6000	5.6812
5.7167	139.92	5.7167	36.834	5.7167	5.7113

toluene + butanone (50/50 vol%)
w_d = 20.07 wt%

Time (min)	□(Pa)
0.0000	17.857
0.1167	17.246
0.2333	17.088
0.3500	16.913
0.4667	16.849
0.5833	16.804
0.7000	16.743
0.8167	16.698
0.9333	16.615
1.0500	16.564
1.1667	16.588
1.2833	16.573
1.4000	16.489
1.5167	16.534
1.6333	16.463
1.7500	16.462
1.8667	16.378
1.9833	16.455
2.1000	16.401
2.2167	16.421
2.3333	16.366
2.4500	16.354
2.5667	16.313
2.6833	16.301
2.8000	16.351
2.9167	16.295
3.0333	16.288
3.1500	16.223
3.2667	16.269
3.3833	16.274
3.5000	16.272
3.6167	16.28
3.7333	16.325
3.8500	16.181
3.9667	16.289
4.0833	16.184
4.2000	16.251
4.3167	16.16
4.4333	16.27
4.5500	16.133
4.6667	16.151
4.7833	16.156
4.9000	16.141
5.0167	16.15

5.1333	16.092
5.2500	16.148
5.3667	16.108
5.4833	16.122
5.6000	16.101
5.7167	16.092

[a] Standard uncertainties u: u(□) = 0.0005 □.